

Identifying Prioritized Areas for Grassed Waterways Implementation

by

Yunhong Tian

A thesis
presented to the University of Waterloo
in fulfillment of the
thesis requirement for the degree of
Master of Environmental Studies
in
Geography

Waterloo, Ontario, Canada, 2021

©Yunhong Tian 2021

Author's Declaration

I hereby declare that I am the sole author of this thesis. This is a true copy of the thesis, including any required final revisions, as accepted by my examiners.

I understand that my thesis may be made electronically available to the public.

Abstract

Soil erosion remains a primary challenge in the 21st century threatening fresh water and cropland that supports more than 95% of global food production. It is of significance to plan for and prevent soil erosion in its initial stages rather than labor intensive repairing later. The Middle Thames River watershed has suffered from severe erosion issues for more than ten years with 21% highly erodible lands throughout the basin, where extensive soil conservation measures are highly encouraged. A series of practical measures that landowners can apply to enhance soil health and water quality while preserving or increasing agricultural production are termed farmland Best Management Practices (BMPs). Among these measures, grassed waterways, as broad and shallow channels to move concentrated surface runoff, are considered as one of the most effective measures to prevent ephemeral soil erosion. Therefore, identifying the site-specific opportunities for grassed waterways implementation in the Middle Thames River watershed can support targeted soil conservation and the watershed planning.

This study aims to identify the potential locations for grassed waterways implementation in the Middle Thames River Watershed using four different techniques with high-resolution data (Compound Topographic Index model, Stream Power Index threshold model, weighted linear overlay, fuzzy logic analysis). The Compound Topographic Index model and Stream Power Index threshold model have been developed to predict the existing and potential grassed waterways at the field level. Then the Compound Topographic Index and Stream Power Index threshold models, the multi-criteria decision analysis (MCDA) has been conducted to map the priority areas for grassed waterways implementation at the watershed scale. The output maps of the Compound Topographic Index model and Stream Power Index threshold model display the location and length of predicted grassed waterways in each field. To better visualize the results of the Compound Topographic Index model and Stream Power Index threshold model, the density distribution maps of predicted grassed waterways throughout the studied watershed have been created based on the outputs from Compound Topographic Index and Stream Power Index threshold model. The performance of the Compound Topographic Index and Stream Power Index threshold model have been assessed by visual evaluation, occurrence evaluation and length evaluation. After developing Compound Topographic Index and Stream Power Index threshold models, the multi-criteria decision analysis (MCDA) has

been conducted to map the priority areas for grassed waterways implementation at the watershed scale. Twelve factors were selected as criteria of MCDA based on literature review, data availability and geographic knowledge. Two methods including weighted linear combination and fuzzy logic analysis were employed in MCDA, which produced two outputs maps of priority areas for grassed waterways implementation. The results of these two maps have been validated using existing grassed waterways.

The results of the Compound Topographic Index model and Stream Power Index threshold model display the existing and predicted grassed waterways in each field. The Compound Topographic Index model with the threshold of 600 has identified 30 existing grassed waterways, while the Stream Power Index threshold model with the threshold of 0.01 standard deviation identified 23 grassed waterways. Several discontinuities exist in predicted grassed waterways along the trajectories of digitized grassed waterways. The lengths of predicted grassed waterways by Compound Topographic Index model have a much better agreement with observation than that of Stream Power Index threshold model. The density distribution map of Compound Topographic Index and Compound Topographic Index model presented high-density areas of predicted grassed waterways which are mainly situated in the northern and central part of the study area, especially the areas along the upstream of Middle Thames River and Nissouri creek. The low-density areas for grassed waterways implementation are mostly located in the southwestern part of the study area.

The results of weighted linear combination and fuzzy logic analysis displayed the high-priority areas mainly located in the northwestern part of the watershed, especially along the upstream of Nissouri creek. It is found that these upstream areas have relatively steeper slope gradient than other areas in the studied watershed, with dominant soil type of sandy loam and silty loam. There are more areas belonging to the lowest priority zone and lower areas falling into the most priority level in the fuzzy logic analysis output map, compared with the map of weighted linear combination. The fuzzy logic analysis required less prior knowledge of the relationship among criteria, which provide more flexibility and convenience to decision makers. The validation of both weighted linear combination and fuzzy logic analysis output maps displays relatively good performance, based on the criteria that a greater percentage of grassed waterways implementation must occur in the higher priority zones (Kanungo et al., 2009).

Acknowledgements

First and foremost, I would like to acknowledge and express my gratitude to my supervisor Dr. Peter Deadman, for his careful guidance and good support throughout my graduate studies. I appreciate his patience, respect, and effort to discuss my research back and forth during the COVID-19, which was a big challenge for my research physically and mentally. Under his supervision, I was introduced to several models and decision-making systems related to Best Management Practices, which laid a solid foundation for my research.

I would also like to thank Dr. Derek Robinson for providing me with professional feedbacks and different research perspectives. I really admire his passion and perseverance for research. Moreover, I would like to extend my thanks to Dr. Merrin Macrae for her assistance in contacting technicians in UTRCA to support my study and answering my questions, which provided significant help during the critical stage of my research. I would like to thank the Upper Thames River Conservation Authority who provide the BMP data as reference data for my research.

I would like to offer my sincere thanks to my friend Siyuan Qiu, who has always encouraged and supported me throughout my graduate studies, especially during the pandemic. I am grateful for the beautiful time spent with him to discuss technical questions.

Last but not least, I would like to offer my special thanks to my parents and grandparents for their love and supports.

Table of Contents

Author's Declaration.....	ii
Abstract.....	iii
Acknowledgements	v
List of Figures.....	ix
List of Tables.....	x
List of Abbreviations.....	xi
Chapter 1 Background.....	1
Chapter 2 Literature Review.....	5
2.1 Best Management Practices.....	5
2.1.1 Introduction of Farmland BMPs.....	5
2.1.2 Factors influencing the effectiveness of BMPs' program	6
2.1.3 BMPs in the Upper Thames River Watershed.....	8
2.2 Grassed Waterways	9
2.3 Ephemeral Gully Erosion	11
2.3.1 Introduction of Ephemeral Gully Erosion	11
2.3.2 Causes and effects of Ephemeral Gully Erosion	12
2.3.3 Research on Ephemeral Gully Erosion.....	14
2.4 Multi-Criteria Decision Analysis in Spatial Decision-Making System.....	19
Chapter 3 Data and Method.....	22
3.1 Study Area	22
3.2 Digitization of Existing Grassed Waterways.....	25
3.2.1 Data.....	25
3.2.2 Digitizing Existing Grassed Waterways.....	27
3.3 Compound Topographic Index Models (CTI).....	28
3.3.1 Data.....	28
3.3.2 Compound Topographic Index Model	29
3.3.3 Threshold Finding and Visual Evaluation.....	30
3.3.4 Post-processing Techniques before Statistical Evaluation	32
3.3.5 Occurrence Evaluation	33
3.3.6 Length Evaluation.....	35
3.4 Stream Power Index (SPI) Threshold Model	36

3.5 Multi-Criteria Decision Analysis (MCDA)	37
3.5.1 Data	38
3.5.2 Constraints in MCDA	38
3.5.3 Criterion for MCDA.....	39
3.5.4 Weighted Linear Combination (WLC)	44
3.5.5 Fuzzy Logic Analysis (FLA)	48
3.5.6 Division of Priority Level.....	52
3.5.7 Validation.....	53
3.5.8 Sensitivity Analysis.....	54
3.6 Summary of Chapter	56
Chapter 4 Results	57
4.1 Digitization of GWWs	57
4.2 CTI model	59
4.2.1 Threshold Finding and Visual Evaluation	59
4.2.2 Occurrence Evaluation.....	61
4.2.3 Length Evaluation.....	62
4.2.4 Visualization of CTI output	62
4.3 SPI Threshold Model	64
4.4 MCDA.....	68
4.4.1 Thematic layers of criteria	68
4.4.2 Weighted Linear Combination.....	70
4.4.3 Fuzzy Logic Analysis.....	73
4.4.4 Validation.....	76
4.4.5 Sensitivity Analysis.....	79
4.5 Summary of Chapter	80
Chapter 5 Discussion	82
5.1 Threshold Finding.....	82
5.2 GWWs predicted by CTI and SPI model.....	83
5.3 Relationship with RUSLE.....	84
5.4 MCDA.....	85
5.5 Limitations and Prospects	86
5.6 Chapter Summery	88

Chapter 6 Conclusions.....	90
References	93
Appendix	109

List of Figures

Figure 3.1 Middle Thames River Watershed in Upper Thames River	23
Figure 3.3.3 Example of extra branches outside the major trajectory of existing GWW	32
Figure 4.1.1 Example of digitized GWWs.....	57
Figure 4.1.2 Distribution of digitized GWWs.....	59
Figure 4.2.1. The Procedure of threshold finding.....	61
Figure 4 .2.3.1 The output map of predicted GWWs by CTI model (threshold = 600)	63
Figure 4.2.3.2 GWWs density distribution map by CTI model.....	64
Figure 4.3.1 the comparison between SPI model output and CTI model output.....	65
Figure 4.3.2 output map of SPI model with 0.01 standard deviation	66
Figure 4.3.3 GWWs density distribution map by SPI model.....	67
Table 4.3 The error matrix of SPI model.....	68
Figure 4.4 Part 1. Criteria Distribution Map of MCA.	69
Figure 4.4 Part 2. Criteria Distribution Map of MCA.	70
Figure 4.4.2 the priority map of GWWs by WLC	72
Figure 4.4.2.2 priority area which should have GWWs from WLC	73
Figure 4.4.3 the priority map of GWWs implementation by fuzzy logic analysis	75
Figure 4.4.3.2 priority area which should have GWWs from FLA	76
Figure 4.4.4 sensitivity analysis plots of selected criteria.....	79

List of Tables

Table 3.3.5. Error matrix to assess occurrence of GWWs predicted by CTI models.....	34
Table 3.5.3 overview of selected criterion. (Part 1)	39
Table 3.5.4.1 Summary of Standardization of Criteria in WLC.....	44
Table 3.5.4.2 summary of ranking and weight assignment (part 1)	47
Table 3.5.5.1 Summary of fuzzy membership functions in FLA.....	49
Table 3.5.7 Validation of Priority Output.....	53
Table 3.5.8 Selected Criteria for Sensitivity Analysis.....	56
Table 4.2.2 Summary of Occurrence Evaluation of CTI model.....	61
Table 4.2.3. Summary of length evaluation of CTI model.....	62
Table 4.4.3.1 Validation of WLC priority map	76
Table 4.4.3.2 Validation of FLA priority map	78

List of Abbreviations

Abbreviation	Term
BMP	Best Management Practices
GWWs	Grassed Waterways
EGE	Ephemeral Gully Erosion
CTI	Compound Topographic Index
SPI	Stream Power Index
MCDA	Multi-Criteria Decision Analysis
WLC	Weighted Linear Combination
FLA	Fuzzy Logic Analysis
SA	Sensitivity Analysis

Chapter 1 Background

A series of practical measures that landowners can apply to enhance soil health and water quality while preserving or increasing agricultural production are termed farmland Best Management Practices (BMPs) (UTRCA, n.d.). Examples of farmland BMPs include vegetated buffer strips, water and sediment control basin (WASCoB) and grassed waterways (Liu et al., 2017). If properly implemented, farmland BMPs can protect soils from erosion and retain sediments (Rao et al., 2009).

Soil erosion and sedimentation can trigger a series of cascading impacts, including declining productivity and biodiversity, reduced food security, sediments added to adjacent watercourses, and nutrient loss (Borrelli et al., 2020). These nutrients, such as nitrogen and phosphorus, are transported into water bodies, contributing to algal and cyanobacterial blooms that can contaminate drinking water (Rao et al., 2009; Schindler & Fee, 1974). These irreparable effects can be seen globally, with soil erosion still considered to be a primary challenge in the 21st century threatening fresh water and crop land that supports more than 95% of global food production (Borrelli et al., 2020; FAO, 2020).

Planning for and preventing soil erosion in its initial stages are increasingly emphasized by many countries as a more cost-effective option than labor intensive repairs later (OMAFRA, 2018). Among series of farmland BMPs, Grassed Waterways (GWWs) stand out for their effectiveness on reducing surface runoff to prevent erosion and reduce catchment sediment yield (Chow et al., 1999; Verstraeten et al., 2002). Although GWWs are accepted as one of the most common BMPs, they have not been the most frequently evaluated practices in recent BMP studies (Porter, 2018). For example, even if it was reported that GWWs can reduce much more sediment yield than vegetative filter strips at the catchment scale (Verstraeten et al., 2000), there existed far more studies concentrated on vegetative filter strips than GWWs, which assessed vegetative filter strips' effectiveness of runoff reduction and trapping sediment (e.g., Schmitt et al., 1999; Delphin and Chapot, 2001). Additional research of BMPs concentrated on GWWs are in great demand.

Grassed waterways (GWWs) are shaped constructed channels planted with grass or other permanent vegetative covers, where concentrated surface water is conveyed slowly across farmland to an outlet at a non-erosive velocity (NRCS, n.d.). Without GWWs, this concentrated flow following heavy rains

can have significant eroding forces to cause channels and deliver sediment (Dosskey, 2002). These temporary erosion channels caused by concentrated overland flow were termed ‘ephemeral gullies’ by Foster (1986).

Ephemeral gully erosion attracts less farmers’ attention than other typical types of erosion such as sheet and rill erosion, since ephemeral gullies are temporary features that can be filled by tillage operations but reappear latter in the same location during the next heavy rainstorm (Bennett & Wells, 2019). Filling the ephemeral gullies with soils from adjoining areas can thin the topsoil layers of borrowing areas, resulting in significant decline in productivity. Even worse, it will accelerate the reforming of ephemeral gully erosion during the next rainstorm since the materials are looser (Dosskey, 2002). Therefore, it is vital to implement GWWs for landowners to prevent ephemeral gully formation and trap sediment (Atkins and Coyle, 1977).

Several studies have demonstrated GWWs’ remarkable performance in runoff reduction and catchment sediment yield reduction, reaching up to 86% and 20% respectively (e.g., Chow et al., 1999; Verstraeten et al., 2002). However, GWWs have not been extensively evaluated in recent BMPs studies, and their performance in erosion reduction under excess infiltration saturation runoff conditions is probably undervalued (Porter et al., 2018). Few studies concentrate on identifying preliminary source areas (the areas most in need) for GWWs implementation using topographic models; Gali et al. (2015) provided a good starting point to predict placement of GWWs in several agricultural fields of the Hickory Grove Lake watershed in Iowa. For the lack of targeted encouragement of implementation and fast preliminary decision-making tools, GWWs are still underutilized in many European countries (Fiener & Auerswald, 2003) and part of steeper agricultural landscapes in North America (Porter et al., 2018). Fast and cost-effective methods for preliminary siting of GWWs are in great demand at the watershed level, enabling better implementation opportunities to control soil erosion and reduce water pollution effectively (Liu et al., 2017).

Considering GWWs’ primary function of preventing ephemeral gully erosion, several studies suggested that identifying areas susceptible to ephemeral gully erosion are necessary for identifying source areas for GWWs implementation (Fiener and Auerswald, 2003). Previous studies have used

terrain attributes and topographic parameters to predict the initiation of ephemeral gully erosion (Moore et al., 1988; Parker et al., 2007; Momm et al., 2013). Whereas most of these studies are subject to grid data resolution and spatial location variance, resulting in dissatisfactory performance in predicting extents and trajectories of ephemeral gullies (Holmes et al., 2000). Pike et al. (2009) conducted logistic regression and neural networks to develop erosion susceptibility maps for GWWs implementation in Kentucky, which provided a scientific basis for determining factors influencing the priority of locations for GWWs implementation and their relative importance. Several GIS and remote sensing techniques have been used by Khawlie et al. (2002), Servenay and Prat (2003), Martin and Franklin (2005) for ephemeral gully erosion mapping, which provided a good starting point to employ GIS methods in ephemeral gully erosion research. GIS-based Multi-criteria analysis (MCA) techniques stand out for their automatable and repeatable execution and flexibility (Majumdar & Chatterjee, 2021). However, these techniques have not been utilized as tools for identifying locations for the placement of GWWs (Gali et al., 2015).

Some researchers developed topographic index models to identify existing and potential ephemeral gully erosion using critical threshold values specific to study areas' geographic and climate conditions (Thorne et al., 1986; Parker et al., 2007; Daggupati et al., 2013). Among these models, the compound topographic index (CTI) model was considered to predict the location and extent of ephemeral gullies better than others (Daggupati et al., 2013). The CTI is defined as product of slope, planform curvature and drainage area, which can detect ephemeral gullies where CTI values are above the critical threshold (Thorne et al., 1986). The U.S. department of Agriculture (USDA) developed the Stream Power Index (SPI) threshold tool to predict candidate locations for GWWs implementation within the fields at the Hydrologic Unit Code (HUC)12 watershed scale (sixth level sub-watershed in 10000 to 40000 acres) (Porter, 2018; U.S. Geological Survey et al., 2013). The grids with SPI values over the user-defined threshold were selected as potential locations for GWWs. The effectiveness of this tool applied in other study sites outside HUC 12 watershed remains to be explored by additional studies (Tomer, 2018).

In recent years, soil and water conservation have gained constant attention in southern Ontario (Watters, 2019). It is estimated that annual cost owing to soil erosion for Ontario farmers is worth over 150 million (OMAFRA, 2016). In southern Ontario, Lake Erie experienced the third severest

algal bloom since the 21st century in 2017 (Daniel et al., 2017). The excessive nutrient loading from adjacent cropland with few BMPs implementation was considered as the primary driver triggering those harmful algal bloom in Lake Erie (Michalak et al., 2013). Proper adoption of BMPs throughout southern Ontario is in great need for preventing soil erosion and improving water quality. A series of programs and strategies have been developed to improve and prevent the deterioration of soil and water resources in southern Ontario, including Southern Ontario Soil and Water Environmental Enhancement Program (SWEEP) (AAFC, 1986), Clean Water Act (Government of Ontario, 2006) and Farmland Health Incentive Program (FHIP) (OSCIA, 2016), which offered financial and technical supports of BMPs implementation for farmers (Rao et al., 2009). Simple and cost-effective methods for identifying candidate locations for specific types of BMPs in southern Ontario are suggested to support targeted planning and promote stakeholder engagement (Tomer, 2018).

This study aims to identify the potential locations for GWWs implementation in the Middle Thames River Watershed using four different techniques with high resolution data (CTI models, SPI threshold, weighted linear overlay, fuzzy logic). Specific objectives were to (1) develop a GIS-based methodology to identify the existing and potential locations for GWWs implementation using two topographic index models respectively (CTI models and SPI threshold) (2) evaluate the performance of two topographic index models in predicting GWWs' occurrence and length under different threshold selection respectively (3) develop multicriteria decision analysis (MCDA) to map prioritized areas for GWWs implementation using weighted linear overlay and fuzzy logic respectively (4) examine the weights' sensitivity of weighted linear overlay analysis using a novel simulation method (5) evaluate the priority division for GWWs implementation of weighted linear overlay and fuzzy logic respectively. This study can be used to facilitate existing hydrology decision-making systems and water quality models, which can help to identify the most suitable locations for implementing GWWs. In addition, the methods can be applied as simple preliminary 'screening' tools for project managers, sponsors and landowners with weak technical background.

Chapter 2 Literature Review

This chapter reviews the required background for this study, including farmland BMPs in the Upper Thames River, existing studies of GWWs, methods of identifying ephemeral gully erosion, the application of MCA in conservation practices. The first section introduces the development of BMPs with their relevant studies and most common farmland BMPs implemented in the Upper Thames River Watershed, including their categories, functions, management plans and relevant studies. Following these initial descriptions, a detailed review of the current studies of GWWs is presented, with the explanation of their impacts on ephemeral erosion and various factors affecting their effectiveness. In this section, the existing gaps in the literature and research need for GWWs placement are stressed, as they relate to the objectives of this thesis. Considering that the primary function of GWWs is to prevent ephemeral gully erosion, the third section describes the cause and effect of ephemeral gully erosion. This description is then followed by a review of various methods of identifying ephemeral gully erosion which have been used by existing studies. A comparison of the CTI model, the SPI threshold model and other commonly used topographic models, together with their potential methods of evaluation is discussed. The last section summarizes the application of multicriteria decision analysis in conservation practices by current studies, which can support the feasibility and rationality of MCA applied in the thesis. Then the sensitivity analysis techniques of MCA and methods of validation are overviewed.

2.1 Best Management Practices

2.1.1 Introduction of Farmland BMPs

Best Management Practices (BMPs) initially referred to pollution control mechanisms for industrial wastewater and municipal sewage in the beginning of the 20th century (Curtiss, 1978). In the area of stormwater management and wetland management, BMPs have been widely used since the middle of the 20th century, as operational practices or management mechanisms focusing on water pollution control in both urban and rural environments (Kincheloe, 1994; Ahiablame et al., 2012; Liu et al., 2016). Farmland Best Management Practices (BMPs), as affordable and effective measures that farmers can take, were developed to target the protection of soil health and water quality while maintaining or improving production, by means of controlling soil loss and surface runoff of

sediments, nutrients, and nonpoint source pollutants into surrounding ecosystems (Srivastava, Hamlett & Robillard, 2013; OMAFRA, n.d.).

The earliest studies of farmland BMP applications mainly concentrate upon tillage management, terraces, crop residue management and so on, which were initially developed to prevent and reduce soil erosion (Schaller & Bailey, 1983; Logan, 1993). From the middle of the 20th century, nutrients and sediments entering waterways began to receive increasing concern in BMP applications (Clark et al., 1985). Additional BMPs application in preventing non-point source pollution entering water bodies were expected (Novotny, 2003; Rao et al., 2009). Based on this situation, Logan (1990) divided BMPs into two categories: structural BMPs and non-structural BMPs. Structural BMPs frequently use permanent facilities and structural changes in the flow system to decrease the pollution by removing contaminations once they leave the sources, such as sediment control basin, detention ponds, riparian buffers (Ackerman & Stein, 2008). The non-structural BMPs are accomplished by changing agricultural behavior with no structural facilities (EPA, 1999). These non-structural measures develop two approaches to mitigate the non-point source pollution from areas susceptible to erosion (Rao et al., 2009). The first approach is to reduce harmful materials on vulnerable fields (e.g., nutrient management), which belongs to source control (Holland, 2004). The second one is to control the transport of sediments, such as conservation tillage (Dabney, 1998).

2.1.2 Factors influencing the effectiveness of BMPs' program

Effective planning strategies for BMPs require integrated decision-making systems involving multi-stakeholders and multi-objectives (Chen, 2019). Garnett et al. (2013) stressed that both factors affecting BMPs' functionality in short and long term and elements influencing landowners' adoption of BMPs play a significant role in effective BMPs' programs.

For conservation managers and government, BMP implementation should spatially target at specific land parcels with most suitable selection of specific BMP types or their combination, with the aim of maximizing the environmental benefits and minimizing the costs (Garnett et al., 2013). Previous studies have assessed the impacts of watershed characteristics on short-term BMP performances, such as topography, metrology, and land use (Rao et al., 2009; Liu et al., 2017). In addition, the design standards, installation and maintenance condition are considered to have relative impacts on BMPs functionality (Rao et al., 2009). Compared with studies of short-term BMPs effectiveness, the

research regarding long-term performance is limited, owing to the inconsistency in the measurable effects and time limitation (Diebel et al., 2008; Koch et al., 2014). There existed several conservation programs developed in previous years which were not able to achieve their water quality improvement goals, such as the program of reducing the excess nutrients (eutrophication) in the Lake Erie basin (Denver et al., 2010; Sharpley et al., 2012). These failures draw increasing attention to recent studies, which reemphasized the essential roles of the intensity and scale of BMP applications at the watershed scale (Reckhow et al., 2011; Sharpley et al., 2012). Various studies highlight that the simple increase of the number of facilities in BMPs region may not be the most cost-effective solution to enhance water quality; on the contrary, the greater effectiveness can be achieved by preferential investment in certain types of BMPs in targeted regions (Strauss et al. 2007; Artita et al. 2013). Diebel et al. (2008) suggested that the BMPs strategies with the goal of reducing water pollution should be designed on the watershed scale, with the priority of upstream stressors rather than local effects.

Despite the studies of BMPs applications and their effectiveness on water quality improvement that are abundant and various, there still exist considerable uncertainties in transferring findings or model thresholds to a different region, due to the localized case-study nature. (Tomer and Locke 2011). Additional research on localized management plans dedicated to specific types of BMPs is high in demand in the watershed level, enabling better implementation opportunities to control soil erosion and reduce water pollution effectively (Liu et al., 2017).

Apart from the factors affecting BMPs' functionality, recent studies stressed that the core of a BMP program is the adoption of BMPs, which is based on farmers' voluntary adoption of BMPs (Prager et al., 2012). The encouragement, financial and technical support in targeted communities or targeted watershed scales can attract more farmers' participation in BMP program (Chen, 2019). There are more and more financial incentives provided by governments to farmers to implement BMPs, with the aim of achieving high production goals and reducing the sediment and nutrient loadings (Chen, 2019). As the final adopters of BMPs, farmers should have a better understanding of their stewardship roles and BMP adoption, which considerably requires effective information conversation between managers and farmers. There are growing concerns about the rationale of adopting BMPs (Chen, 2019). Several researchers have identified the relationship between farmers' characteristics and their

BMP adoption (Baumgart-Getz, Prokopy, & Floress, 2012). There are also several studies conducting the analysis about the farmers' attitudes change to BMP adoption and their perception of innovation (Floress et al., 2008; Trujillo-Barrera et al., 2016).

In view of the important role of information in BMP adoption, the promotion of effective communication between stakeholders, and the application of participatory mechanisms have gained influence in decision support programs focused on BMPs. For instance, there were several workshops and one-to-one consultations held by the Canada Ontario Environmental Farm Plan, which worked on supporting stakeholders on decision-making of BMP adoption (Smither & Furman, 2003; Chen, 2019). According to the European Union's rural development policy, the State Members in the European Union were also required to encourage stakeholders' involvement in BMP adoption and support the partnership program (Chen, 2019). Nevertheless, there still exist difficulties and obstacles. According to Prager and Freese (2009), the decision support programs and system of BMPs have a long way to go, which still faces challenges including limited funding of conservation, farmers' lack of knowledge and awareness, and poor efficiency in communication.

2.1.3 BMPs in the Upper Thames River Watershed

The Upper Thames River Watershed got second place in overall good water quality for all of the 28 sub-watersheds in 2017 (UTRCA, 2017). This grading was according to bacterial abundance, phosphorous loading, and other significant indexes (UTRCA, 2017). To maintain and improve this ranking, the UTRCA has developed several goals, such as "improve each sub-watershed's water quality score by one grade by 2037" (UTRCA, 2017). Based on these targets, the UTRCA initiated the Clean Water Program (CWP) offering technical and financial support for farmers to implement BMPs (UTRCA, n.d.). Eight different categories of BMPs are mainly adopted in the Upper Thames River Watershed, including Bio-Filters, Buffer Strips, Cover Crops, Drain Modifications, Fragile Land Retirement, Wetland Construction, Windbreaks and Erosion Control Structures (UTRCA, 2017). These BMPs all fit with the cost-effective approach to protect soil health and improve water quality without sacrificing productivity (OMAFRA, n.d.). The Erosion Control Structures include three different methods depending on the types of erosion, size of the watershed and characteristics of

farm fields, including Water and sediment control basins, diversion terraces, and grassed waterways (UTRCA, n.d.).

The earliest studies of BMPs in the Upper Thames River mainly focus on the effects of BMPs implementation on water quality improvement (Yates et al., 2007). However, the results showed no significant correlation between BMPs intensity and stream quality, owing to the limited number of BMPs implemented in 2007 (Yates et al., 2007). Recent studies have found significant correlation between BMPs implementation and water quality indexes (Liu et al., 2017), with several studies aiming to optimize the BMPs distribution for best performance in erosion control and water quality improvement (Rao et al., 2009; Gaddis et al., 2014). Other researchers analyzed the relationship between BMP adoption and farmers' characteristics such as behaviors through regression modelling (Srivastava et al., 2003; Nebel et al., 2017). It was found that there existed positive correlation between BMPs adoption and farmland size, term of land ownership and good attitudes on conservation (Srivastava et al., 2003; Nebel et al., 2017). In these studies, voluntary surveys were conducted for collecting data for regression modelling. However, there were only 18% of voluntary respondents in the survey, which may result in non-response bias when representing overall population. (Srivastava et al., 2003; Nebel et al., 2017). Although the existing studies of BMPs in the Upper Thames River provide adequate findings of BMPs' functionality of water quality improvement, the studies focusing on facilitating targeted planning are still limited. The additional research of identifying potential location for BMPs placement in the Upper Thames River is in need.

2.2 Grassed Waterways

Grassed waterways refer to permanently vegetated channels which are designed for transporting runoff to a stable outlet and mitigating soil erosion when it happens during rainstorms and snowmelt (UTRCA, n.d.). With the increase of surface roughness by vegetation cover, the water flow can be slowed down, and the sediment can be trapped. Therefore, the sediment and nutrient loading can be relatively reduced, and the soil can be protected from ephemeral gully erosion. The vegetation cover provides the habitat for birds and animals, which relatively increase the biodiversity of the field. (Clean water Iowa, n.d.). Compared with other measures of erosion control, the GWWs have some specific advantages; for instance, the cost of maintenance is relatively low after the establishment of

vegetation. Moreover, GWWs can carry large runoff from large watersheds during a heavy rainstorm. GWWs can be crossed by farm machinery on the field (OMFRA, n.d.). Generally, the GWW is supposed to follow the natural drainage way and fit the watershed's characteristics (UTRCA, n.d.). It is recommended to construct grassed waterway when the drainage area covers more than 35 acres. According to Stone and McKague (2009), the shape of waterways, the dimensions such as width, height need to be considered according to the soil characteristics and runoff volume. For instance, it is suggested to select the side slope greater than 1% to protect against out-of-bank flow (Stone and McKague, 2009). It is noted that the appropriate side slope can prevent drainage tile buried under the GWWs from offsetting from the grassed waterway's center, which can also make farm machinery easily move (OMFRA, n.d.). To achieve higher efficiency, grassed waterways are usually implemented with the combination of other BMP methods; for instance, it was found that the system combining terraces and GWWs can effectively reduce approximately 86% of runoff and 95% sediment delivery in fields with potato cultivation (Chow et al., 1999).

Porter et al. (2018) explained 3 reasons why GWWs are relatively effective and efficient measure for preventing ephemeral gully erosion. First, the growing vegetation can slow down the surface run off, which can prevent soil detachment at the same time. Second, if the grass is flushed to lie flat on the field, it can also function as a physical barrier to discourage ephemeral gully formation. Last, the soil strength can be enhanced by grasses' root system, thus restricting soil detachment (Port, 2018). Several researchers have highlighted GWWs' remarkable effectiveness in runoff reduction and catchment sediment yield reduction, reaching up to 86% and 20% respectively (Chow et al., 1999; Verstraeten et al., 2002). One study found that the GWWs were able to reduce 56% of weedicide loss in surface runoff (Briggs et al., 1999). In addition, substantial hydrologic models were conducted to analyze the relationship between GWW properties and its effectiveness on runoff reduction and sediment control (Fiener and Auerswald, 2006; Dermisis et al., 2010). Fiener and Auerswald (2006) found that there is minor influence of seasonal variation of GWW characters (e.g., hydraulic roughness) on the effectiveness of runoff reduction and sediment control. Another study analyzed the impacts of GWW length on its functionality through Water Erosion Prediction Project (WEPP) model (Dermisis et al., 2010). It was found that GWW length had a significant impact on the effectiveness of sediment reduction. Moreover, the researchers demonstrated peak run off as the primary factors affecting GWW's performance of sediment reduction (Dermisis et al., 2010).

While GWWs are among the most common and effective BMPs, they are still not fully used in part of countries, for the lack of targeted encouragement of implementation and fast preliminary decision-making tools (Port et al., 2018). The annual expense of implementing grassed waterway is approximately 18.13 dollars per hectare which is far lower than buffer strips' 40.71 dollars per hectare (Schroter and Kansas, n.d.). This difference of the annual expense is probably owing to different planting and installation cost (e.g., some buffer stripes need woody plating stock and tile extensions), different maintenance cost, and different opportunity cost of the land taken out of the production (Tyndall & Bowman, 2016). Simple and user-friendly tools or methodology for preliminary placement of GWWs are suggested at the watershed level, which can promote implementation opportunities to control ephemeral gully erosion (Liu et al., 2017). Gali et al (2015) tried to identify the potential locations of GWWs using CTI considering the GWWs' primary function of preventing ephemeral gully erosion, which present a good starting point in GWW placement studies (Port et al., 2018). However, there still existed obvious discontinuities in the predicted trajectory of GWWs, likely due to the omission of soil properties in the CTI model (Gali et al., 2015). The U.S. department of Agriculture (USDA) developed an SPI threshold tool to predict candidate locations for GWWs implementation within the fields at the Hydrologic Unit Code (HUC) 12 watershed scale (Porter, 2018). The grids comprising SPI values over the user-defined threshold were post-processed, such as excluding the non-agricultural grids, and then selected as potential locations for GWWs. This tool was comprised in Agriculture Conservation Planning Framework (ACPF) toolbox, which contains a set of GIS-based tools using high-resolution data to predict potential locations for different types of BMPs in the Midwest (Porter, 2018). Although the effectiveness of this toolbox applied in other study sites outside the U.S. remains to be explored by additional studies (Tomer, 2018), it has provided a guideline for analyzing placement opportunities for BMPs from the field scale to watershed scale.

2.3 Ephemeral Gully Erosion

2.3.1 Introduction of Ephemeral Gully Erosion

Ephemeral gullies refer to temporary erosion channels caused by concentrated overland flow, which was firstly explored by Foster (1986). Poesen (1993) supplemented Foster's definition of ephemeral gully erosion, indicating that ephemeral gully erosion may also occur along linear landscape features

where overland runoff concentrates such as parcel borders. Ephemeral gullies are typically developed by disequilibrium between erosional forces and erosional resistance of soils. Either the erosion forces increase (for the increasing concentrated flow or discharge), or the erosion resistance decreases (owing to the decreasing vegetation cover or the disturbance) to initiate the formation of ephemeral gully erosion (Bernard et al., 2010). Several studies emphasized that the initiation of ephemeral gully erosion is also affected by subsurface flow on hillslopes (Huang et al., 1999; Zheng et al., 2000).

Ephemeral gully erosion is distinguished from other types of erosion such as rill erosion and classic gully erosion, owing to ephemeral gully erosion's 'ephemeral' nature of temporary features that can be filled by tillage operations but reappear latter in the same location during the next heavy rainstorm (Foster 1986, Bennett & Wells, 2019). Classic gully erosion refers to very deep erosion in channels that farming equipment can not cross (Hutchinson and Pritchard, 1976). In contrast to ephemeral gully erosion, classic gully erosion is mainly evolved by a complex combination of erosion processes including 'head-cut migration and erosion of gully walls' (Nachtergael et al., 2002). For ephemeral gully erosion, it is mainly evolved by repeated incision process, which is less impacted by 'head-cut migration and erosion of gully walls' (Nachtergael et al., 2002). Rill erosion is characterized as erosion in many small channels spreading along the slope, which has a different way of contributing to the drainage pattern from ephemeral gully erosion (Nachtergael, 2002). The distribution of rill erosion is restrained by field boundaries, while ephemeral gully erosion usually crosses several fields. This difference indicates that rill erosion and ephemeral gully erosion have different impacts on soil transport: rill erosion usually moves soil within a single field, whereas ephemeral gully erosion can redistribute soil particles cross numerous farmlands in the watershed.

2.3.2 Causes and effects of Ephemeral Gully Erosion

Ephemeral gully erosion phenomena are relatively impacted by interaction between natural factors (such as heavy rainstorm and soil erodibility) and social factors (such as excessive cultivation). Huge ephemeral gully erosion s usually present in the arid and semi-arid areas with exiguous vegetation and abundant clay minerals. With respect to social factors, unsustainable land management practices have exacerbated ephemeral gully erosion and their cascading effects over the last decades. (Majumdar et al., 2021). For instance, filling the ephemeral gullies with soils from adjoining areas can thin the

topsoil layers of borrowing areas, resulting in significant decline in productivity. Even worse, the looser materials will raise the chance of ephemeral gully erosion's reoccurrence in the same location during the next rainstorm (Den Biggelaar et al., Dosskey, 2002; AEP 2005). It is noticeable that badlands are instance of these erosion areas where topsoil layers are removed and incision occur into the land (Valentin et al., 2005).

Ephemeral gully erosion features are usually overlooked by landowners and scientific communities, since it is difficult to predict their location and timing of occurrence (Soil Science Society of America, 2008). These complicated problems originate from dynamic interaction between: (1) the surface and subsurface runoff's intensity (2) the earth materials' erodibility (3) variations in vegetation cover resulted from conservation practices and landscape (Nachtergaele et al., 2002). Owing to these complex interrelation problems, the previous studies on ephemeral erosion account for less than 10% of soil erosion research during the past decades (Majumdar, 2021). There emerged increasing instances of damage from sediment and chemical in concentrated runoff to surrounding watercourses, in relation to ephemeral gully erosion (Boardman, 2001; Poesen et al., 2003). These damages attract more and more attention to field studies, indicating that ephemeral gully erosion do not merely act as sediment sources but as transporting links of sediment between uplands and lowlands (Verstraeten and Poesen, 1999; Poesen et al., 2003). Apart from the sediment production and delivery, various studies begin to explore gully erosion's significant impacts on soil loss (e.g., Bocco 1991; Poesen et al., 1996b; Poesen et al., 2003). It is found that the ephemeral gully erosion's impacts on soil loss vary significantly from spatial locations across the world, with soil loss rates ranging from 10% to 94% (Poesen et al., 2003). In addition to spatial factors, the environmental factors relatively impact the ephemeral gully erosion's contribution to soil loss rate, such as land use, topography, soil type and climate condition (Poesen et al., 2003). However, ephemeral gully erosion's contribution to soil loss is currently over-subscribed in current soil loss prevention and assessment projects (Garen et al., 1999; Poesen et al., 2003). It was found that the reformation of ephemeral gully erosion prevention is considerably limited compared with the research in ephemeral gully erosion's development (Poesen & Valentin, 2003). There existed many studies stressing that a number of existing ephemeral gully erosion prevention measures were not valid as expected (e.g., Poesen et al., 2003; Poesen & Vanwalleghem, 2011). More research efforts of ephemeral gully erosion's impacts are expected to assist better conservation strategies.

2.3.3 Research on Ephemeral Gully Erosion

The previous studies on ephemeral erosion account for less than 10% of soil erosion research during the past decades (Majumdar, 2011). In recent years, various research on ephemeral gully erosion with relevant tools and software have widely increased (e.g., Poesen 2011; Majumdar, 2011). Existing research on ephemeral gully erosion typically involves three categories: (1) predicting erosion retreat rates at different spatial and temporal scales (e.g., Oostwoud and Bryan, 2001; Hu et al. 2007); (2) assessing the impacts of ephemeral gully erosion on soil loss, sediment yield and hydrology (e.g., Nyssen et al., 2008); (3) monitoring ephemeral gully erosion's initiation and development (e.g., Poesen et al., 2003).

2.3.3.1 Prediction of Erosion Rate

Several scientific literatures have used physically-based models or field-based techniques to evaluate ephemeral gully erosion's erosion rate quantitatively and qualitatively. Poesen et al. (2003) explored the variation of erosion rates during the evolution of ephemeral gully erosion, with the highest rate at its initiation and drastic decrease as ephemeral gully erosion grows steadily. Wu and Wang (2005) developed a model to simulate the headcut migration vertically in two dimensions, considering the hydraulic erosion on the headcut's vertical headwall and technical faults caused by the scour. However, this model ignores both concentrated flows and sided bank erosion (Bernard et al., 2010). There emerged several models able to predict ephemeral gully erosion rate (Poesen et al., 2003), including CREAMS (Chemicals, Runoff and Erosion from Agricultural Management Systems) (Knisel, 1980), GLEAMS (Groundwater Loading Effects of Agricultural Management Systems) (Knisel, 1993), WEPP (Water Erosion Prediction Project (Ascough et al., 1997) and REGEM (Revised Ephemeral Gully Erosion Model) (Bingner et al., 2007). These models are based on the assumption of the proportional relationship between the rate of concentrated flow detachment and the difference between (1) the flow's delivery capacity and sediment load and (2) "flow sheer stress applied on the bed material" (Majumdar, 2011).

Despite these models professed to be capable of estimating soil losses from ephemeral gully erosion, there existed no thorough tests on the erosion process of these models (Majumdar, 2011).

Nachtergaele et al. (2001) conducted a test of predictive capability of EGEM in multiple cropland environments. Although the preliminary tests presented good alignment between estimated and observed ephemeral gully volumes, there was a weak relationship between the estimation and observation of ephemeral gully erosion cross-sections, since the ephemeral gully volumes need to be divided by the ephemeral gully length (Majumdar, 2011). This test by Nachtergaele et al. (2001) reveals that the predictive capability of EGEM is relatively weak for the cropland environments in the test. In addition, the ephemeral gully length becomes an increasingly important parameter in these prediction models.

2.3.3.2 Prediction of EGE's Location

Prediction of ephemeral gully erosion's location is significant for decision makers to prevent and mitigate ephemeral gully erosion. Both universal models (such as RUSLE) and existing prediction models of EGE's erosion rate lack routines to predict the potential location of EGE (Poesen et al., 1998). For instance, AnnAGNPS (the Annualized version of the Agricultural Non-point Source Pollution Model) is a well-accepted model to predict the origin, movement, amount, and probability of sediment and chemical at any location within the watershed. The magnitude and length of ephemeral gully erosion caused tillage can also be predicted by AnnAGNPS. However, both the prediction of pollutants and E ephemeral gully erosion's magnitude need users to identify location of ephemeral gully erosion e

specially the mouth of ephemeral gully erosion in advance, which reveals the important roles of predicting ephemeral gully erosion's location (Parker et al., 2007).

Various studies have used multivariate statistics techniques and data mining methods to predict areas prone to ephemeral gully erosion, including logistic regression modelling (Bou Kheir et al., 2007), artificial neural networks (Geissen et al., 2007) and classification and regression trees (Gómez-Gutiérrez et al., 2009). These studies commonly use topographic parameters, soil erodibility, lithology, climate parameters and land cover as explanatory variables (Gómez-Gutiérrez et al., 2015). However, these studies typically demand large databases and high spatial resolution environmental

data, such as ephemeral gully erosion inventory data in large temporal scales. Obtaining this inventory data require integrated monitoring system, abundant field-based determination, or advanced satellite image processing techniques. In addition, the accessibility and availability of high spatial resolution environmental data are not always adequate, especially in undeveloped countries (Gómez-Gutiérrez et al., 2015). These limiting factors have negative impacts on the application of statistical methods and data mining techniques in well-accepted, universal, and user-friendly tools.

2.3.3.2.1 Topographic Index Methods

In recent years, there emerges relative development in Light Detection and Ranging (LIDAR) technologies and global mapping missions to obtain high-resolution digital elevation models (DEMs). In addition, more and more topographic data with high resolution in global scale is published and shared through projects (Gómez-Gutiérrez et al., 2015). These advancements promote the development of precision conservation, which can identify the areas prone to erosion accurately and suggest the placement of BMPs (Gali et al., 2015). Various studies have used topographic threshold to predict the potential location of ephemeral gully erosion (Thorne et al., 1986; Moore et al., 1988; Desmet et al., 1999; Parker et al., 2007; Knapen and Poesen, 2010; Daggupati et al., 2013). The application of topographic threshold was firstly introduced by Horton (1945), claiming that “a channel incision occurs when a threshold force is exceeded” (Daggupati et al., 2013). Based on Horton’s study, several researchers explored the channel incision by slope and drainage area, finding that there is inverse correlation between slope and drainage area (Patton and Schumm, 1975; Begin and Schumm, 1979). Other studies used stream power to identify the potential ephemeral gully erosion location, which are according to the theory that “the ephemeral gully formation is generated when the concentrated surface runoff have abundant magnitude and duration” (Thorne and Zevenbergen, 1984). The stream power can be obtained by multiplying the discharge, slope, and channel width (or other power-type function), which can represent the sufficient concentrated surface runoff (Desmet et al. 1999). Apart from stream power, Zevenbergen and Thorne (1987) found that plan curvature is another significant parameter contributing to ephemeral gully erosion’s development, which indicate the convergence and divergence of flow along the cross-section.

With growing knowledge of important topographic parameters contributing to ephemeral gully erosion formation, researchers began to apply these parameters in some combination to describe the spatial variations in ephemeral gully erosion processes (Moore et al., 1988). Since these topographic parameters can be obtained directly from DEM data, the combination of these parameters is defined as topographic index model or compound indices (Moore et al., 1991; Daggupati et al., 2013). When the topographic index value is over the specific threshold, it indicated the occurrence of ephemeral gully erosion.

Several topographic models have been explored to identify the potential location of ephemeral gully erosion during the past decades. Thorne et al. (1986) developed compound topographic index model (CTI) to predict the location of ephemeral gully erosion. The CTI is defined as product of slope, planform curvature and drainage area, which can detect ephemeral gullies where CTI values are above the critical threshold (Thorne et al., 1986; Gali et al., 2015). Moore et al. (1988) developed slope area index model (SA) and wetness topographic index (WTI) model to predict the location of ephemeral gully erosion. SA model refers to the product of slope gradient and contributing drainage area. WTI model is derived by Napierian logarithm of the quotient of upstream drainage area divided by slope. (Moore et al., 1988). Vandaele et al. (1996) developed slope area power index model (SAP) to detect the location of ephemeral gully erosion. SAP model is defined as the product of slope gradient of empirical power of drainage area. Daggupati et al (2013) evaluated the predictable capability of these four topographic index models in Kansa. It is concluded that the CTI model can predicted the extent of ephemeral gullies in relatively good agreement with existing GWWs' using specific threshold values (Daggupati et al., 2013).

There is still no standard methodology to evaluate the topographic index models (Gali et al., 2015). Desmet et al., (1999) evaluated the models' performance by the percentage of estimated pixels of ephemeral gully erosion aligned with the observed pixels of ephemeral gully erosion. Parker et al. (2007) assessed the models by comparing predicted ephemeral gully erosion trajectories with satellite images visually. Daggupati et al. (2013) used three methods to evaluate the predictable performance of four topographic models, including visual evaluation, error matrix assessment and assessing the predicted ephemeral gully erosion length by statistical indicators. These studies highlighted that there exist inevitable discontinuities in predicted ephemeral gully erosion trajectories (Desmet et al., 1999;

Parker et al., 2007; Gali et al., 2015). In addition, soil properties are not considered in the topographic index models, which may result in overestimate of the number and magnitude of ephemeral gully erosion s (Gali et al., 2015). As for the threshold selection, it is unsuitable to utilize the threshold used in the previous studies with different environmental conditions directly, for the localized case-study nature of threshold selection (Parker et al., 2007). However, the cost-effective advantage and relative outstanding predictable performance enable topographic index models as simple and user-friendly tools to assist land managers and policy makers. Compared with complex methods of predicting ephemeral gully erosion s such as neural network and regression modeling, the CTI model requires minimal input data and cost, with relatively good performance of identifying the location and extent of ephemeral gully erosion s, which stands out as preliminary “screening” tool to identify the location of ephemeral gully erosions.

2.3.3.2.2 Multi-Criteria Decision Analysis

In recent years, increasing decision makers and researchers used various GIS and remote sensing techniques for prioritizing the BMPs placement and mapping the areas susceptible to erosion and landslides. Among these techniques, GIS-based Multi-criteria analysis (MCA) techniques stand out for their automatable and repeatable execution and flexibilities (Majumdar & Chatterjee, 2021). GIS-based Multi-criteria analysis (MCA) refers to the analysis through converting and integrating multiple geographic data in order to generate new information of the problem (Greene et al., 2011; Malczewski & Rinner, 2015; Domazetović, 2019). Other researchers define GIS-based MCA as a ‘complementary approach to cost-benefit analysis (CBA)’ (APFM, n.d.). The application of GIS-based MCDA is typically related to explore the areas with different levels of vulnerability of hazards (e.g., Erener et al., 2016; Kumar et al., 2017) or different degrees of suitability of the placement (Young et al., 2010). Various studies have used GIS-based MCA to analyze the susceptibility of ephemeral gully erosion (e.g., Conoscenti et al., 2011; Rahmati et al., 2017). These application of MCA in these studies is based on existing factors impacting the ephemeral gully erosion’s initiation and development (Domazetović et al., 2019). Rundquist (2002) developed a ranking system for mapping fields where ephemeral gully erosion is susceptible to develop, using multiple layers derived from topographic data and multi-temporal ortho images such as normalized difference vegetation index (NDVI). Domazetović et al. (2019) developed a GIS automated MCA (GAMA) methodology, which simplified the multicriteria grouping and weighting assignment. This GAMA methodology can be developed as an automatable and repeatable tool for decision makers in various regions, where the

factors and weights can be adjusted according to different objectives. The existing statistical modeling results of predicting ephemeral gully erosion occurrence have provided abundant information of established criteria and weight assignment for MCA of ephemeral gully erosion susceptibility (e.g., Zabihi et al., 2018). Although there still lack of inventory data of gully erosion and existing GWWs recognized as efficient and sufficient which is required by statistical models, the coefficients and summary statistics in existing studies of statistical modeling can provide the relative importance of conditioning factors of implementing GWWs in MCA. The common established criteria include topographic wetness index (TWI), plan curvature, Stream Power Index (SPI), lithology, distance from river, distance from road, slope aspect, land use, slope length and steepness (Lucà et al., 2011; Conoscenti et al., 2013).

2.4 Multi-Criteria Decision Analysis in Spatial Decision-Making System

Apart from the application of detecting an area's susceptibility of ephemeral gully erosion, MCA has also been applied in spatial decision-making system of BMPs placement. The application of MCA to both the susceptibility of ephemeral gully erosion and a spatial decision-making system provide sufficient rationales for applying MCA in identifying GWW's placement. A series of BMP planning decision support systems have been developed in recent years (Jia et al., 2013; Wang et al., 2017). One of the most famous systems is System for Urban Stormwater Treatment and Analysis Integration systems (SUSTAIN) (Shoemaker et al. 2009), which can provide detailed BMP process simulations and optimal analysis and applications in multiple scales. However, these professional models and systems are usually complex, which is not user-friendly for the stakeholders with weak technical background (Balmforth et al., 2006). In some situations, it can be adequate to apply a simple analysis on BMPs' decision-making, as a central data integration and communication tool, much like a precursor or monitory tool to assist the complex modeling process (Jia et al., 2013; Ellis et al., 2004). Therefore, there emerged several studies implementing multi-criteria analysis in the BMP decision-making framework (e.g., Young et al., 2010; Raines et al., 2010).

There are three common techniques in MCA related to criteria standardization, weight assignment and aggregation: (1) Analytical Hierarchal Process (AHP) (2) Fuzzy Logic Analysis (3) Weighted Linear Overlay. The fundamental for AHP is the pairwise comparison matrices, based on which the

comparison and rank of the various alternative BMPs can be obtained. The weights of each thematic layer will be calculated by creating the pair-wise comparison matrix according to the relative significance between two thematic layers. The numeric scales will be used to illustrate the intensity of importance between the two layers (Chen et al., 2010). And the weights of layers can be calculated by normalization of the principal eigenvectors with the largest eigen value (Chen et al., 2010). Then the consistency ratio (CR) will be calculated to check ‘the inconsistencies among pair-wise judgements’ (Chen et al., 2010). For examples, Young et al. (2010) applied analytical hierachal process (AHP) in BMP site selection, which developed priority ranking of stormwater control and BMP efficiency metrics. However, there seems to be an inherent limitation in these methods, since the weights are determined by the knowledge of researchers and experts, thus introducing bias while being time-consuming (Alvarez-Guerra et al., 2009). Apart from AHP, some researchers used Fuzzy Logic Analysis to construct the benchmarks and indicators. Fuzzy logic analysis is an overlay analysis technique, with the basic premise regarding inaccuracies in both attributes and geometry of spatial data, through which the possibility of the phenomenon is a member of a set is defined (Esri, 2017). Ki et al. (2014) used fuzzy logic function in the Spatial Analyst toolbox in ArcGIS 10 to select suitable sites to implement different BMPs, which was recognized as brand-new BMP decision-making structure using initial site screening and final index map developing. It is concluded by Martin (2007) that the suitability scores from fuzzy logic will be skewed in low score zones. The AHP is expected to be skewed in high suitability scores with a negative skewness distribution (Martin, 2007).

Many strengths of MCA in spatial decision support system have been highlighted in the literature. MCA can be used to perform assessments of complicated problems in epistemic and standard dimensions, which are significant in environmental management evaluation (Vatn, 2019). In addition, multiple objectives of decision-making problems can be considered simultaneously ranging from natural requirements, social issues, cultural issues, economic issues, and human demand issues. The multi-stakeholder scenarios can also be facilitated (Marttunen et al., 2015; Khosravi et al., 2019). Moreover, its capacity of dealing with both quantitative and qualitative information or their mixed set can support environmental planning problems with much uncertainty and incomplete information (Locatelli et al., 2008).

The literature also highlights limitations. In some cases, the best alternatives may not be the most appropriate alternatives in the decision-making process (Triantaphyllou, 2000). There exist some exterior factors which seem to be uncertain and difficult to be considered such as government policies (Triantaphyllou, 2000). In addition, the methods of quantifying the criteria may average the tradeoffs of the criteria. Moreover, some stakeholders' objectives may be contradictory, and the analysis methods can only serve for relatively small group of partnerships. The dearth of covering the whole population's objectives and preferences lead this analysis less representative (Saarikoski et al., 2013).

Chapter 3 Data and Method

3.1 Study Area

The Middle Thames River watershed is one of the four river watersheds of the Upper Thames River in southern Ontario. On a wider scale, the Middle Thames River watershed is a component of the Lake Erie watershed. There are 2 out of 28 sub-watersheds of the Upper Thames River basin in the Middle Thames River Watershed, which are Middle Thames Corridor watershed and Mud Creek watershed (Board et al., 2000; UTRCA, n.d.). The Middle Thames River watershed sits in the south-central part of the Upper Thames River basin (shown in figure 3.1), spanning the East Zorra-Tavistock and the Zorra township (UTRCA, 2017a).

The Thames River rises from northeast of London flowing downstream into southwest of Lake St. Clair. Water from Mud Creek runs north of the Middle Thames River joining it downstream of Embro. As a major branch of South Thames River, the Middle Thames enters the South Thames at the downstream area of Dorchester and runs through London and Chatham joining Lake St. Clair, which meets Lake Erie through Detroit River (Board et al., 2000; UTRCA, 2017b).

The total length of watercourses within the Middle Thames River watershed is 517km, including 248km in the Mud Creek watershed and 269 km in the Middle Thames Corridor watershed. The Mud Creek Watershed covers an area of 171 km² taking up approximately 5% of the Upper Thames River basin, while the Middle Thames Corridor Watershed occupied 157 km². The agricultural lands constitute the majority land use types in the Middle Thames River watershed, covering 85% of the total land in the Mud Creek Watershed and 81% in the Middle Thames Corridor watershed (UTRCA, 2017a). In the Mud Creek watershed, approximately 49% of the basin has agricultural field tile. The dominant soil type in this watershed is silty loam and sandy loam, covering 68% and 25% respectively (UTRCA, 2017a). As for the Middle Thames Corridor watershed, the agricultural field tile covers 49% of the total watershed. The major soil type is sandy loam and silty loam, both of which account for 42% of the total area. (UTRCA, 2017b). The climate in the Middle Thames River is humid continental, with significant seasonal fluctuation. During the growing season from mid-April to late October, rainfall composes about 60% of all forms of precipitation, marked with an average of

160 frost-free days annually (CCDS, 2020). The annual precipitation is about 999mm on average from 2001 to 2020, with the standard deviation of 168mm (Watershed Evaluation Group, 2018).

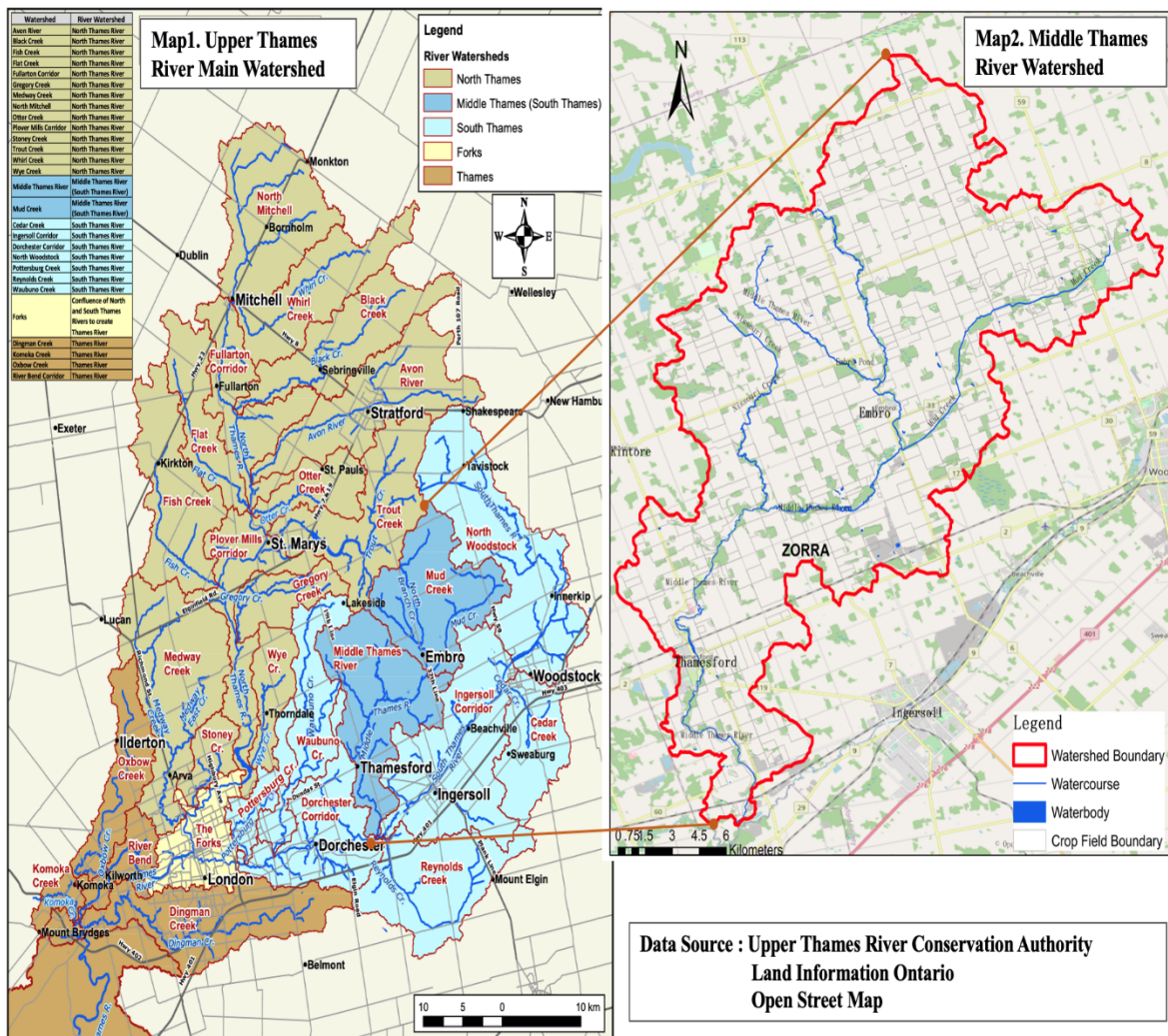


Figure 3.1 Middle Thames River Watershed in Upper Thames River

Note: Upper Thames River Main Watersheds Map (left) and Middle Thames River Watershed Map (right). (Left map) Reprinted from 2017 Upper Thames River Watershed Reports Card, Retrieved August 1, 2021, from <https://thamesriver.on.ca/wp-content/uploads//WatershedReportCards/Map3-UpperThamesRiverMainWatersheds.pdf>. Copyright 2017 by UTRCA. Reprinted with permission.

The Middle Thames River watershed has suffered from severe erosion issues for more than ten years. It is noticeable that up to 20% of lands in the Mud Creek watershed is highly erodible, indicating

more than 7 tons of soil per hectare annually contributed to the adjacent watercourse (UTRCA, 2017a). The Middle Thames Corridor experiences more serious erosion issues with 21% highly erodible lands throughout the basin (UTRCA, 2017b). The average portion of highly erodible lands in the total Upper Thames River watershed is 9%, which is much lower than that of the Middle Thames River watershed (UTRCA, 2017a). The Watershed Report Card (2017) stressed that the overall water qualities of the Mud Creek watershed and the Middle Thames Corridor watershed keep the grade of D and C respectively during the last ten years. The concentrations of Phosphorus in these two sub-watersheds are both higher than three times of provincial aquatic life guideline, dominantly contributing to excess algae and low oxygen in waterbodies (UTRCA, 2017a; b). The Middle Thames River watershed has been identified as one of the polluting sources to Lake Erie through speeding the formation of algal blooms, which is responsible to provide millions of people with drinking water, business development and recreation (UTRCA, 2017a), with 21% highly erodible lands throughout the basin.

To control soil erosion and improve water quality in the Upper Thames River Watershed, the Upper Thames River Conservation Authority has initiated multiple Clean Water Program Projects throughout the Upper Thames River basin from 2011 to 2015. The number of projects completed in the Mud Creek Watershed is the largest among 28 sub-watersheds. The Middle Thames Corridor watershed also has the third largest quantity of projects completed (UTRCA, 2017c). Although plenty of projects have been completed in these two watersheds, the water quality and soil health still need to be improved through more targeted management strategies (UTRCA, 2017a). Few studies of BMPs have focused on this region to facilitate the existing decision-making systems of BMPs. Considering the severe erosion issues in the Middle Thames River watershed, more research efforts on identifying the potential locations for erosion control BMPs are in highly demand. Numerous BMP projects in the Middle Thames River watershed can provide plentiful BMP data available for modeling and calibration. Therefore, the Middle Thames River watershed is selected as study area for identifying the potential locations for GWWs implementation.

3.2 Digitization of Existing Grassed Waterways

The locations and shapes of existing GWWs were used as observed data to evaluate the performance of topographic index models and MCA in previous studies. For the lack of accurate inventory data of existing BMPs, the existing GWWs need to be delineated. In this study, the digitization of existing GWWs were conducted to retrieve reference data to assess performance of CTI model, SPI model and MCDA. The Section 3.2.1 introduces the relevant data used in the digitization of GWWs. In Section 3.2.2, the process of digitization is presented.

3.2.1 Data

The process of digitizing existing GWWs requires three layers of data, including watershed boundary, aerial imagery, and BMP project data. The boundary data provide the scope of digitization. The aerial imagery is used as the base map offering landscape information. The BMP project data provide approximate locations of the fields with GWWs supported by UTRCA, which can assist the identification of GWWs. The Section 3.2.1.1 introduces detailed information of the required boundary data, including data sources and how they were processed. In Section 3.2.1.2, details of aerial imagery and BMP project data are explained.

3.2.1.1 Boundary Data

The digitization of existing GWWs required the primary layer of buffered Middle Thames River watershed boundary, to ensure that land use, soils and slope can adequately represent the watershed's extent. This buffered watershed boundary data were created at a distance from the union of original Middle Thames River watershed boundary and the crop field boundary data (intersect with the watershed). The 'union' operation and 'buffer' operation were both conducted in ArcGIS using the Union tool and Buffer tool respectively. The buffer distance in this study is 1000 meters, referring to the buffer distance used in the Agricultural Conservation Planning Framework (Porter et al., 2018) and the extent of agricultural fields within the watershed.

The quaternary Ontario Watershed Boundary (OWB) data provided by Land Information Ontario (LIO) were used as the source of watershed boundary data. This boundary data were generated based on the latest Ontario Integrated Hydrology (OIH) data published in 2019. During the generating

process, the involvement of several advanced interpolation and smoothing techniques improved the data's consistency with present local hydrology (MNRF, 2019; LIO, 2021). The division of each watershed primarily followed the 'Drainage Area' hierarchical reporting framework proposed by Water Survey of Canada. This division aimed to ensure that all the land mass and waterbodies within the same suitably sized 'Drainage Areas' were contained in the same polygon, which can facilitate conservation management research and setting hydrometeorological sites (LIO, 2021).

The field boundary data were retrieved from the Agricultural Resource Inventory (ARI) 1983 dataset. This dataset was published by Ontario Ministry Agriculture, Food and Rural Affairs, with a recent update in 2019. Instead of only representing discrete ownership patterns, these shapefile data reflected the crop mix and crop proportions within each ownership block, where each polygon represented crop-specific land use (OMAFRA, 2019). This kind of crop-specific field boundary data have been increasingly used in recent conservation planning projects such as Agricultural Conservation Planning Framework in the U.S. (Porter et al., 2018). The identification of cropping systems rather than ownership patterns or land use information can be valid for a longer period, which facilitates field-level conservation planning process. During the generating process of the ARI, the crops growing in each field were identified through field surveys with the latest 1:40000 and 1:50000 aerial images as references. These observations were managed in units of ownership block, based on the ownership data from the local assessment offices (OMAFRA, 2019).

3.2.1.2 Aerial Imagery and BMP Project Data

The Southwestern Ontario Orthophotography (SWOOP) 2015 embedded in the Goggle Earth Engine was used as the aerial base map for digitization. This aerial imagery was provided by Land Information Ontario coordinating several organizations from public and private sectors, covering the entire Ontario province. The pixel resolution of the imagery is 20 centimeters, with 90% accuracy in 50 centimeters on the ground. (LIO, 2020). The aerial imagery was captured in the spring of 2015 with leaf off, under ideal conditions when there is no cloud, snow, ice, and smoke (LIO, 2020). This high-resolution imagery can provide explicit landscape information for reference of digitization, ensuring most of GWWs were not covered by canopies.

The BMP project data in the Upper Thames River Basin was provided by the technician in the Upper Thames River Conservation Authority. These data were stored in comma-separated values (CSV) file, providing approximate coordinates of GWWs or the starting point of fields with GWWs supported by UTRCA. These point data can be displayed on the aerial base map layer on Google Earth Engine through importing the CSV file. Although it is not an accurate and exhaustive list of GWWs, it can provide a guideline for digitizing GWWs.

3.2.2 Digitizing Existing Grassed Waterways

The existing GWWs in the Middle Thames River watershed were identified and digitized using drawing tools of geemap in Google Earth Engine (Wu, 2020; Wu et al., 2019). Field reconnaissance surveys of GWWs were not possible owing to the restricted access to agricultural fields (private property) during the pandemic. In view of this limitation, the identification of GWW features was cross-checked with the technician from UTRCA and relevant experts throughout the digitizing process. The location of each digitized GWWs was checked with the technician, ensuring that the open watercourses and low-lying lawn were not misidentified as existing GWW.

The existing GWWs were recognized only as features inside crop fields; GWWs found along property lines or development boundaries were not recorded, which were not considered as “in-field” GWWs according to previous studies (e.g., Gali et al., 2015; P. Daggupati et al., 2013). The shapefiles of buffered watershed boundary, field boundaries and BMP points were overlaid on the aerial base map on the Google Earth Engine, supporting to locate the possible GWWs. The visual interpretation standards for identifying GWWs referred to expert judgment and previous studies of GWWs (e.g. Boardman, 2016; Gali et al., 2015; P. Daggupati et al., 2013); specifically:

- (1) Curved or tortuous features in 6 to 20 meters width within cultivated fields especially in the thalweg, with different color or texture from surroundings.
- (2) Presence of grass or vegetative cover along linear features, sometimes along the natural drainage way and providing outlets for terraces or diversions.

Every identified GWW was digitized as a polygon feature on Google Earth Engine, which was performed at scales from 1:3500 to 1:1000. The map scale during the manual tracing process was fixed at 1:3500; while the scale was zoomed out gradually until 1:1000 to check the surrounding landscape of identified GWWs. The minimum mapping unit was 50 meters. To prevent

misinterpretation, special attention was paid on straight and parallel traces in the agricultural fields, which were likely to be trails of agricultural machinery. In addition, great care was required in the determination of starting and ending points of GWWs, which can influence the accuracy of GWWs length. The digitized GWWs were verified with technicians in the UTRCA, ensuring that intermittent headwater streams or open watercourses were not misinterpreted as GWWs. GWWs that appeared on the aerial imagery but were not stored in BMP project dataset were also digitized, which were possibly supported by other projects. The digitized GWWs were used as observed data to assess the predictable performance of CTI model, SPI model and MCDA.

3.3 Compound Topographic Index Models (CTI)

3.3.1 Data

The Ontario Digital Elevation Model (DEM) data were used as the source of primary topographic information to generate terrain attributes and compound topographic indices. These data were the product of the Southern Ontario Orthophotography Project (SWOOP) with 2-meter resolution, provided by Ontario Ministry of Natural Resource and Forestry (MNRF) in 2015. These data are a set of raster elevation tiles (1km * 1km) retrieved from the Ontario Classified Point Cloud data, representing the general elevation of surface and ground (MNRF, 2016). The name of each file in the data package reflects the corresponding tile's boundary coordinates and UTM zone, which facilitates the mosaic of contiguous tiles within the study area. During the generating process, the “pixel-autocorrelation” and “steam rolling” algorithm were conducted to ensure the DEM data closer to ground true elevation (MNRF, 2016). After these processes, the elevations of several types of bumped features such as small buildings and small forest cover were reduced which was closer to the ‘bare earth’ (MNRF, 2016).

The Annual Crop Inventory 2019 data provided by the Agriculture and Agri-Food Canada (AAFC) were used as land-cover data to mask non-agricultural fields. These raster data display the crop type distribution of individual fields throughout Canada with 30-meter resolution. A decision tree algorithm combined with crop insurance data and ground-truth information were used in the generating process of this data layer, with overall accuracy of 85% in land-cover type classification (AAFC, 2019). To better describe the agricultural landscape information, several series of multi-temporal optical images were used in the critical stages of the generating process. For the Ontario

region, 66 categories of land-cover types were included in the dataset with more than 82% classification rate (AAFC, 2019).

The Ontario Hydro Network (OHN) data were used as hydrology data source to remove the cells corresponding to the open drainage network and stream network. This dataset is a polyline layer covering the entire Ontario province, provided by the Ministry of Natural Resource and Forestry (MNRF) through digitization. The OHN captures all the watercourses feature in Ontario, including stream, ditches, and virtual flow (MNRF, 2020). During the generation process of the OHN, the GPS data, LIDAR and hydrologic modeling were used to enhance the data quality (MNRF, 2020).

3.3.2 Compound Topographic Index Model

The CTI model was primarily developed to predict the presence or absence of ephemeral gully erosion at each point in earliest studies (Thorne et al., 1986; Moore et al., 1988; Parker et al., 2007). Considering GWWs' major function of preventing ephemeral gully erosion, recent research began to use CTI model to predict the locations of GWWs where ephemeral gully erosions are prone to occur (Gali et al., 2015). In this study, the CTI model was conducted on each DEM raster within the Middle Thames River watershed, to predict the existing and potential locations with GWWs implementation. The output of the CTI model is a map, where each raster cell is assigned a topographic index value. The presence of GWWs at each DEM raster was detected when the CTI value of the pixel was higher than the critical threshold. The selection of critical threshold was based on values reported in previous studies through a trial-and-evaluation approach, which will be explained in the next section. In the CTI model, three terrain attributes including upstream drainage area, slope and plan curvature were used to describe the topographic variability of the drainage network. The following equation

was applied to calculate the CTI value for each raster.

$$\text{CTI} = A \cdot S \cdot \text{PLANC} \quad \text{Equation 3.3.2}$$

where A represents the drainage area (m^2), S refers to the slope (m m^{-1}), and PLANC represents the plan of curvature ($\text{m per } 100 \text{ m}$). The slope and drainage area represent the flow intensity, which is a proxy for forecasting sediment delivery capacity. The plan curvature reflects the lateral concavity or convexity at the cell, indicating the degree of concentration of the runoff by the plan curvature value.

The concave surface has negative value, indicating the convergence of flow in that pixel across the surface. A positive value represents the convex of the surface and the divergence of flow (Zevenbergen and Thorne, 1987).

These three terrain attributes are derived from DEM data using ArcGIS function. The slope was obtained by calculating maximum rate of elevation change between the cell and its surroundings through “Slope” function in ArcGIS (Burrough & McDonell, 1998; Esri, 2016). Before calculating drainage area, the “filling” operation was performed on the DEM data through ArcGIS to remove depressions. After filling sinks, the “Flow Direction” and “Flow Accumulation” were conducted on each raster sequentially to calculate the accumulated number of upland raster (flow) draining into each cell. The contributing drainage area of each raster was the product of raster size and flow accumulation. The plan curvature measured the local flow geometry perpendicular to the direction of maximum slope using “Curvature” function on DEM data (Esri, 2016). The plan curvature layer was multiplied by -1 to convert the values of convergent pixels to positive value, allowing for more direct interpretation of the output and easier threshold finding (Gali et al., 2015). Based on the CTI output raster, the land-use data were used to clip the output raster into cultivated fields. The pixels corresponding to open drainage network and stream network were excluded from the CTI output map.

3.3.3 Threshold Finding and Visual Evaluation

In this study, a trial-and-evaluation approach was adopted to iteratively adjust the threshold until the most suitable threshold of the CTI model is determined. Considering that the critical threshold cannot be currently derived from theoretical basis, this study first tested critical threshold values reported in the literature and conducted visual evaluation on the outputs. The poor performances of the outputs with critical thresholds suggested iterative increments in the threshold until the output achieved the visual evaluation criterion. After identifying the range of eligible threshold values from visual evaluation, this study conducted a quantitative assessment with two methods to identify the most suitable threshold values, which will be illustrated in the next section.

This study first tested five critical threshold values (12, 30, 62, 75, 100) reported as most appropriate thresholds in the literature (Daggupati et al., 2013; Parker et al., 2007; Thorne et al., 1986; Thorne

and Zevenbergen, 1990). Five output maps of potential locations for GWWs using these empirical thresholds were developed respectively. Visual evaluation was conducted on the output maps of potential locations for GWWs. The digitized GWWs and predicted GWWs along the trajectory of existing GWWs were visually compared. The criterion for qualitative assessment of CTI performance using suitable thresholds referred to the relevant literature (Boardman, 2016; Gali et al., 2015; P. Daggupati et al., 2013; Parker et al., 2007; Thorne et al., 1986; T); specifically:

- (1) Most (more than 90%) of the existing GWWs' occurrences in the study area are identified.
- (2) The shape of each predicted GWW is consistent with the trajectory of digitized GWW. Neither significant distortions nor missing parts exist in the shape of predicted GWWs along the trajectory of existing GWWs.
- (3) There are few "branches" outside the trajectory of the digitized GWWs in the shape of the prediction.

The shapes of predicted GWWs in five output maps display poor consistency with shapes of existing GWWs based on the criteria for visual evaluation above, with quantities of extra "branches" outside the major trajectories of existing GWWs. An example was presented in Figure 3.3.3. According to previous studies of CTI model (e.g., Boardman, 2016; Gali et al., 2015; P. Daggupati et al., 2013; Parker et al., 2007; Thorne et al., 1986; T) and numerous trials, the shapes of predicted GWWs can be simplified when the threshold value is increased, through which the extra "branches" outside the existing GWWs' trajectories can be reduced. Therefore, it can be concluded that the suitable threshold values are larger than the five critical threshold values selected from the existing studies. The increment iteration of the threshold value started from 100 (the maximum value of critical threshold in the literature) is suggested, with an increment of 100 in each loop. This increment step size was selected based on numerous trials since there were no theoretical basis for critical threshold values. The increment iteration process was stopped when significant discontinuities and missing parts existed in the predicted GWWs along the trajectories of existing GWWs. After the increment iteration process, a range of threshold values were identified as eligible values meeting visual evaluation standards, above which significant discontinuities and missing parts existed in the predicted GWWs along the trajectories of existing GWWs. Based on the range of suitable threshold values, following statistical assessments using two methods were conducted to evaluate CTI model's performance and identify the most suitable threshold values.



Figure 3.3.3 Example of extra branches outside the major trajectory of existing GWW

Significant extra branches are denoted by green circle.

(Left) existing GWWs; (Right) Predicted GWWs with threshold value of 100

3.3.4 Post-processing Techniques before Statistical Evaluation

Before the statistical evaluation, a series of post-processing techniques were applied using ArcGIS to derive length of GWWs from the output maps of CTI models with each eligible threshold value respectively. These techniques were developed to smooth the trajectories of predicted GWWs without distorting their original shapes and link the discontinuities along the trajectories, in reference to previous studies of predicting GWWs by topographic index models (Daggupati et al., 2013; Parker et al., 2007; Thorne et al., 1986; Thorne and Zevenbergen, 1990). The main steps are as follow:

- (1) Pixels with CTI values greater than the selected threshold were recoded as a value of 1. Then the majority filter function was applied to smooth the recoded pixels.
- (2) The smoothed pixels with the value of 1 were extended by 1 pixel using “expand” function to enhance the connection between cells, then narrowed to a maximum width of 1 cell using “thin” function in ArcGIS.
- (3) The post-processed pixels representing GWWs in the output raster layer were converted to a polyline output layer.
- (4) The output polylines were snapped to nearest edge and end of polylines within 3 meters. This specified snapping distance was based on previous studies, beyond which the shape of trajectories would be distorted. The polylines with a common endpoint were dissolved into one polyline features using “dissolve” function.

(5) The lengths of post-processed polylines were calculated. The dangled polylines with length less of 10 meters were excluded.

(6) The polylines within the digitized GWW polygons were selected. All individual polylines within the same polygon were merged into one polyline feature, representing the GWWs present in both predicted and observed dataset with unique identification number. The sum of lengths of polylines within each GWW polygon was used as the length of predicted GWWs.

(7) For the polylines outside the digitized GWW polygons, all individual polylines within the same crop field boundary were dissolved into one GWW polyline feature. The GWWs with cumulative length less than 50 meters were excluded, according to the typical scales of GWWs which are more than 50 meters and existing studies of GWWs using the CTI model (e.g., Gali et al., 2015; Parker et al., 2007).

3.3.5 Occurrence Evaluation

In this study, the error matrix approach was used to assess the occurrence of predicted GWWs and evaluate the suitability of threshold values. An error matrix summarized the agreement between predicted dataset and ground truth dataset, which was also called covariance matrix or confusion matrix. This approach was used in previous studies of predicting the locations of ephemeral gully erosions with CTI models and regression analysis (Daggupati et al., 2013; Gutierrez et al., 2009). This matrix used a binary variable to describe the occurrence of GWWs (1= present, 0 = absent). There were four entries in this matrix, recording frequencies of four categories of prediction from comparing the predicted and digitized GWWs respectively. For each CTI model with the eligible threshold value selected, the occurrence evaluation using an error matrix was conducted respectively using the format in Table 3.3.5. The entries in the Table 3.3.5 are defined as follows:

a = the number of GWWs that presented in both predicted dataset (by CTI model) and digitized dataset., which was also called as true positive value.

b = the number of GWWs that were predicted by the model but absent in the ground truth dataset, which was also called as false positive value.

c = the number of GWWs that were not predicted by the model but present in the ground truth dataset, which was also called as false negative value.

d = the number of GWWs that were absent in both predicted dataset and observed dataset, which was also called as true negative value

Table 3.3.5. Error matrix to assess occurrence of GWWs predicted by CTI models

Observation			
Prediction	Present	Absent	Totals
Present	a (true positive)	b (false positive)	(a+b)
Absent	c (false negative)	d (true negative)	(c+d)
Totals	(a+c)	(b+d)	
False positive rate	b/(a+b)		
False negative rate	c/(a+c)		

Several statistics can be derived from the error matrix table to evaluate the performance of CTI model. The performance of the CTI model can also indicate the suitability of the threshold selected. (Daggupati, 2012; Daggupati et al., 2013; Gali et al., 2015). In this study, false positive rate, false negative rate, and Kappa (κ) statistics were calculated to assess the performance of each CTI model with eligible threshold respectively. The false negative rate was calculated as the number of false negative GWWs divided by the total number of GWWs predicted by the model. The false positive rate was derived from the number of false positive GWWs divided by the total number of existing GWWs.

A model with good performance is supposed to have low false positive rate and low false negative rate. In the study of GWWs prediction, a high false positive rate did not necessarily reflect poor performance of the CTI model, because the model may predict potential locations in great need of GWWs implementation where GWWs have not been adopted at the time of capturing aerial imagery. However, a high false positive rate was considered as an indicator of poor performance of CTI model, which also indicated the poor suitability of the corresponding threshold value (Daggupati et al., 2013; Gali et al., 2015). It is noticeable that the present study conduct occurrence evaluation on the cropping fields with existing GWWs. Cropping fields without any existing GWWs but predicted as

potential locations for GWWs implementation were not considered in the occurrence evaluation. The suitable threshold values were identified with which the CTI model had considerably low false positive rate.

3.3.6 Length Evaluation

There is no established method of assessing GWWs' length predicted by CTI model. This study applied the cumulative length evaluation method developed by Daggupati et al. (2013) in GWWs' length evaluation, which was previously used to assess the ephemeral gully erosion length predicted by topographic index models. The total accumulated length of each GWW derived from the CTI model was compared with the corresponding GWW's length in ground truth dataset, which was extracted from the centerline of the digitized GWWs polygon. This comparison was conducted on "true positive" GWWs that were present in both predicted and observed dataset. The Nash-Sutcliffe efficiency (NSE) and percent bias (PBIAS) were statistics used in this comparison. These statistics were commonly used to assess the predictive performance of hydrological models relative to observed data, such as SWAT evaluation (Gali et al., 2015; Moriasi et al., 2007).

The NSE is derived from one minus the estimation error variance, as the Equation 3.3.6.1 illustrated:

$$NSE = 1 - \frac{\sum_{n=1}^N (L_p^n - L_o^n)^2}{\sum_{n=1}^N (L_o^n - \bar{L}_o)^2} \quad \text{Equation 3.3.6.1}$$

where \bar{L}_o represents the average length of observed GWWs, and N is the total number of existing GWWs; L_o^n is the nth observed GWW's length, and L_p^n is the nth predicted GWW's length. The higher NSE represents the better predictable performance of the CTI model, indicating the better suitability of the threshold value. The optimal value of 1 indicates the perfect predictable performance of the CTI model, with the ideal agreement between predicted GWWs' length and observed length.

The PBIAS measures the magnitude of the bias between prediction and simulation. The Equation 3.3.5.2 was applied to calculate PBIAS. The low-magnitude values of PBIAS indicate good predictable performance, with the value of 0 indicating the perfect estimation of GWWs length. The positive value of PBIAS displays the underestimation of GWWs' length. The negative PBIAS value indicates that the CTI model overestimates GWWs' length relative to digitized GWWs (Daggupati et al., 2013).

$$PBIAS = 100 * \frac{\sum_{n=1}^N (L_p^n - L_o^n)}{\sum_{n=1}^N L_o^n} \quad \text{Equation 3.3.6.2}$$

of CTI models with each eligible threshold value respectively. The threshold values of with high NSE and low PBIAS were considered as suitable threshold values.

3.4 Stream Power Index (SPI) Threshold Model

In Section 3.4, the SPI threshold model was applied as the second method using topographic index to predict the locations of GWWs in the Middle Thames River watershed. The SPI threshold method was developed by the United States Department of Agriculture (USDA) to predict the potential placement of GWWs in sub-watersheds at the scale of 10000 to 40000 acres in the U.S. (Porter et al., 2018). The USDA applied this method in the Agriculture Conservation Planning Framework (ACPF), as one of the ArcGIS tools to support the implementation of GWWs in each field. In the SPI threshold tool, a specified threshold was applied to the stream power index (SPI) raster layer of the study area. The cells with SPI values greater than the user-defined threshold were identified as potential locations for GWWs, followed by several post-processing techniques to derive the polyline layer of potential locations of GWWs.

SPI is a topographic index indicating the erosive power of flows across the surface, based on the assumption that the flow of water is in proportion to the contributing drainage area. Both net erosion in convex areas and net deposition in concave areas are estimated by SPI. In this study, the SPI raster layer was derived from the DEM raster data following the Equation 3.4, where A refers to the contributing drainage area (m^2) and β refers to the slope ($m m^{-1}$). These two terrain attributes in the Equation 3.4 had been derived in Section 3.3.2 using ArcGIS. Based on the SPI raster, the land-use data were used to clip the output raster into cultivated fields. The pixels corresponding to open drainage network and stream network were excluded from the SPI raster layer.

$$SPI = A * \tan \beta \quad \text{Equation 3.4}$$

After deriving SPI output layer, this study first tested 4 threshold values suggested by ACPF (from 2 to 5 standard deviations greater than the average SPI values of the study area). The raster cells with SPI values greater than each standard deviation threshold values were selected respectively, and four output maps of GWWs were generated. Visual evaluation was conducted on these output maps, which followed the same criterion of that of CTI models in Section 3.3.2. Numerous absences of

predicted GWWs at the locations of existing GWWs suggested the iterated decrement of the threshold values. The decrement iteration of the threshold value started from 1 standard deviation above the average SPI values of the study, with a decrement of 0.01 standard deviation in each loop. A range of threshold values were identified as eligible values meeting visual evaluation standards. Based on the output maps using each eligible threshold values selected, a series of post-processing techniques were conducted to smooth the trajectories of predicted GWWs and derive the lengths of predicted GWWs, which followed the same steps in the post-process of CTI models in Section 3.3.4. Following the post-process, the same statistical assessments (occurrence evaluation and length evaluation) applied in Section 3.3.5 and 3.3.6 were conducted to evaluate SPI threshold model's performance and identify the most suitable threshold values.

3.5 Multi-Criteria Decision Analysis (MCDA)

In Section 3.5, the GIS-based multi-criteria decision analysis is applied to identify prioritized areas for GWWs implementation. The present study adopted two approaches for MCDA including weighted linear combination (WLC) and fuzzy logic analysis (FLA). The differences between their priority maps and advantages of each method are compared.

The MCDA process consisted of six major steps: (1) setting a MCDA goal (2) selecting the criteria and constraints (3) standardization of criteria (4) weight assignment (5) aggregating criteria (6) validation. The primary goal of the MCDA in this study was identifying the prioritized areas for GWWs implementation and creating the priority maps. Based on the main goal, the factors influencing the priority of GWWs implementation were selected through comprehensive analysis of existing studies conducted on similar sites. The detailed explanation of each criterion and constraints will be given in Section 3.5.2 and 3.5.3. The data used for deriving criterion and constraints will be illustrated in Section 3.5.1. According to selected criterion, the WLC and FLA employ different techniques in step (3), (4), and (5), which produce biases between the results. The detailed illustration of WLC and FLA process will be presented in Section 3.5.4 and 3.5.5 respectively.

3.5.1 Data

The MCDA of GWWs requires 6 categories of data, including elevation data, land cover data, soil information data, stream network data, road data and boundary data. The Ontario Digital Elevation Model (DEM) data provided by OMNRF are used as the source of elevation information, simultaneously providing primary topographic information to generate terrain layers in MCDA. The Annual Crop Inventory (ACI) 2019 data provided by the Agriculture and Agri-Food Canada (AAFC) is used as land-cover data to mask non-agricultural fields and provide crop type information in each field. The detailed information of the DEM data and ACI data has been illustrated in Section 3.3.1. The soil survey complex data are used as the source of soil information, providing depictive information such as soil texture, soil erodibility, and soil component. This dataset is a polygon layer, generated from a number of soil surveys throughout the Southern Ontario on a county-by-county basis from the 1920s to the 2000s (LIO, 2015). These surveys were developed by Ontario Ministry of Agriculture, Food and Rural Affairs (OMAFRA) and the Ministry of Nature Resources (MNR). During the primary stage of the production, the soil information of each soil polygon was checked by a GIS specialist using various resources, such as surveys from regional municipal and existing soil data maps (LIO, 2015). The Ontario Hydro Network (OHN) data provided by OMNRF is used as stream network data source to generate drainage density, which has been introduced in Section 3.3.1. The Ontario Road Network (ORN) Segment with Address provided from OMNRF is used as road network data source. This polyline layer data comprise municipal roads and provincial highways covering the entire Ontario province, which was authorized as the official source of road data for the Government of Ontario (LIO, 2019). The boundary data provide the scope of MCDA, which is used to clip the data into the buffered Middle Thames River watershed. This buffered watershed boundary data were created at a 100-meter distance from the union of original Middle Thames River watershed boundary and the crop field boundary data (intersect with the watershed), which has been illustrated in detail in Section 3.2.1.1.

3.5.2 Constraints in MCDA

In GIS-based MCDA, the constraints commonly refer to Boolean criterion, using binary classification to exclude non-satisfactory alternatives (Jiang & Eastman, 2000). The present study selected two constraints including land use and waterway grade, which classified study area into areas where GWWs are possible to be constructed (1-true) and areas where GWWs are impossible to be

constructed (0-false). The selection of these constraints was based on the primary goal of MCDA and the construction manual of erosion control structures by OMAFRA (2016).

Land use is the constraint which can identify agricultural areas and non-agricultural areas. Since the object of this study is agricultural GWWs implemented within fields, the non-agricultural areas are considered as impossible alternatives in MCDA. The pixels belonging to farmland were classified as 1(true), and pixels belonging to non-farmland were classified as 0 (false).

Waterway grade is the constraint classified study area into areas with suitable grade for constructing GWWs and areas with steep grades impossible for GWWs construction. According to OMAFRA (2016), a grade of more than ten percent is not suitable for GWWs, which has a potential for erosion. Therefore, the pixels with grades less than ten percent are classified as 1, and pixels with grades more than 10 percent are classified as 0.

3.5.3 Criterion for MCDA

Since the locations of GWWs implementation is influenced by various factors including the susceptibility of ephemeral gully erosion and suitability of GWWs construction, this study selected 12 parameters as criterion for MCDA, which can affect (1) the likelihood of ephemeral gully erosion's occurrence and (2) the efficiency of GWWs. The selection of the criterion was based on previous studies (Domazetović et al., 2019; Mohsen et al., 2017; Majumdar et al., 2021), data accessibility, and hydrological and geological knowledge. Table 3.5.3 presents an overview of selected criterion. The criterion selected in MCDA included: (1) slope (2) aspect (3) drainage density (4) topographic wetness index (TWI) (5) stream power index (SPI) (6) slope length and steepness (LS Factor) (7) profile curvature (8) plan curvature (9) distance from stream (10) distance from road (11) soil erodibility (12) crop type.

Table 3.5.3 overview of selected criterion. (Part 1)

#	Criteria	Literatures using certain criteria	Data Source
1.	Slope	Conforti et al., 2011; Domazetović et al., 2019a; Domazetović et al., 2019b; Ki & Ray, 2014; Pournader et al., 2018; Zabihi et al., 2018;	DEM

Table 3.5.3 (continued) overview of selected criterion. (Part 2)

#	Criteria	Literatures using certain criteria	Data Source
2.	Aspect	Rahmati et al., 2016; 2017; Domazetović et al., 2019a; Ki & Ray, 2014; Pournader et al., 2018;	DEM
3.	Drainage density	Boufeldja et al., 2020; Majumdar et al., 2021; Zabihi et al., 2018; Samira et al., 2020	Ontario Hydro Network (OHN)
4.	TWI	Agnesi et al., 2011; Conforti et al., 2011; Domazetović et al., 2019a; b; Rahmati et al., 2016; 2017; Ki & Ray, 2014;	DEM
5.	SPI	Agnesi et al., 2011; Conforti et al., 2011; Domazetović et al., 2019a; b; Rahmati et al., 2016; 2017;	DEM
6.	LS factor	Conforti et al., 2011; Domazetović et al., 2019a; b; Lucà et al., 2011;	DEM
7.	Profile curvature	Conforti et al., 2018; Domazetović et al., 2019a; b; Zabihi et al., 2018;	DEM
8.	Plan curvature	Lucà et al., 2011; Pournader et al., 2018; Zabihi et al., 2018;	DEM
9.	Distance to stream	Ki & Ray, 2014; Pournader et al., 2018; Zabihi et al., 2018;	Ontario Hydro Network (OHN)
10.	Distance to road	Ki & Ray, 2014; Zabihi et al., 2018;	Ontario Road Network (ORN)
11.	Soil erodibility	Agnesi et al., 2011; Conforti et al., 2011; Pournader et al., 2018; Lucà et al., 2011;	soil survey complex data
12.	Crop type	Boufeldja et al., 2020; Pournader et al., 2018;	Annual Crop Inventory (ACI)

Slope is one of the major factors of landform formation, which has a direct impact on the intensity of erosion process. The steeper slope increases the intensity of surface runoff and risk of ephemeral gully erosion. In addition, the slope gradient can influence the efficiency of GWWs. The OMAFRA

(2019) recommended that the suitable range of slope for GWWs was between 1 percent to 5 percent. A grade of more than 10 percent is not suitable for implementing GWWs, where there is likely to be erosions in the waterways. A slope of less than 1 percent is not suggested either. The slope of 5 percent is considered as optimal slope for implementing GWWs (OMAFRA, 2019). The slope layer was derived from the DEM data, throughly calculating maximum rate of elevation change between the cell and its surroundings using “Slope” function in ArcGIS (Burrough & McDonell, 1998; Esri, 2016).

Aspect is one of the significant factors influencing both erosion process and efficiency of GWWs. The aspect of the slope controls the exposure of terrains to climate conditions such as the duration of sunlight and wind speed (Dai et al., 2001; Rahmati et al., 2016; Wijdenes et al., 2000). It also has an impact on vegetation cover, evapotranspiration, and water content, which affect both the erosion process and vegetation growth in GWWs (Cevik and Topal 2003; Conforti et al., 2011; Pulice et al. 2009). Southern, south-eastern, and south-western slope was proven to be exposed to longer sunlight duration in Canada (Avalance Canada, n.d.). The aspect layer was extracted from the DEM data using “aspect” function in ArcGIS.

The drainage density measures “the mean length of channels per unit area” (Horton, 1945). Existing studies have concluded that there existed significant positive relationship between drainage density and erosion rate (Clubb et al., 2016). The drainage density layer was derived from the stream network data using “line density” function in ArcGIS.

The topographic wetness index (TWI) is a topographic index indicating the water saturated areas with low surface water infiltration (Conforti et al., 2011; Beven and Kirkby, 1979). This saturated area is prone to concentrated surface runoff, where ephemeral gully erosion is more likely to occur (Domazetović et al., 2019). The TWI layer was derived from the DEM data, based on the Equation 3.5.2.1 below (Beven and Kirkby, 1979), where α is contributing drainage area (m^2/m), and β is slope (degree). The extraction of contributing drainage area has been given in Section 3.3.2.

$$TWI = \ln \left(\frac{\alpha}{\tan \beta} \right) \quad \text{Equation 3.5.2.1}$$

The stream power index (SPI) is a topographic index indicating the erosive power of flows across the surface, based on the assumption that the flow of water is in proportion to the contributing drainage area. The extraction of SPI layer has been illustrated in Section 3.4.

The slope length and steepness (LS) factor is a parameter used in the Universal Soil Loss Equation (USLE), indicating the sediment transport capacity of surface flow. This factor depends on two relevant factors: the slope length factor (L) and slope steepness factor (S), which have a significant impact on surface runoff speed. The cells in the areas with steeper slope and larger catchment area have large LS factor values, representing high susceptibility of erosion. There are various methods applied in previous studies to calculate the LS factor. In this study, the LS layer was derived from the DEM data using the Equation 3.5.2.2 given in Moore and Burch (1986), where A is contributing drainage area (m^2/m), and β is slope (degree).

$$\text{LS} = 1.4 * \left(\frac{A}{22.13}\right)^{0.4} * \left(\frac{\sin \beta}{0.0896}\right)^{1.3} \quad \text{Equation 3.5.2.2}$$

The profile curvature reflects the upward concavity or convexity at the cell, indicating the velocity of surface runoff by the profile curvature value. It described the local flow geometry parallel to the direction of maximum slope, which affects the erosion and deposition process (Esri, 2016). An upwardly convex surface has negative value of profile curvature, indicating the deceleration of the runoff across the surface. A positive value of profile curvature indicates the upward concavity of the surface with the acceleration of the flow. (Esri, 2016). The profile curvature layer was derived from DEM data using “Curvature” function in ArcGIS.

The plan curvature reflects the lateral concavity or convexity at the cell, indicating the degree of concentration of the runoff by the plan curvature value. It measured the local flow geometry perpendicular to the direction of maximum slope using “Curvature” function on DEM data (Esri, 2016). The concave surface has negative value, indicating the convergence of flow in that pixel across the surface. A positive value represents the convexity of the surface and the divergence of flow (Zevenbergen and Thorne, 1987). The plan curvature layer was derived from the DEM data using “Curvature” function in ArcGIS.

The distance to road is an indirect factor influencing the susceptibility of erosion, which was used by several studies of mapping ephemeral gully erosion (Domazetović et al., 2019; Mohsen et al., 2017;

Majumdar et al., 2021). Xiao et al. (2016) concluded the indirect impacts of roads on the erosion process including the fragment landscapes and pollution from the transportation. The construction of roads disturbs the original stream systems and soil systems, with the vegetation removed simultaneously. The distance to road layer was derived from the ORN data, using raster-based distance tool in ArcGIS.

The distance to stream is a factor influencing the erosion process and sediment delivery, which was used in several studies of predicting ephemeral gully erosion and landslides (Domazetović et al., 2019; Majumdar et al., 2021). The areas in shorter distance to stream bed are prone to ephemeral gully erosion. The distance to stream layer was derived from the OHN data, using raster-based distance tool in ArcGIS.

The soil erodibility (also known as K factor) is a parameter used in the Universal Soil Loss Equation (USLE), indicating the susceptibility of the soil to erosion with the influence of runoff and rainfall. The soil texture, structure and organic matter can affect the soil particles detachment and transport, thus generating different susceptibility of soil loss (OMAFRA, 2015). This soil erodibility layer is derived from soil survey complex data. The soil erodibility of each soil polygon was the weighted average K factor value of each textural class within the polygon. The soil polygon layer was converted to 2-meter raster layer with cell values indicating soil erodibility.

The crop type is a factor indicating different cropping management systems with different effectiveness of preventing soil erosion. The farmlands with different crop types and tillage methods can prevent soil loss in different effectiveness in compare with fallow and tilled lands (OMAFRA, 2015). The crop type layer was derived from ACI data, which was resampled to 2-meter resolution consistent with other 2-meter raster layers.

3.5.4 Weighted Linear Combination (WLC)

3.5.4.1 Standardization of Criteria

To ensure all criterion are comparable, the values contained in all criteria layer maps require to be reclassified and scored with the same scale, through the process of standardization. In this study, the selected criteria were divided into several categories and scored on a numeric scale from 1 to 5, where 1 was given to the least priority categories of a certain criteria, and 5 was assigned to the highest priority categories. Similar studies have applied standardized scale of 1-3, 1-4, 1-5 and 1-16 (Aguilar-Manjarrez & Ross, 1995; Domazetović et al., 2019a; Pournader et al., 2018; Salam & Ross 2000). However, it is found that the standardized scores of 1-3 and 1-4 presented insensitive results and the scale of 1-16 was relatively complex. The standardization in the present study was based on the detailed analysis of existing studies of predicting ephemeral gully erosion conducted on the similar sites and geology knowledge. The referenced studies mainly applied frequency ratio (FR) model, index of entropy (I of E), weight of evidence (W of E), analytical hierarchical process (AHP) logistic regression analysis to evaluate the susceptibility of ephemeral gully erosion (Conforti et al., 2011; Domazetović et al., 2019a; Lucà et al., 2011; Zabihi et al., 2018), based on which the relative correlation between each category in the criteria and the occurrence of ephemeral gully erosion can be obtained. The standardization of criteria was adapted to local characteristics of the study area and GWWs construction manual provided by OMAFRA (2016). Table 3.5.4.1 presented the summary of standardized criteria and corresponding references.

Table 3.5.4.1 Summary of Standardization of Criteria in WLC

#	Criteria	Categories	Scores	References
1.	Slope	0 - 1	2	OMAFRA, 2016;
		(in percent) 1-5	5	
		5-10	4	
		>10	1	
2.	Aspect	Flat	1	Conforti et al., 2011; Majumdar &
		North	1	Chatterjee, 2011; Zabihi et al., 2018;
		North East	2	
		East	3	
		South East	4	

#	Criteria	Categories	Scores	References
		South	5	
		South West	4	
		West	3	
		North West	1	
3.	Drainage	<0.5	1	Boufeldja et al., 2020; Majumdar &
	Density	0.5 - 2	2	Chatterjee, 2011; Zabihi et al., 2018;
	(m/m ²)	2 - 4	3	
		4 - 6	4	
		>6	5	
4.	TWI	<4	1	Conforti et al., 2011; Lucà et al., 2011;
		4-6	2	Zabihi et al., 2018;
		6-8	3	
		8-10	4	
		>10	5	
5.	SPI	0-3	1	Conforti et al., 2011; Lucà et al., 2011;
		3-8	2	
		8-50	3	
		50-1000	4	
		>3000	5	
6.	LS Factor	0-0.3	1	Conforti et al., 2011; Lucà et al., 2011; Zabihi
		0.3-0.7	2	et al., 2018;
		0.7- 3	3	
		3 - 9	4	
		>9	5	
7.	Plan Curvature	<-58	5	Conforti et al., 2011; Lucà et al., 2011; Zabihi
		-58 - -10	4	et al., 2018;
		-10 - 0	3	
		>0	1	
8.	Profile Curvature	<0 (convex)	1	Lucà et al., 2011; Zabihi et al., 2018;
		0 (flat)	3	
		>0(concave)	5	

9.	Distance to stream (m)	0 - 100 100- 300 (m) 300 - 550 550 - 850 >850	5 4 3 2 1	Majumdar & Chatterjee, 2011; Pournader et al., 2018; Zabihi et al., 2018;
10.	Distance to roads (m)	0-250 250-400 400-600 600-800 >800	5 4 3 2 1	Ki & Ray, 2014; Zabihi et al., 2018;
11.	Soil Erodibility	0-0.19 0.19-0.33 0.33-0.42 0.42-0.47 0.47-0.63	1 2 3 4 5	OMAFRA, 2015; Majumdar & Chatterjee, 2011;
12.	Crop type	Corn system Continuous row crop Orchard Grain system Mixed system Tabaco system Berries Field vegetables others	5 5 2 5 4 2 2 3 1	OMAFRA, 2015;

3.5.4.2 Weight Assignment

After the standardization of criteria, the weight coefficient of each criteria needs to be determined to differentiate the selected criteria based on their importance. This study adopted the Simple Multi Attribute Rating Technique Exploiting Ranking (SMARTER) approach to determine weight coefficients in WLC (Barron and Barret, 1996). This method was commonly used in planning,

environmental construction, and site selection, owing to its efficiency, simplicity, and repeatability (Barron and Barret, 1996). The SMARTER was developed by Edwards and Barron, as a simplified version of the Simple Multi Attribute Rating Technique (SMART) method to determine the weights of criteria. Different from Analytical Hierarchical Process (AHP) and other objective weighting methods, the SMARTER does not require various experts' opinions or sufficient historical data for statistical analysis, which is suitable for the present study conducted during the pandemic (Odu, 2019).

The first step in SMARTER process was to rank the criteria in (descending) order of importance. The criteria ranking of this study was based on the research goals and detailed analysis of existing studies, including frequency ratio (FR) model, index of entropy (I of E), weight of evidence (W of E), analytical hierarchical process (AHP) logistic regression analysis, which provide relative importance of each criterion in predicting ephemeral gully erosion and implementing GWWs. Based on the ranked criteria, "surrogate" weights were assigned to corresponding criteria as the "true" weights indicating the relative importance of the criteria. There are four methods of calculating "surrogate" weights, including rank order distribution (ROD) method, rank order centroid (ROC) weights method, rank sum (RS) weights method, and rank reciprocal (RP) weights method. Among these methods, the RS method is considered as a relatively practical and accurate solution to problems with plentiful criteria (Roberts and Goodwin, 2002), which was used in this study. The calculation of RS weights is given in Equation 3.5.4.2, where n is the count of criteria, i represents the rank of the criteria and $\sum_{i=1}^n W_i = 1$. The overview of criteria ranking, and weight assignment is given in Table 3.5.4.2.

$$W_i \text{ (RS)} = \frac{(n + 1 - i)}{n(n + 1)/2}, i = 1, 2, \dots, n. \quad \text{Equation 3.5.4.2}$$

Table 3.5.4.2 summary of ranking and weight assignment (part 1)

Criteria	Ranking	Weight
SPI	1	0.1538
LS factor	2	0.1410
Slope	3	0.1282
Soil erodibility	4	0.1154

Table 3.5.4.2 (continued) summary of ranking and weight assignment (part 2)

Criteria	Ranking	Weight
Aspect	5	0.1026
Profile Curvature	6	0.0898
Distance to stream	7	0.0769
Drainage Density	8	0.0641
TWI	9	0.0513
Distance to road	10	0.0385
Plan Curvature	11	0.0256
Crop type	12	0.0128

3.5.4.3 Criteria Aggregation

The last step in WLC is the criteria aggregation, which is used to aggregate constraints and sum of weighted criteria to produce priority map. Equation 3.5.4.3 was applied to conduct criteria aggregation, where S is the priority score of each raster cell; X_i is the standardized value of i^{th} criteria; w_i is the weight of the i^{th} criteria; C_j is the constraint value. Based on the Equation 3.5.4.3., the priority score of each cell was derived from 14 raster layers using “raster calculator” tool in ArcGIS.

$$S = \sum_{i=1}^n w_i X_i * \prod C_j \quad \text{Equation 3.5.4.3}$$

3.5.5 Fuzzy Logic Analysis (FLA)

In this study, the fuzzy logic analysis (FLA) was applied as the second method of MCDA. The FLA is an overlay analysis technique, with the basic premise regarding inaccuracies in both attributes and geometry of spatial data, through which the possibility of the phenomenon is a member of a set defined (Esri, 2016). Compared with other approaches of MCDA, the FLA requires least prior knowledge during the standardization and weighting process (Ki & Ray, 2014). The FLA process comprises two major steps including fuzzy membership function and fuzzy overlay (Joss et al., 2008). The fuzzy membership function is presented in Section 3.5.5.1. The fuzzy overlay process is explained in Section 3.5.5.2.

3.5.5.1 Fuzzy Membership Function

Fuzzy membership function is a standardization process where the criteria values in each thematic layer are rated between 0 and 1 (Joss et al., 2008). This transforming process, also known as fuzzification, ranks the criteria value as a possibility of “being a member of a fuzzy set”, with 1 representing the absolute belonging to the set (Ki & Ray, 2014). There are seven categories in fuzzy membership function, which all belong to continuous functions. Each function is based on different types of transforming process to achieve different expected effect (Esri, 2016). Table 3.5.5.1 presents the overview of fuzzy membership functions selected for each criterion and corresponding statistical properties. The selection of fuzzy membership function was based on geological knowledge and existing studies (Conforti et al., 2011; Gigović & Pamučar; 2019; Lucà et al., 2011; Ki & Ray, 2014;). The fuzzy membership functions used in this study included fuzzy Guassian, fuzzy large, and two types of fuzzy linear (decrease and increase). It is noticeable that the fuzzy membership function could not be applied to crop type layer which consists of discrete classes, since the membership function should be continuous for all input values (Gigović & Pamučar; 2019). To maintain the consistency with the remaining criteria layers for the aggregation, this study used the crop type layer standardized in Section 3.5.4.1 and divided each cell values by 10 to be scaled from 0 to 1.

Table 3.5.5.1 Summary of fuzzy membership functions in FLA

Factors	Fuzzy Membership	Parameters	
Drainage density	Linear (increase)	minimum	0
		maximum	8.693
aspect	Guassian	midpoint	202.5
		spread	0.001
slope	Guassian	midpoint	5
		spread	0.01
TWI	Large	midpoint	5
		spread	1
SPI	Linear (increase)	minimum	30
		maximum	3000
profile Curvature	Linear (decrease)	minimum	549.0114
		maximum	-58.38
plan curvature	Linear (increase)	minimum	-499.57
		maximum	430.27
distance to road	Linear (decrease)	minimum	1382.0332
		maximum	100
distance to stream	Linear (decrease)	minimum	1599.93
		maximum	5
ls factor	Linear (increase)	minimum	0.8
		maximum	50

soil k factors	Linear (increase)	minimum	0
		maximum	0.63

Among the criteria in Table 3.5.5.1, the distance to road is an indirect factor influencing the susceptibility of erosion, which was used by several studies of mapping ephemeral gully erosion (Domazetović et al., 2019; Mohsen et al., 2017; Majumdar et al., 2021). Xiao et al. (2016) concluded the indirect impacts of roads on the erosion process including the fragment landscapes and pollution from the transportation. The construction of roads disturbs the original stream systems and soil systems, with the vegetation removed simultaneously. The selection of fuzzy ‘linear’ function for the distance to road was according to the existing studies (e.g., Mohsen et al., 2017; Majumdar et al., 2021). The distance to stream is a factor influencing the erosion process and sediment delivery, which was used in several studies of predicting ephemeral gully erosion and landslides (Domazetović et al., 2019; Majumdar et al., 2021). The areas in shorter distance to stream bed are prone to ephemeral gully erosion. The selection of fuzzy ‘linear’ function for the distance to stream was based on the existing studies of fuzzy logic analysis on ephemeral gully erosion (e.g., Domazetović et al., 2019; Majumdar et al., 2021).

The fuzzy Gaussian function is a transformation process based on Gaussian or normal distribution, which is around a defined midpoint, with a user-defined spread declining to zero (Esri, 2016). The fuzzy Gaussian function is suggested when the membership is around a certain value. Considering that the areas with the slope gradient closer to 5 percent and the aspect closer to south are more favorable for GWWs implementation, the aspect and slope criteria were transformed by Gaussian function with midpoint of 5 and 202.5 respectively (OMAFRA, 2015; Gigović & Pamučar; 2019). The formula for the fuzzy Gaussian function is given in Equation 3.5.5.1.1, where f1 is the user-defined spread; f2 is the midpoint, and x is the input criteria value.

$$\mu(x) = e^{-f1*(x-f2)^2} \quad \text{Equation 3.5.5.1.1}$$

The fuzzy linear function is a linear transforming process, within the range from specified minimum value to user-defined maximum value (Esri, 2016). The minimum value is assigned a membership of 0 and the maximum value is assigned a membership of 1 (Gigović & Pamučar; 2019). When the specified minimum parameter was larger than the specified maximum parameter for a certain

criterion, the linear transformation is in a negative slope. The linear function is suggested when the membership value linearly increases (or decreases) with the increase of corresponding criteria value. The drainage density, SPI, plan curvature, LS factor and soil erodibility were applied increase linear function, based on their positive linear correlation between criteria value and membership value. The profile curvature, distance to road and distance to stream were applied decrease linear fuzzy function.

The fuzzy large function is a transforming process through which the larger input values are transformed to higher membership closer to 1 (Esri, 2016; Gigović & Pamučar; 2019). The fuzzy large function is suggested when the large values of criterions possess larger membership. The formula for the fuzzy large function is given in Equation 3.5.5.1.2, where f_1 is the user-defined spread; f_2 is the midpoint, and x is the input critera value. The TWI layer was applied fuzzy large function, based on the existing literatures (Gigović & Pamučar; 2019).

$$\mu(x) = \frac{1}{1+(\frac{x}{f_2})^{-f_1}} \quad \text{Equation 3.5.5.1.2}$$

3.5.5.2 Fuzzy Overlay

After deriving multiple thematic layers by fuzzy membership function, this study conducted fuzzy overlay to aggregate all the criteria layers using fuzzy overlay tool in ArcGIS. The output of the fuzzy overlay is a raster layer where each cell with the value representing the priority level of implementing GWWs. There are five optional approaches of overlay provided in the tool, including fuzzy And, fuzzy Or, fuzzy Product, fuzzy Sum and fuzzy Gamma (Esri, 2017; Gigović & Pamučar; 2019). The fuzzy overlay aggregates the input data through set theory analysis, with different methods addressing distinct aspects of pixels' membership relative to the multiple input layers (Esri, 2016). The selection of appropriate overlay approach should be based on the goals of MCDA and expected results (Gigović & Pamučar; 2019).

Fuzzy And and fuzzy Or approach are suggested when the output map is expected to extract the minimum and maximum values from the aggregation of multiple input sets (Gigović & Pamučar; 2019). Fuzzy Product is suggested when the values of cells in the aggregated output map are less important than those of any single criteria layer. The fuzzy Sum approach is suggested when the value of each cell in the output map is more important than that of any single criteria layer (Gigović &

Pamučar; 2019). Fuzzy Sum is an increasing linear combination of input layers rather than algebraic sum, which is not commonly utilized in the analysis. Fuzzy Gamma is a compromised approach to neutralize fuzzy Sum's increasing effect and fuzzy Product's decreasing effect (Esri, 2016). This method is suggested when the value of each cell in the output is expected to be larger than fuzzy Product and smaller than fuzzy Sum. The formula of fuzzy Gamma is given in Equation 3.5.5.2 below.

$$\mu(x) = (\text{FuzzySum})^\gamma * (\text{FuzzyProduct})^{1-\gamma} \quad \text{Equation 3.5.5.2}$$

In this study, the fuzzy Gamma was applied to combine 12 criteria layers in FLA. The value of 0.9, which were most used in previous studies as default value of Gamma, were applied to produce the priority maps (Ki & Ray, 2014; Raines et al., 2010). The suitability of the Gamma value was evaluated through the subsequent validation process given in Section 3.5.7.

3.5.6 Division of Priority Level

After WLC and FLA, different output raster layers were obtained, where the value of each cell indicates the priority score of GWWs implementation. To generate the priority maps for GWWs implementation, the priority scores need to be divided into several categories indicating different levels of priority zone. The traditional methods of segmentation used in previous studies are relatively subjective, owing to the random central tendencies in criteria layers (Saha et al., 2005). This study applied a new probabilistic method of priority level division, which was employed in recent studies to segment susceptibility zones of landslide (Saha et al., 2005; Kanuago et al., 2009). The priority values were divided into five categories including least priority, low priority, median priority, high priority, and most priority, with boundaries fixed at $(\mu - 1.5m\sigma)$, $(\mu - 0.5m\sigma)$, $(\mu + 0.5m\sigma)$ and $(\mu + 1.5m\sigma)$, where μ is the average priority value of cells in the output layer, σ is the standard deviation of priority values in the output layer, and m is a positive, non-zero value (Saha et al., 2005; Kanuago et al., 2009). Based on the range of value assigned to m in previous studies, this study tested the value of 0.9, 1, 1.1 and 1.2 assigned to m , through the subsequent validation process given in Section 3.5.7. The suitable value of m was selected when greater percentage of existing GWWs occur in higher priority zones.

3.5.7 Validation

The validation of priority map is a significant process in MCDA to evaluate the predictive ability of the method and the suitability of the parameters selected (Yilmaz, 2010). The most common method of validation adopted in previous studies is AUC (Area Under the Curve) -ROC (Receiver Operating Characteristics) curve, which can assess the model's ability of predicting occurrence or non-occurrence of natural hazards (Fawcett, 2006; Kanuago et al., 2009; Nandi and Shakoor, 2009; Saha et al., 2005;). In this study, there exist locations with non-occurrence of existing GWWs in demand of GWWs implementation, which cannot be treated as “non-occurrence” used in natural hazards. These locations should be predicted as potential locations with occurrence of GWWs. Therefore, the AUC-ROC method is not a suitable validation method in this study. A statistics summary method was adopted in this study to validate priority maps and the suitability of selected parameters. This validation method summarized the distribution of priority zones and GWWs within each zone. The performance of the priority maps is evaluated by the fact that greater percentage of GWWs implementation must occur in the higher priority zones. Table 3.5.7 presented the statistics required in the validation process.

Table 3.5.7 Validation of Priority Output

Priority level	I. Percent Watershed Area (%)	II. Percent GWWs Field Area (%)	III. Percent GWWs per level (%)	IV. GWWs Field in watershed density	V. GWWs in GWWs Field density	VI. GWWs in watershed density
Least Priority	a	f	k	f/a	k/f	k/a
Low Priority	b	g	l	g/b	l/g	l/b
Median Priority	c	h	m	b/c	m/h	m/c
High Priority	d	i	n	n/d	n/i	n/d
Most Priority	e	j	o	o/e	o/j	o/e

The percentage of total study area in five priority level zoned were summarized in column I. The percentage of the agricultural fields with existing GWWs in each priority level were summarized in column II. The column III summarized the portions of pixels within existing GWWs polygon

belonging to each priority level zone. The column IV recorded the distribution of various densities of the fields with GWWs belonging to each zone. The column V summarized the GWWs density in the field belonging to various priority level. The column VI recorded the GWWs density of the watershed in different priority zones. The performance of the priority map and the suitability of the parameter selected can be validated following two criteria: (1) the greater percentage of existing Grassed Waterways occur in the higher priority zone of the watershed (2) greater percentage of crop fields with existing Grassed Waterways occur in higher priority zone (3) the greater percentage of existing Grassed Waterways occur in higher priority areas within the field.

3.5.8 Sensitivity Analysis

Sensitivity analysis (SA) is a crucial step in the evaluation of MCDA, which assesses the stability of the MCDA. It examines the extent of variation in the output when specific input parameters are changed in a specified range (Archer et al., 1997; Delgado and Sendra, 2004; Ravalico et al. 2010;). This study examined the criteria sensitivity of WLC by changing criteria weights using a cost-effective approach known as OAT. This method changes input factors one-at-a-time and examines the change in the output (Chen et al., 2010). It was commonly used in existing studies owing the strong operability and low cost (Archer et al., 1997; Chen et al., 2010; Delgado and Sendra, 2004; Ravalico et al. 2010).

At the beginning of the OAT process, a range of weight deviations from the initial weight value needs to be defined. This range can be specified as either range of percent change (RPC) or a group of discrete percent change. Either the same range is assigned to all criteria, or different ranges can be applied to selected criteria (Chen et al., 2010). After determining the RPC, a series of SA simulation runs are conducted through increment of percent change (IPC) in each criterion within the specified range (RPC). In each simulation run, the main changing criterion weight is changed in percent increments, and the weights of the remaining criterions are altered in proportion to their relative importance, under the constraint that the sum of the criteria weights is always equal to one. The base run of the simulation is the original criteria weights used in MCDA with no IPC.

The Equation 3.5.8.1 is applied to calculate the weight of the main changing criterion at a certain percent change (PC) level (Chen et al., 2010), where c_m is the main changing criterion (also the m^{th} criterion in the criteria set) and $W(c_m, 0)$ refers to the weight of criterion c_m at the base run.

$$W(c_m, pc) = W(c_m, 0) + pc * W(c_m, 0) \quad \text{Equation 3.5.8.1}$$

The additivity constraint of criteria weights at a certain percent change (PC) level is given in equation 3.5.8.2, where $W(pc)$ is the sum of the total criteria weight at PC level; $W(c_k, pc)$ refers to the weight of the k^{th} criterion at a certain percent change (PC) level, and n is the number of criteria in MCDA.

$$W(pc) = \sum_{k=1}^n W(c_k, pc) = 1 \quad \text{Equation 3.5.8.2}$$

The weights of the remaining criteria $W(c_i, pc)$ are altered through Equation 3.5.8.3, where $W(c_i, pc)$ is the weight of i^{th} criterion at a certain PC level; $W(c_i, 0)$ refers to the weight of criterion c_i at the base run; $W(c_m, pc)$ and $W(c_m, 0)$

$$W(c_i, pc) = (1 - W(c_m, pc)) * \frac{W(c_i, 0)}{1 - W(c_m, 0)}, \quad i \neq m, \quad 1 \leq i \leq n \quad \text{Equation 3.5.8.3}$$

For each simulation, a priority map is generated after changing the criteria weight at a specific PC level, and the number of cells in five priority levels are summarized. For each main changing criterion, the variation in distribution of each priority level throughout the specified RPC are summarized.

Owing to the huge computation and time limitation, the present study examined the sensitivity of six criteria representing different levels of importance in generating priority scores of WLC (most important, moderately important, least important), which were selected according to their quantile ranking order in weight assignment (as Table 3.5.8 illustrates). The sensitivity of six criteria in WLC were examined through OAT method, including SPI, LS factor, profile curvature, distance to stream, plan curvature and crop type. For each selected criterion, the SA simulation was conducted with an RPC of $\pm 20\%$ and an IPC of $\pm 1\%$, consisting of 40 simulation runs. There were 240 simulation runs in total where each run created a new priority map with corresponding attribute table recording the distribution of cells' priority scores. Six plots were generated for each criterion, where the variations of the cells in different priority level were summarized.

Table 3.5.8 Selected Criteria for Sensitivity Analysis

Criteria	Rank	Importance
SPI	1 st	Most important
LS factor	2 nd	
Profile Curvature	6 th	Moderately important
Distance to Stream	7 th	
Plan Curvature	11 th	Least important
Crop type	12 th	

3.6 Summary of Chapter

This chapter illustrates the methodology of identifying existing and potential areas for GWWs implementation in the studied watershed, as well as the required data. The identification and digitization of GWWs have been conducted using ariel images to delineate the existing GWWs as reference data. The CTI model and SPI model has been developed to predict the existing and potential GWWs at the field level. The process of threshold finding and visual evaluation were described. The performance of CTI and SPI model were assessed through occurrence evaluation and length evaluation. After CTI model and SPI model, the MCDA was conducted to predict the priority areas for GWWs implementation. The WLC and FLA were developed, which produced two output maps respectively. The validation of priority maps of WLC and FLA was conducted following the criteria that greater percentage of GWWs implementation must occur in the higher priority zones (Kanungo et al., 2009). In the end, the sensitivity analysis was employed to examine the stability of WLC and sensitivity of selected criteria.

Chapter 4 Results

4.1 Digitization of GWWs

A total of 30 GWWs were identified and digitized in the study area. These identified GWWs are distributed in 28 cropping fields. Figure 4.1 presented an example of digitized GWWs polygon. The lengths of the digitized GWWs range from 83 to 588 meters, with an average of 283 meters; the widths of the GWWs vary from 5 to 32 meters, with an average of 15.8 meters. The total surface area covered by the digitized GWWs is approximately 33.9 ha. The elevation at which the GWWs were identified ranges from 278.22 to 355.227 meter, with an average of 325.69 meter; the slope gradient of digitized GWWs varies from 0.03% to 15%, with an average of 4.35%.

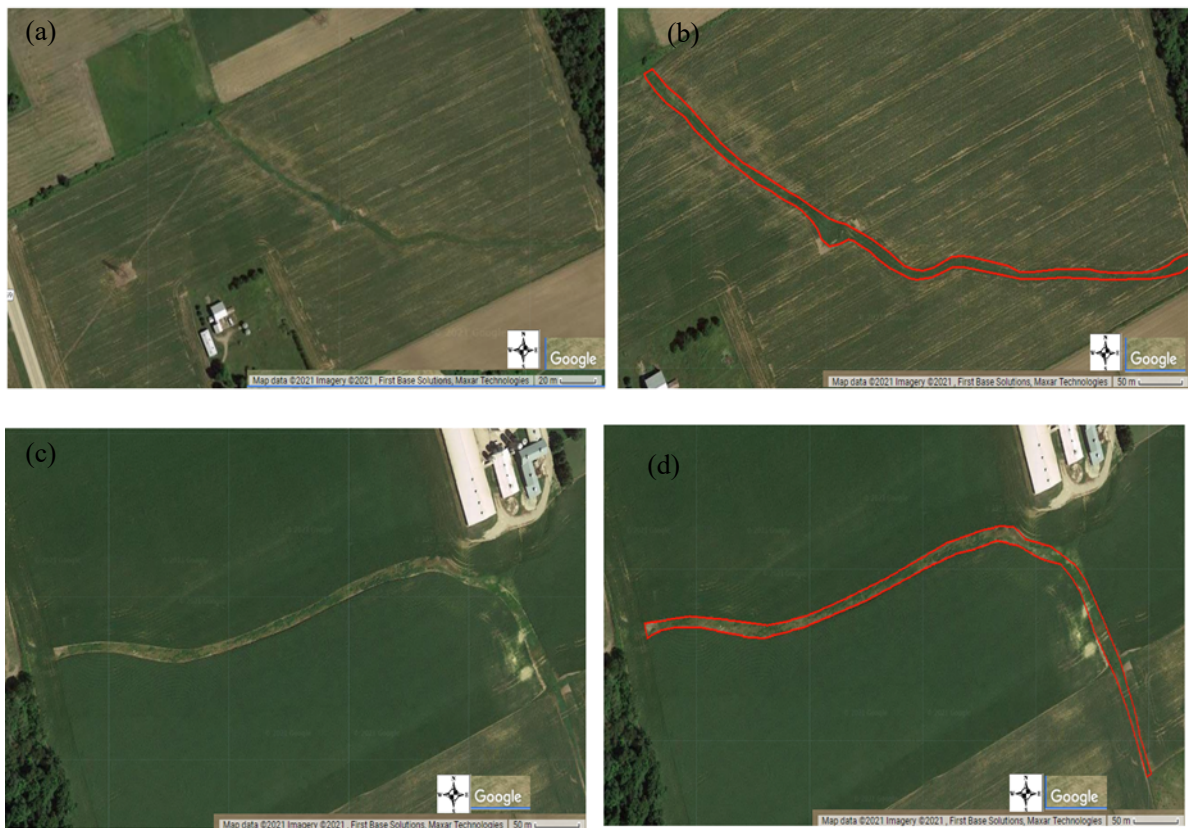


Figure 4.1.1 Example of digitized GWWs. (a)identified GWW (near $80^{\circ}48'52.165''W$, $43^{\circ}14'55.992''N$). (b)close view of digitized GWW of (a). (c)identified longest GWW ($80^{\circ}58'55.285''W$, $43^{\circ}11'53.147''N$). (d) close view of digitized GWW of (c)

In geographic terms, most of the identified GWWs are situated in the north part of the Middle Thames River Watershed, with denser distribution in the east part around Strathallan. Specifically, most digitized GWWs are distributed along the upstream of watercourses, including Mud Creek, Middle Thames River, Nissouri Creek and Phelam Creek. The geographic distribution of digitized GWWs is presented in figure 4.1.2. It was found that the GWWs were identified mainly in corn system (13 out of 31 cases), continuous row crops (10 out of 31 cases), and mixed system (5 out of 31 cases).

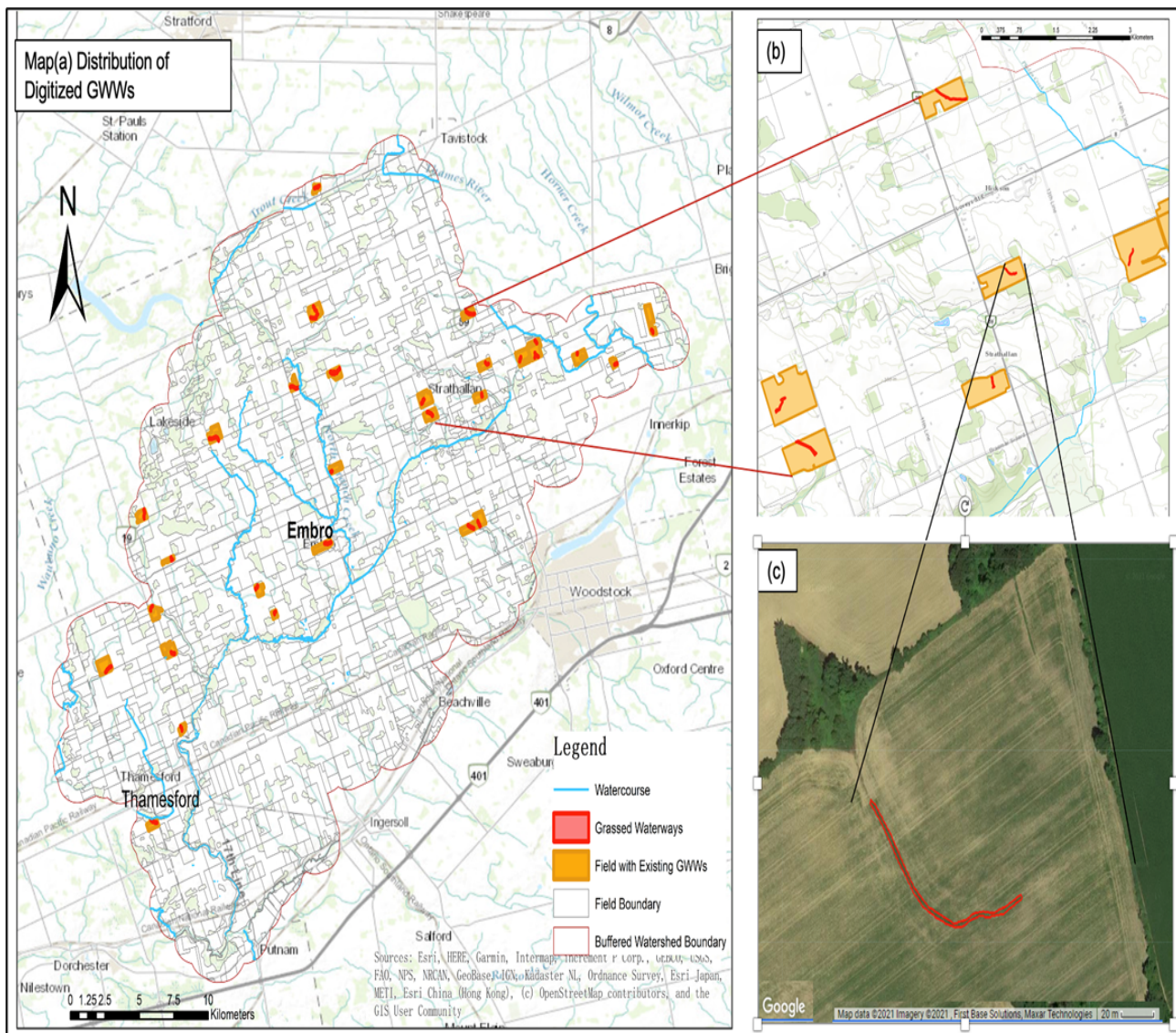


Figure 4.1.2 Distribution of digitized GWWs. (a) Distribution map (b) close view of distribution map (c) close view of digitized GWW on Google Earth Engine

4.2 CTI model

4.2.1 Threshold Finding and Visual Evaluation

In CTI model, a trial-and-evaluation approach was adopted to iteratively adjust the threshold until the most suitable threshold of the CTI model is determined. This study first tested five critical threshold values (12, 30, 62, 75, 100) reported as most appropriate thresholds in the literature (Daggupati et al., 2013; Parker et al., 2007; Thorne et al., 1986; Thorne and Zevenbergen, 1990). Five output maps of potential locations for GWWs using these empirical thresholds were developed respectively. The visual evaluation was conducted on five output maps by comparing the existing GWWs and predicted GWWs. It reveals that the shapes of predicted GWWs using 5 critical thresholds display poor consistency with trajectories of existing GWWs, with quantities of “branches” outside the trajectories, which suggested iterative increase of the threshold values. After the iterative increments in the threshold, the visual interpretation of the CTI model output showed that the models with threshold from 500 to 1100 can correctly predict most of GWWs’ trajectories up to standard of qualitative assessment. The representative results of this procedure for the trial-and-evaluation are presented in figure 4.2.1. As this figure illustrates, with the increase of the threshold value, the areas predicted to be GWWs placement reduce in size, with better consistency with the trajectory of digitized GWW. When the threshold value is under 500, there still exist distortions and several significant “branches” outside the trajectory of GWW. When the threshold value is 500 or higher, there are few “branches” outside the trajectory of the digitized GWWs in the shape of the prediction, and the shape of predicted GWWs better match the shape of existing GWW. Closer observations reveal that there exist more discontinuities and missing parts along the trajectory, as the threshold value increases to 1000 or higher. Overall, the visual evaluation reveals that the range of suitable CTI threshold is from 500 to 1100.

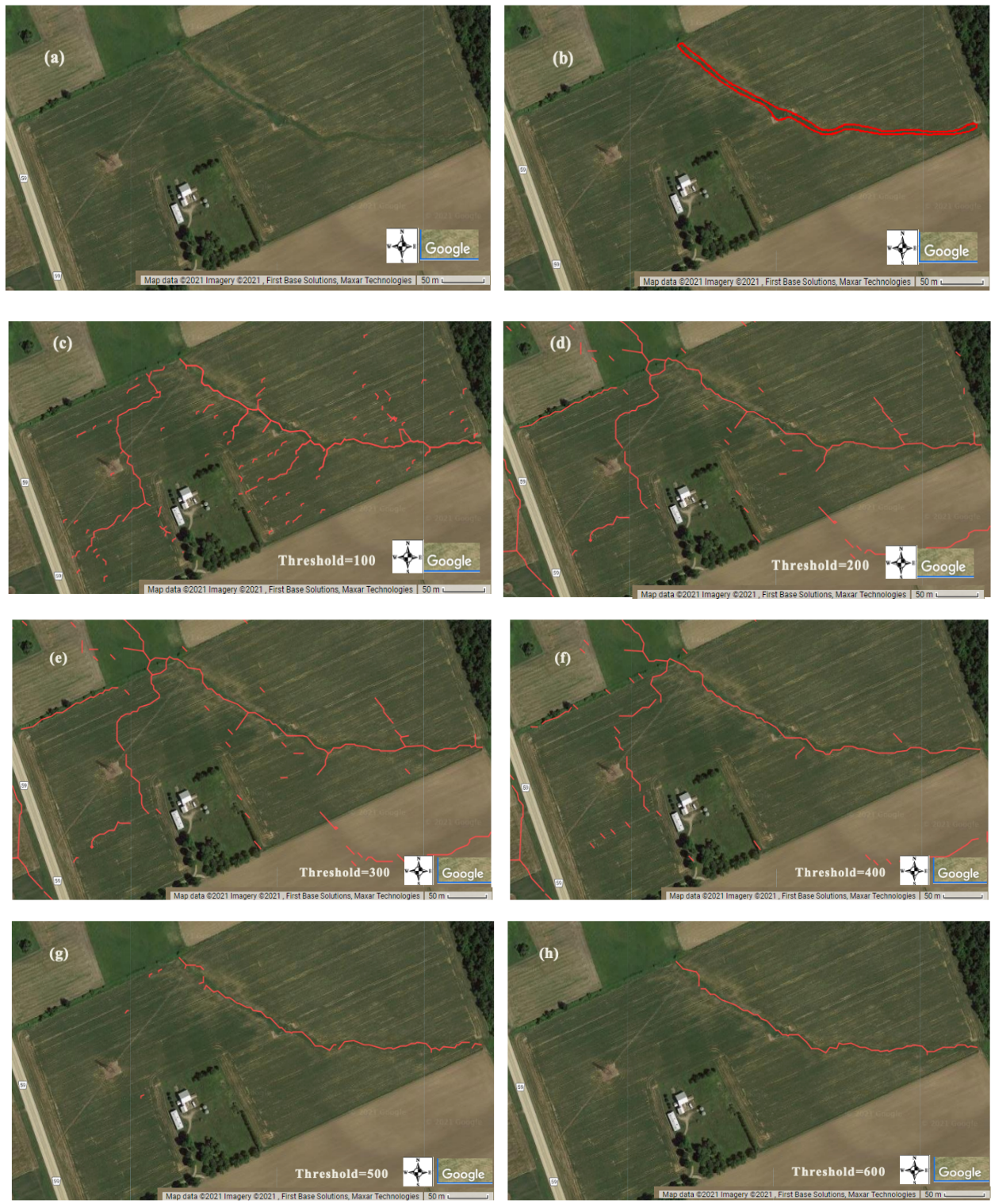




Figure 4.2.1. The Procedure of threshold finding. The predicted GWWs are denoted by red lines. The significant discontinuities are denoted by green circle.

4.2.2 Occurrence Evaluation

The occurrence evaluation shows that the CTI models with threshold from 100 to 600 can identify 30 of 31 existing GWWs in the study area. The models with threshold from 700 to 1000 can identify 29 of 31 existing GWWs in the study area. The false positive rate and false negative rate for the models with series of suitable threshold values are summarized in Table 4.2.2. The models with threshold of 500 and 600 have lower false negative rate (0.0323). As the threshold value increases, the false positive rate decreases. In this study, the false positive rate does not necessarily reflect poor performance of the CTI model. This rate can indicate (1) potential locations in great need of GWWs implementation where GWWs have not been adopted at the time of capturing aerial imagery, or alternatively (2) overestimated GWWs by CTI models, which could be eroding channels or low-lying drawn; (3) Locations where the imagery's time differs from that of prior or existing GWWs. (4) Locations where there should have been GWWs but do not. In general, the model with threshold of 600 have relatively better performance in occurrence evaluation.

Table 4.2.2 Summary of Occurrence Evaluation of CTI model

Threshold Value	False Positive Rate	False Negative Rate
500	0.898	0.0323
600	0.756	0.0323
700	0.736	0.0645
800	0.727	0.0645
900	0.691	0.0645
1000	0.689	0.0645
1100	0.638	0.0645

4.2.3 Length Evaluation

The statistics of length evaluation is summarized in Table 4.2.3. In terms of PBIAS, all the models obtain relatively low-magnitude values close to 0, revealing the little bias between estimated and observed lengths of GWWs. The models with threshold of 800 and 1100 have negative values in PBIAS, indicating the underestimation of GWWs' lengths. The positive PBIAS values from the models using 500, 600, 700, 900, 1000 as threshold values indicate the overprediction of the lengths of GWWs. As for the NSE value, the model with the threshold of 600 obtains the value closest to 1, indicating the best agreement between prediction and observation. Overall, the model with the threshold of 500, 600 and 700 have better performance in length evaluation.

Table 4.2.3. Summary of length evaluation of CTI model

Threshold Value	PBIAS	NSE
500	2.099	0.616
600	3.006	0.684
700	2.187	0.443
800	-1.854	0.388
900	2.184	0.442
1000	2.378	0.427
1100	-1.163	0.328

4.2.4 Visualization of CTI output

Based on the visual evaluation, occurrence evaluation and length evaluation, it is found that the CTI model with the threshold of 600 has overall better performance than others. The output map from CTI model with the threshold of 600 is presented in Figure 4.2.3.1. To better visualize the output result, the distribution of predicted GWWs density map is given in Figure 4.2.3.2, where each raster value indicates the length density (m km^{-2}) of GWWs in the neighborhood of the raster cell. The bandwidth of the density map is specified as the default value, which can guarantee the relative robustness to spatial outliers (Esri, 2016).

As Figure 4.2.3.2 illustrates, high-density areas of predicted GWWs are mainly situated in the northern and central part of the study area. Specifically, the areas along the upstream of Middle Thames River, Nissouri creek and Phelan Creek within the study area are predicted as potential areas for intensive GWWs implementation. The low-density areas for GWWs implementation are mostly

located in the southwestern part of the study area. It is noticeable that the predicted GWWs density has similar geographic distribution of existing GWWs which is illustrated in Figure 4.1.2.

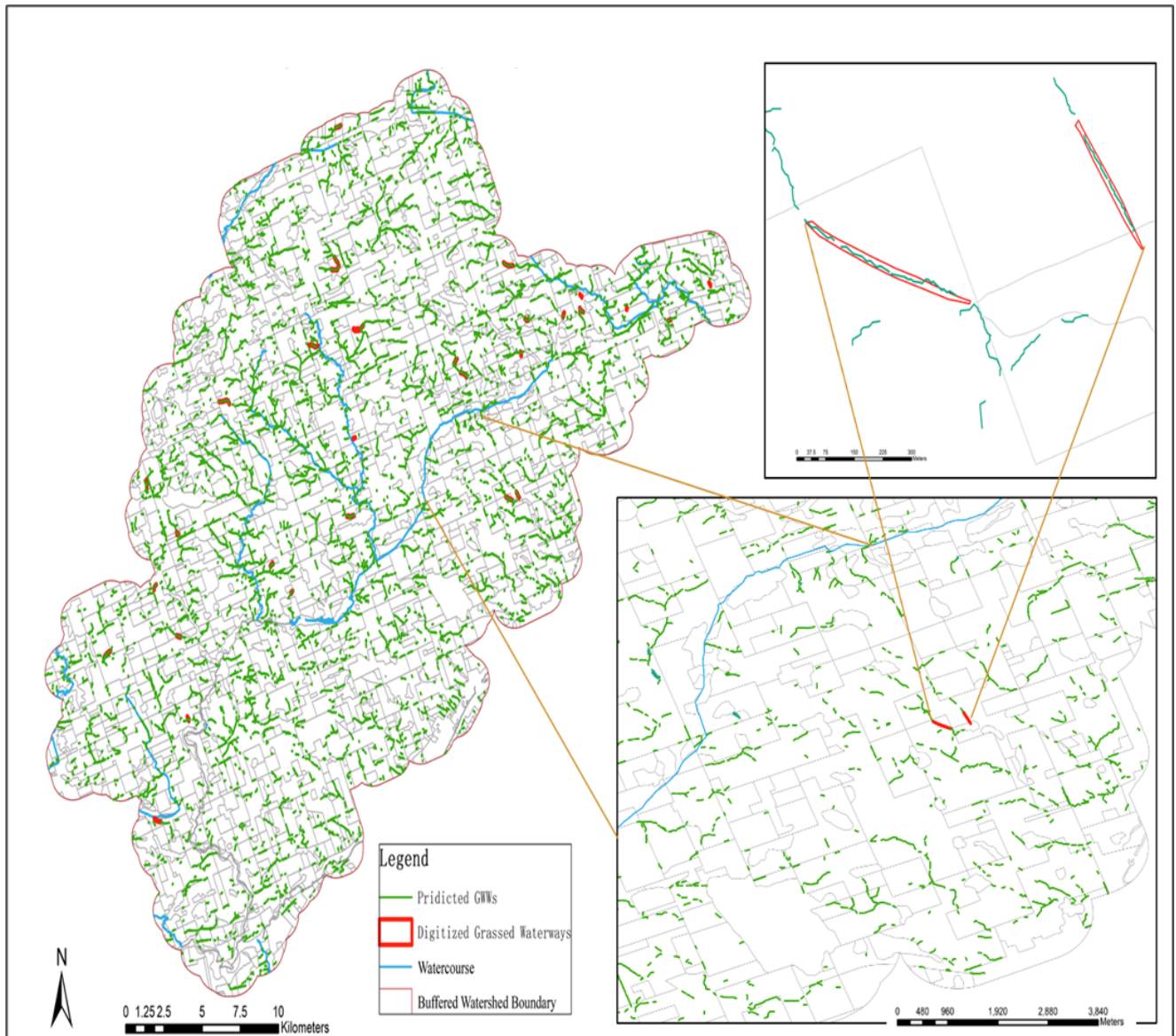


Figure 4 .2.3.1 The output map of predicted GWWs by CTI model (threshold = 600)

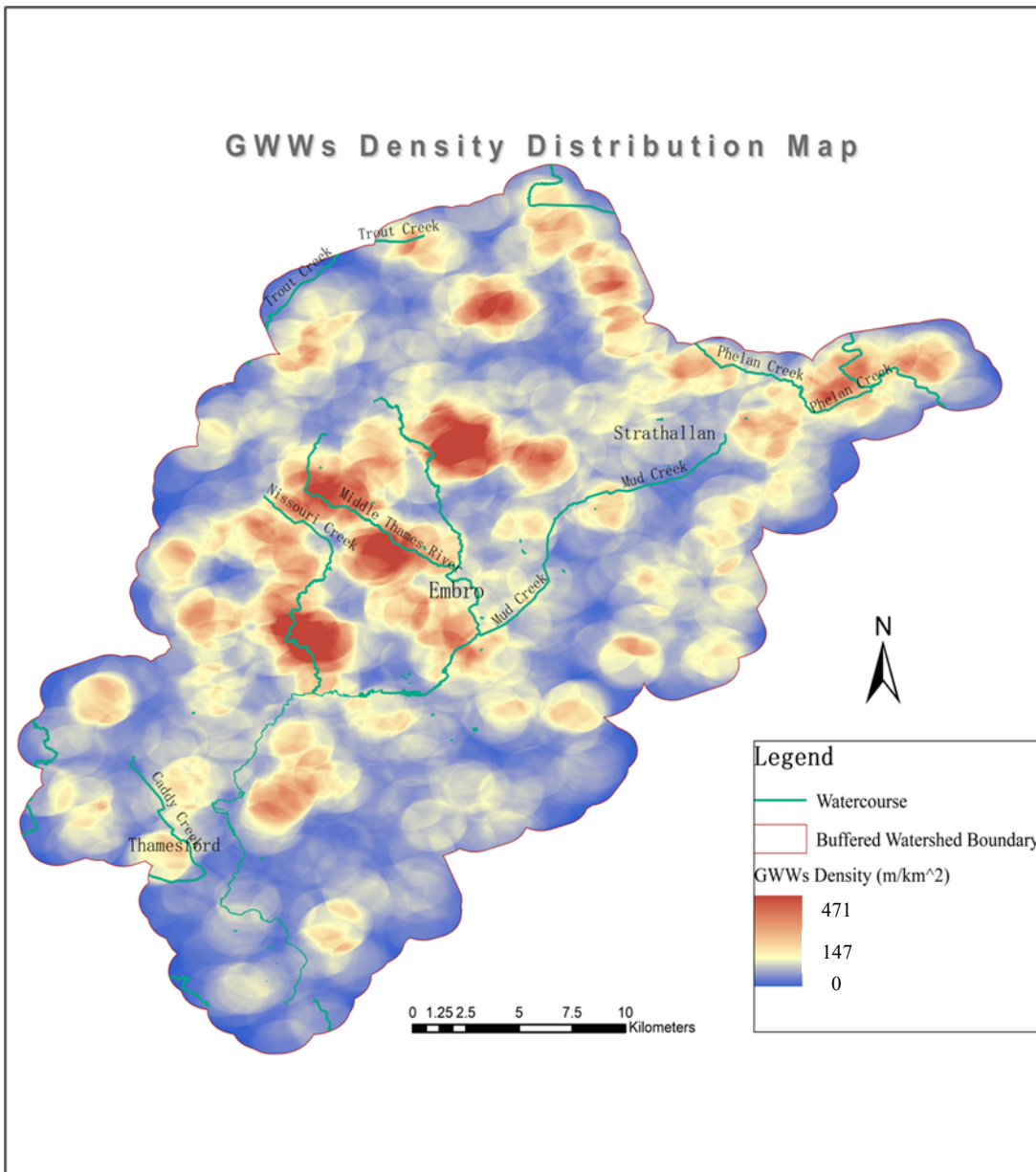


Figure 4.2.3.2 GWWs density distribution map by CTI model

4.3 SPI Threshold Model

For SPI threshold model, four threshold values suggested by ACPF (from 2 to 5 standard deviations greater than the average SPI values of the study area) have been tested and visually evaluated. There are no existing GWWs identified by SPI model with threshold from 2 to 5 standard deviation above the mean, indicating that these thresholds are not capable of predicting GWWs correctly. The model with the threshold of one standard deviation is not able to identify the existing GWWs as well, which

can only identify several open drainage lines with significant discontinuities. During the iterated decrement of the threshold values, it showed that the models can predict increasing number of locations of existing GWWs gradually until 23 GWWs with 0.01 standard deviation above the mean. For the models with the threshold from 0.05 to 0.09 standard deviation, there exist numerous absences of predicted GWWs at the locations of existing GWWs, with considerably significant discontinuities along the trajectories of existing GWWs. Figure 4.3.1 presents an identified GWWs with SPI threshold model with comparison of output from CTI model. It is found that there exist lots of missing parts in the output SPI model along the trajectory of existing GWWs. Figure 4.3.2 presented the output map of SPI model with 0.01 standard deviation. Figure 4.3.3 presented the GWWs density distribution map by SPI model with 0.01 standard deviation.



Figure 4.3.1 the comparison between SPI model output and CTI model output.

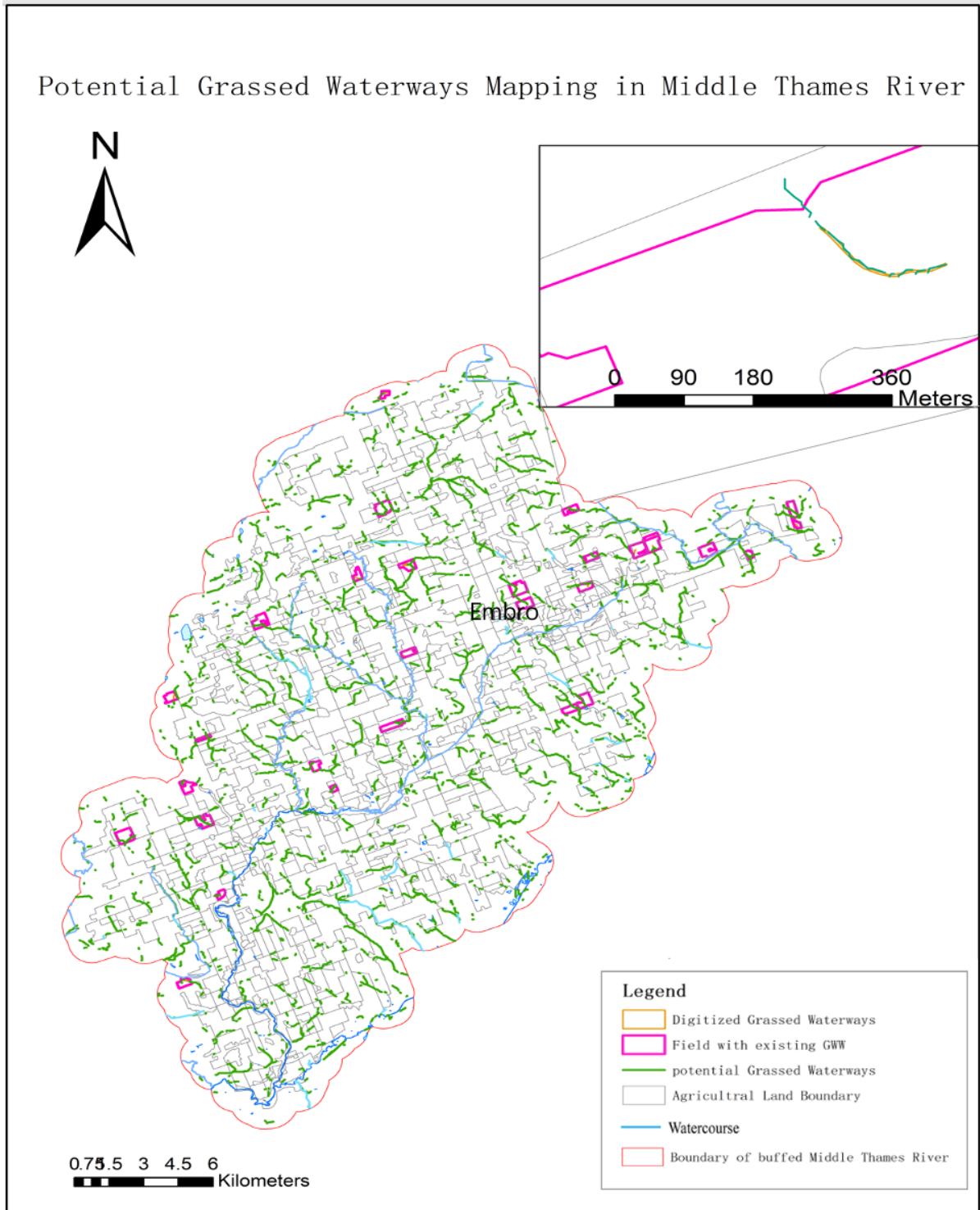


Figure 4.3.2 output map of SPI model with 0.01 standard deviation

GWWs Density Distribution Map by SPI model

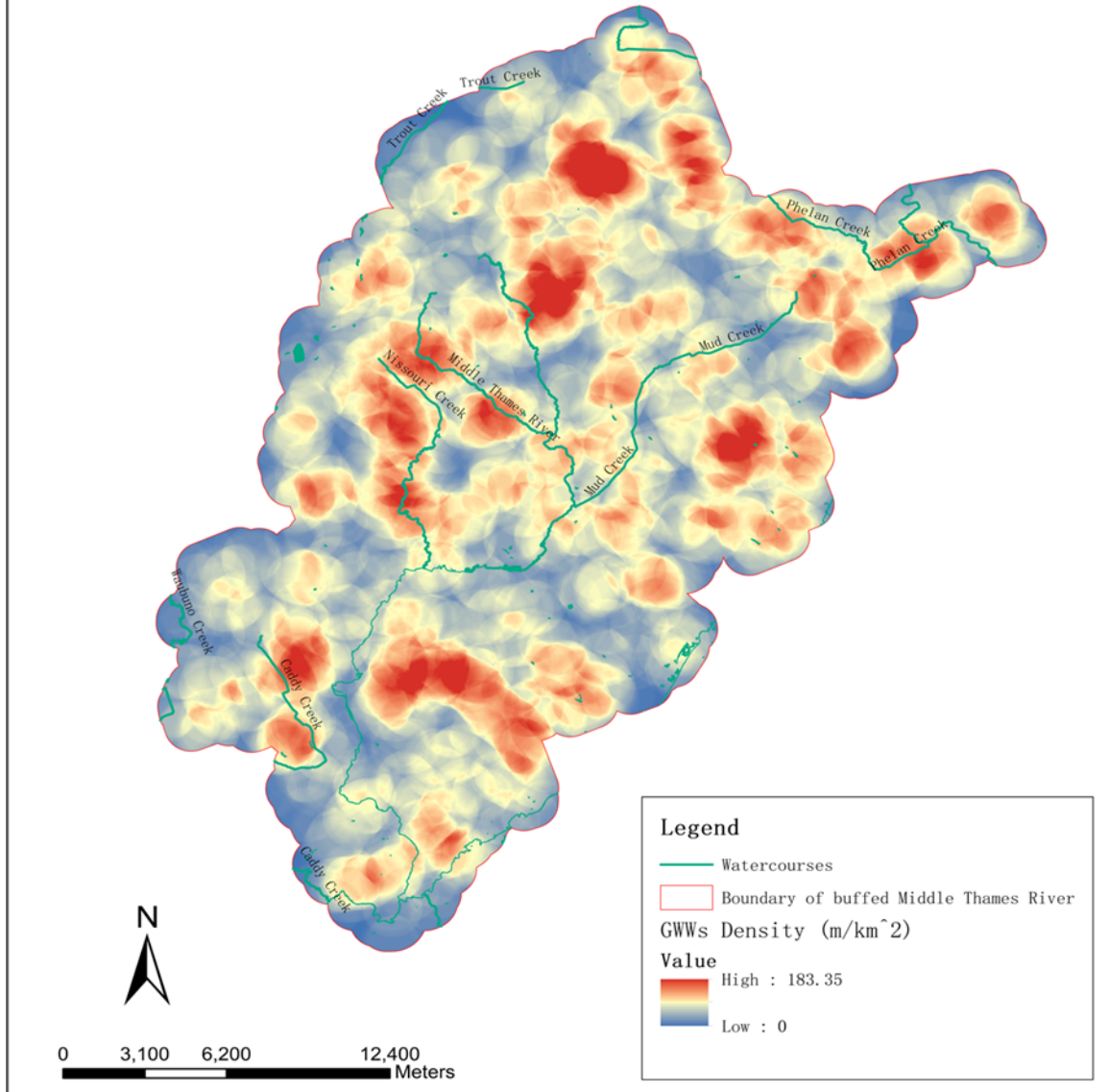


Figure 4.3.3 GWWs density distribution map by SPI model

As Figure 4.3.3 presents, the distribution of GWWs density predicted by SPI threshold model is roughly similar to that of CTI model in figure 4.2.3.2. The maximum GWWs density is around 183.35 meter per square kilometer, which is much less than that of CTI model. The high-density areas are mainly located along the watercourses in the northern part of the Middle Thames River watershed.

There exist high-density areas in the southwestern part of the study area, which is different from the density distribution by SPI model.

The occurrence evaluation is summarized in Table 3.4. There are 23 GWWs identified by SPI threshold model. The absent values for the observations referred to the number of predicted GWWs by SPI model which were not identified during the digitization process (which have not been implemented). The false negative rate is 0.258065, which is much higher than that of CTI model. The Kappa statistics of SPI model is 0.2574, indicating the moderately agreement between prediction and observation. As for the length evaluation, the PBIAS and NSE of SPI model area -0.128 and -1.08 respectively, revealing the underestimation of the lengths and poor agreement between predicted lengths and observed lengths, owing to numerous absences of predicted GWWs at the locations of existing GWWs and significant discontinuities along the trajectories of existing GWWs.

Table 4.3 The error matrix of SPI model

		observation		total
		Present	Absent	
prediction	Present	23	26	49
	Absent	8		
total		31		
False positive rate		0.530612		
False negative rate		0.258065		

4.4 MCDA

4.4.1 Thematic layers of criteria

The thematic layers of MCDA are presented in figure 4.4, which displays the distribution of 12 criteria in the Middle Thames River Watershed respectively. As map (a) illustrates, the soil erodibility of the study area ranged from 0 to 0.063, with the highest value in northwestern of the watershed where there may contain rocky structures. The minimum values of soil erodibility are mainly distributed in the southeastern part of the study area, which is around the outlet of Mud Creek. There exist areas with lowest soil erodibility in the northernmost part of the watershed, which is possibly the outlet of North Woodstock watershed. The topographic layer in map (i) displays that the slope of the watershed varied from 0.09% to 1.26%, with relatively steep slope along the Middle Thames River and Nissouri Creek. The overall slope of the northwestern part is steeper than others. Map (b)

displays the distribution of the LS factor value, which is similar to that of slope layer. The high LS values are mainly distributed in the northern part especially the northeastern part of the study area. The crop type layer shows that the corn systems and continuous row crops dominate the crop type by more than 85% of the watershed area. In terms of terrain attribute layers, the profile curvature and plan curvature layers distinguish the road ditches, valleys, and concave surface of the study area. The SPI layer, TWI layer and stream density layer display geographic distribution patterns respectively which are closely associated with drainage pattern and erosive power of the surface.

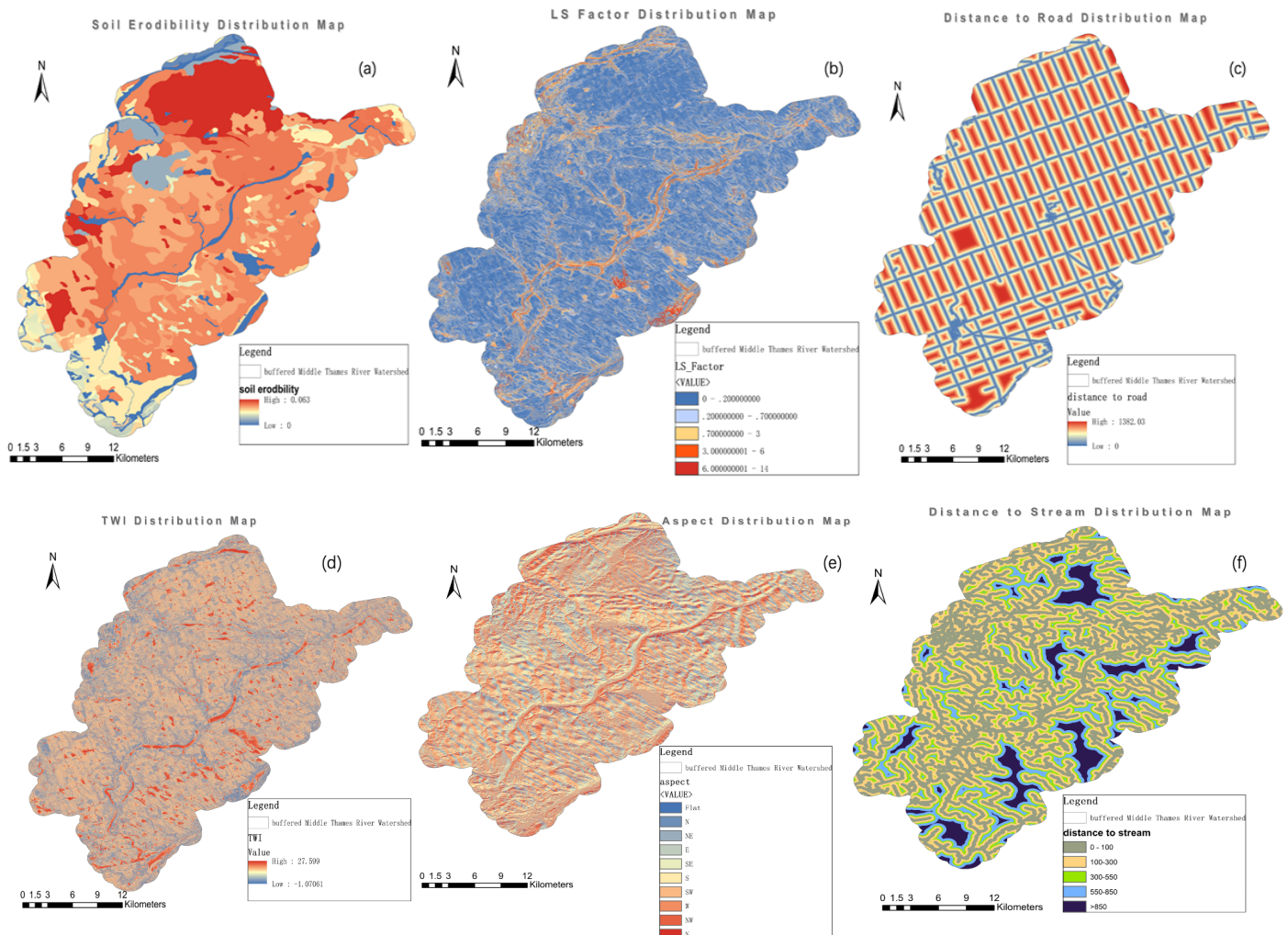


Figure 4.4 Part 1. Criteria Distribution Map of MCA.

- (a) Soil Erodibility Map (b) LS Map (c) Distance to Road Map
- (d) TWI Map (e) Aspect Map (f) Distance to Stream Map

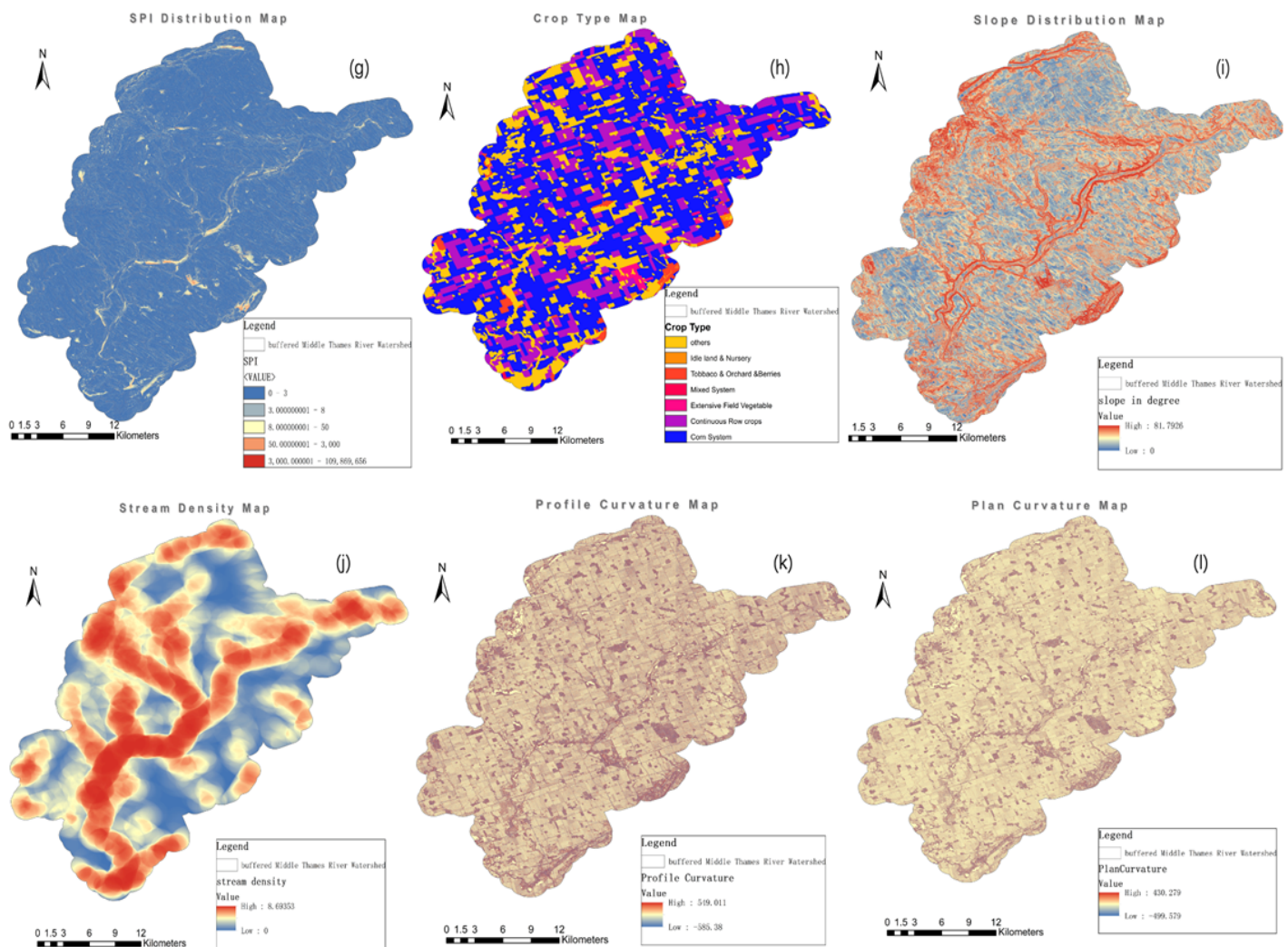


Figure 4.4 Part 2. Criteria Distribution Map of MCA.

(g) SPI MAP (h) Crop Type Map (i) Slope Map

(j) Stream Density Map (k) Profile Curvature Map (l) Plan Curvature Map

4.4.2 Weighted Linear Combination

The propriety map of WLC is presented in figure 4.4.2 below. Figure 4.4.2 illustrates the distribution of priority for GWWs implementation in the Middle Thames River watershed, with priority scores ranging from 0 to 4.56. The priority scores in watershed are devided into 5 classess: least priority zone, low priority zone, median priority zone, high priority zone and most priority zone. There also exist constraint areas where the implementation of GWWs is impossible. The boundaries of these

priority level division are located at value of $0.405 (\mu_0 - 1.5m\sigma_0)$, $1.357(\mu_0 - 0.5m\sigma_0)$, $2.309(\mu_0 + 0.5m\sigma_0)$ and $3.261(\mu_0 + 1.5m\sigma_0)$, where μ_0 is observed mean value of scores; σ_0 is the standard deviation and m is set to 0.8. The rationale of priority division and the selection of m are validated in Section 4.4.4. Maximum area of priority level is devoted to low priority category taking up 39.6% and 2.3% of the area have the most priority of GWWs implementation. The high and median priority categories of priority cover 15.3% and 29.6% respectively, while the least priority area accounts for 13.2% of the studied watershed. As figure 4.4.2 displays, the areas with the highest priority are located in northwestern part and northeastern part of the watershed, especially along the upstream of Phelan Creek and Nissori Creek. It is found that these upstream areas have relatively steeper slope gradient than other areas in the studied watershed, with dominant soil type of sandy loam and silty loam. In macroscopical sight, the priority map of GWWs implementation from WLC has the similar geographic distribution of GWWs density map from CTI model and SPI model, where the areas in the northwestern part along the Nissori Creek and upstream of Mud creek are in highly demand of GWWs implementation.

Several highest priority areas are retrieved from the priority map of WLC through post-processing techniques, including raster calculation using operator “Condition” and “raster to polygon” in ArcGIS (Esri, 2016). Three priority areas with pixels comprising highest average priority scores are presented in Figure 4.4.2. These three priority areas are located in large farmlands, two of which belong to mixed system. In terms of geographic distribution, they are clustered at central part of the studied watershed, closely along the watercourses. There are totally 26 priority areas retrieved from the priority map, covering the area from 0.35ha to 1.89ha. These priority areas are primarily located in large crop fields covering an area more than 990 acres. The predominate crop type of these priority areas are mixed system and corn system.

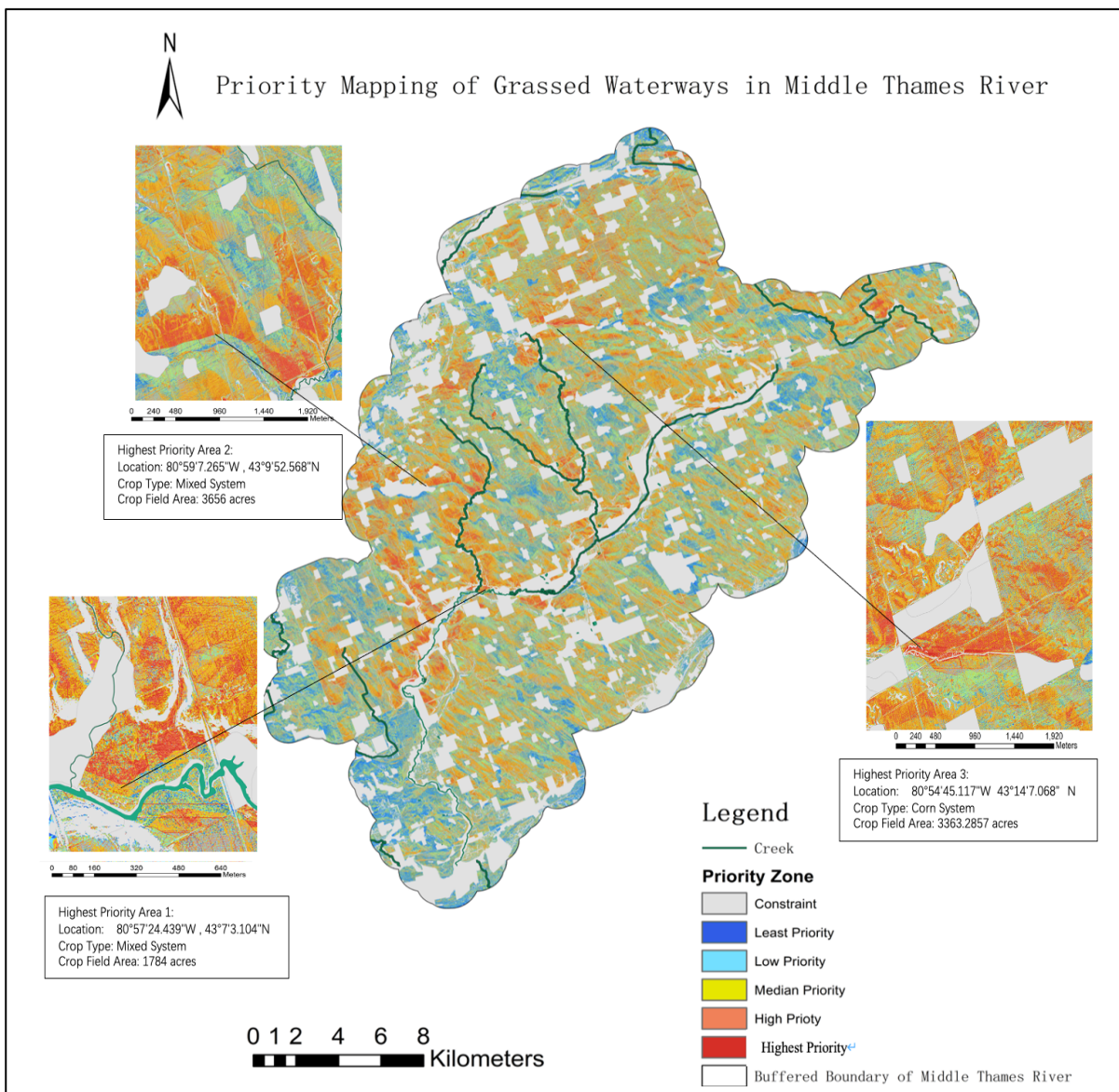


Figure 4.4.2 the priority map of GWWs by WLC

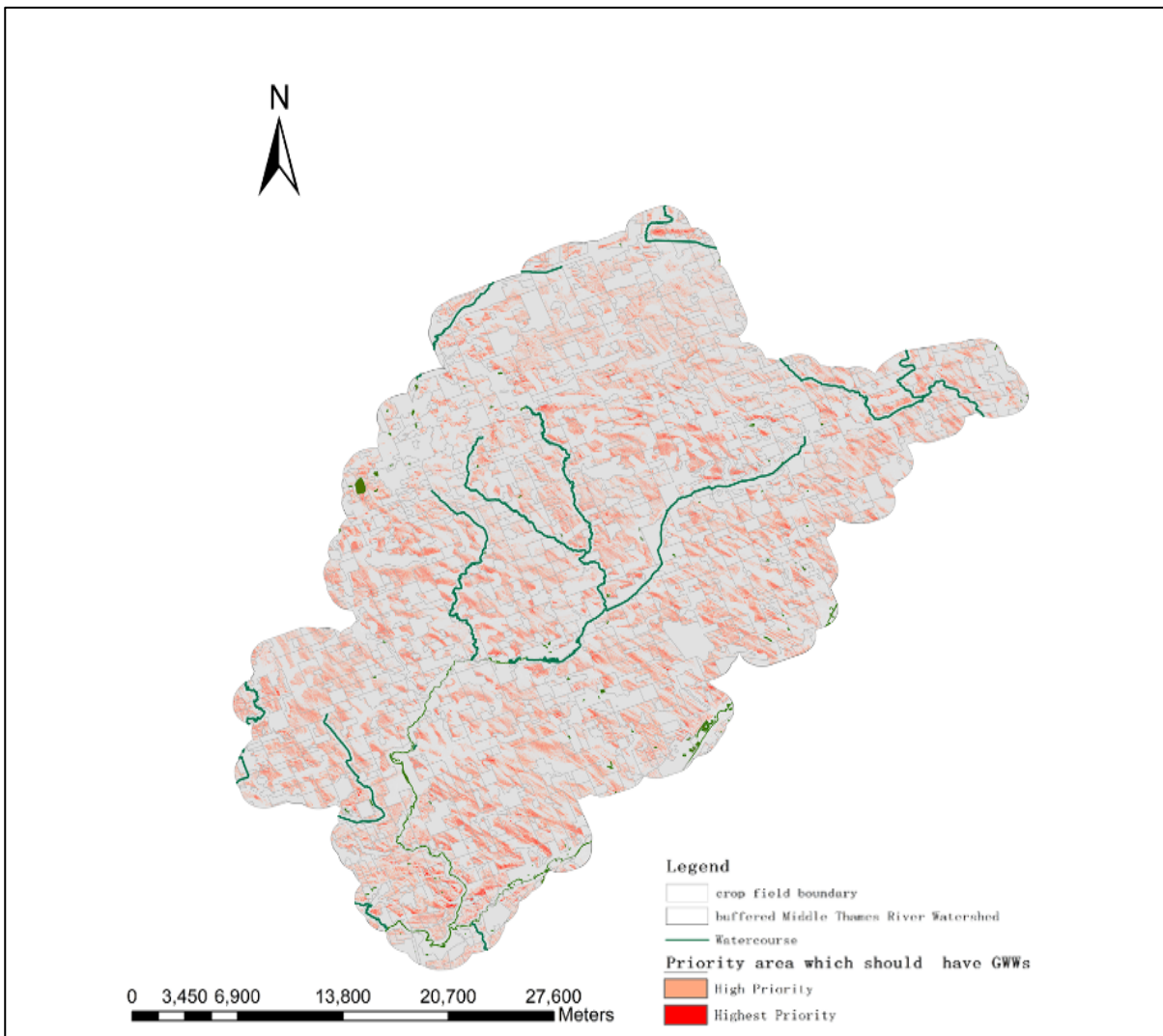


Figure 4.4.2.2 priority area which should have GWWs from WLC

4.4.3 Fuzzy Logic Analysis

The propriety map by FLA is presented in Figure 4.4.3 below. Figure 4.4.3 illustrates the distribution of priority for GWWs implementation in the Middle Thames River watershed, with priority scores ranging from 0 to 0.4835. The priority scores in watershed are divided into 5 classes: least priority zone, low priority zone, median priority zone, high priority zone and most priority zone. There also exist constraint areas where the implementation of GWWs is impossible. The boundaries of these priority level division are located at value of 0.000768, 0.01137, 0.2267, 0.3396 and 0.4835.

Maximum area of priority level is devoted to median priority category accounting for 30.24%, and 1.27% of the area have the most priority of GWWs implementation. The high and low priority

categories of priority cover 30.24% and 17.15% respectively, while the least priority area accounts for 21.04% of the studied watershed. As Figure 4.4.2 displays, the areas with the most priority are located in north central part and northwestern part of the watershed. Although there exist highest priority areas along the watercourses, it displays less agreement with drainage pattern compared with the map from WLO. The spatial tendency of each priority categories cannot be visualized directly. It is noticeable that there exist more areas with lowest priority in the northern part of the watershed, which is possibly owing to the fuzzy Gamma overlay.

Several highest priority areas are retrieved from the priority map of FLA through post-processing techniques, including raster calculation using operator “Condition” and “raster to polygon” in ArcGIS (Esri, 2016). Three priority areas with pixels comprising highest average priority scores are presented in Figure 4.4.3. These three priority areas are located in median and large farmlands, which are relatively smaller than that of WLC. The central locations of these three priority areas are (81°3'50.285"W 43°6'2.429"N), (80°52'28.855"W 43°13'36.647"N) and (80°48'48.726"W 43°13'32.964"N), which are relatively dispersed. There are totally 18 highest priority areas retrieved from the priority map, covering the area from 0.25ha to 1.49ha. These priority areas are primarily located in median to large crop fields covering an area more than 590 acres. The predominate crop type of these priority areas is corn system followed by mixed system.

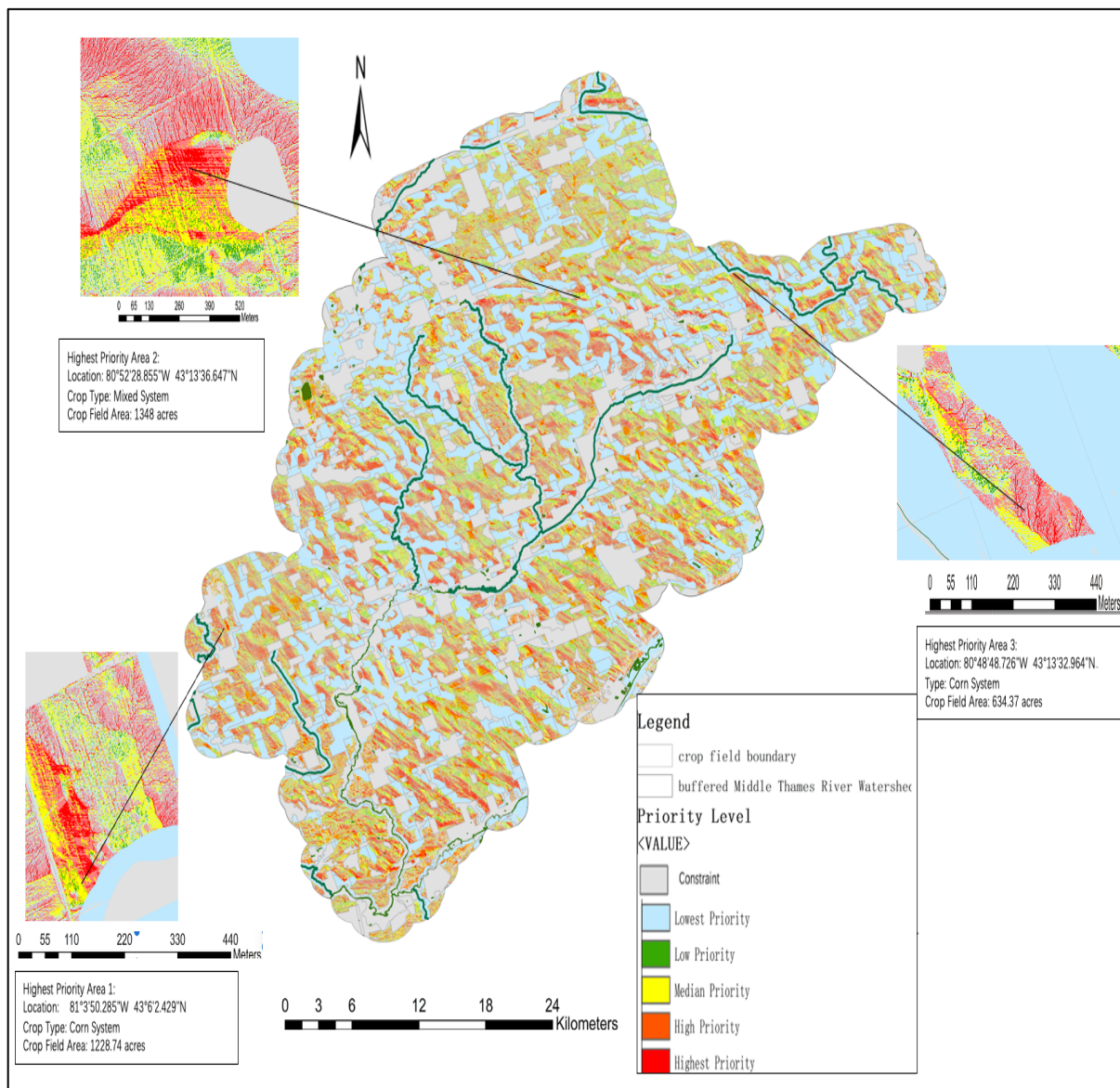


Figure 4.4.3 the priority map of GWWs implementation by fuzzy logic analysis

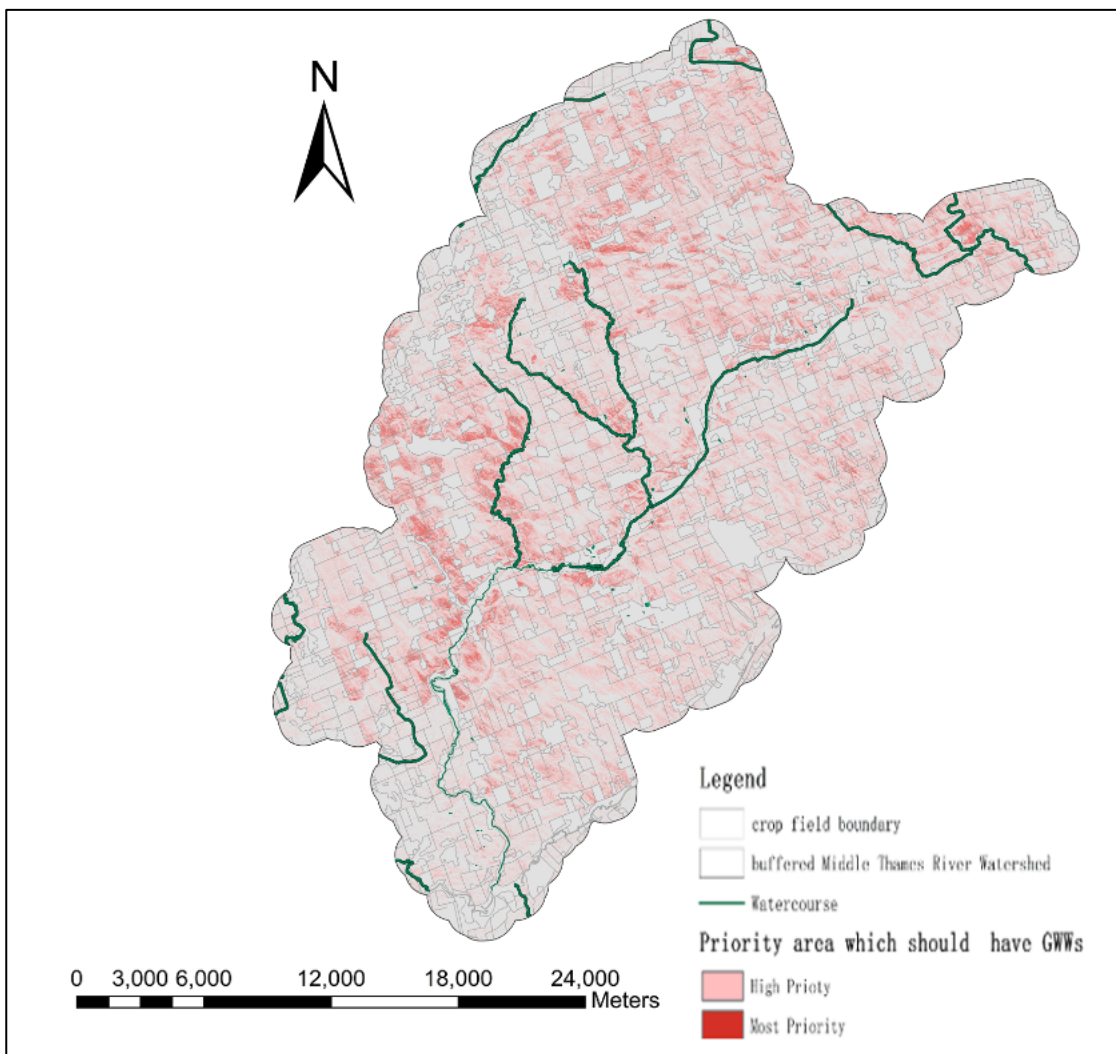


Figure 4.4.3.2 priority area which should have GWWs from FLA

4.4.4 Validation

The performance of priority maps from WLC and FLA and their priority division were validated based on the criteria that greater percentage of GWWs implementation must occur in the higher priority zones (Kanungo et al., 2009). The validation statistics of WLC priority map and FLA priority map were summarized in Table 4.4.3.1. and Table 4.4.3.2 respectively.

Table 4.4.3.1 Validation of WLC priority map

Priority level	I. Percent Watershed	II. Percent GWWs	III. Percent GWWs per Field Area	IV. GWWs per level (%) km ² / km ²	V. GWWs in watershed	VI. GWWs in GWWs
	Area per level (%) km ² / km ²	Field Area per level (%)	km ² / km ²	density (km ² / km ²)	Field density (km ² / km ²)	density (km ² / km ²)
Least Priority	13.2%	7.55%	2.6%	0.572	0.344	0.196
Low Priority	15.3%	10.89%	6.7%	0.711	0.615	0.438
Median Priority	39.6%	34.06%	30.5%	0.860	0.895	0.770
High Priority	29.6%	37.70%	46.6%	1.274	0.615	1.574
Most Priority	2.3%	9.80%	13.6%	4.261	0.344	5.913

It can be observed from Table 4.4.3.1 that 2.3 % of the studied watershed is occupied by most priority zone, while 13.2%, 15.3%, 39.6% and 29.6% areas are occupied by least priority, low priority, median priority, and high priority zones respectively. The distribution of digitized GWWs in different priority zones and crop fields with existing GWWs in different zones are compared respectively. It is found that 13.6% of occupied area of existing GWWs is predicted over most priority zones, while 37.7%, 34.06%, 10.89% and 7.55% of GWWs area are predicted as high priority, median priority, low priority and least priority zones respectively. These statistics displays that 47.5% area of most priority and high priority zones can predict 60.2% GWWs area, indicating that the distribution of GWWs over studied watershed tends to the higher priority zones. In addition, Table 4.4.3.1 displays that the GWWs density in most priority zone is higher than those of lower priority zones, which indicates the relatively good performance of priority map and priority division. Similarly, it can be obtained from the Table 4.4.3.1 that the distribution of cropping fields with existing GWWs over priority zones is skewed to the higher priority zones. Within each cropping fields with existing GWWs, the GWWs density over most priority zone is relatively higher than those of lower priority zones.

Table 4.4.3.2 Validation of FLA priority map

Priority level	I. Percent Watershed	II. Percent GWWs	III. Percent GWWs per area per level (%) km ² / km ²	IV. GWWs Field in watershed	V. GWWs in GWWs	VI. GWWs in watershed
Least Priority	21.04%	5.26%	0.57%	0.0269	0.108	0.0269
Low Priority	17.15%	6.50%	9.55%	0.557	1.470	0.557
Median Priority	30.30%	13.94%	35.1%	1.158	2.517	1.158
High Priority	30.24%	14.52%	39.63%	1.308	2.730	1.308
Most Priority	1.27%	0.622%	1.728%	1.361	2.778	1.361

As for the priority map from FLA, it can be observed from Table 4.4.3.1 that 1.27 % of the studied watershed is occupied by most priority zone, while 21.04%, 17.15%, 30.30% and 30.24% areas are occupied by least priority, low priority, median priority, and high priority zones respectively. The distribution of digitized GWWs in different priority zones and crop fields with existing GWWs in different zones are compared respectively. It is found that 1.728% of occupied area of existing GWWs is predicted over most priority zones, while 39.63%, 35.1%, 9.55% and 0.57% of GWWs area are predicted as high priority, median priority, low priority and least priority zones respectively. These statistics displays that 31.51% area of most priority and high priority zones can predict 41.358% GWWs area, indicating that the distribution of GWWs over studied watershed tends to the higher priority zones. In addition, Table 4.4.3.2 displays that the GWWs density in most priority zone is higher than those of lower priority zones, which indicates the relatively good performance of priority map and priority division. Similarly, it can be obtained from the Table 4.4.3.2 that the distribution of cropping fields with existing GWWs over priority zones is skewed to the higher priority zones. Within each cropping fields with existing GWWs, the GWWs density over most priority zone is relatively higher than those of lower priority zones.

4.4.5 Sensitivity Analysis

Within the range from -20% to +20% of the baseline weight value, a total of 240 simulation runs of sensitivity analysis were conducted on 6 selected criteria to analyze the sensitivity of the criteria and stability of the WLC model created in the present study. For each selected criteria, the number of cells falling into each priority zones during each simulation run are summarized and plotted, as Figure 4.4.4 illustrates.

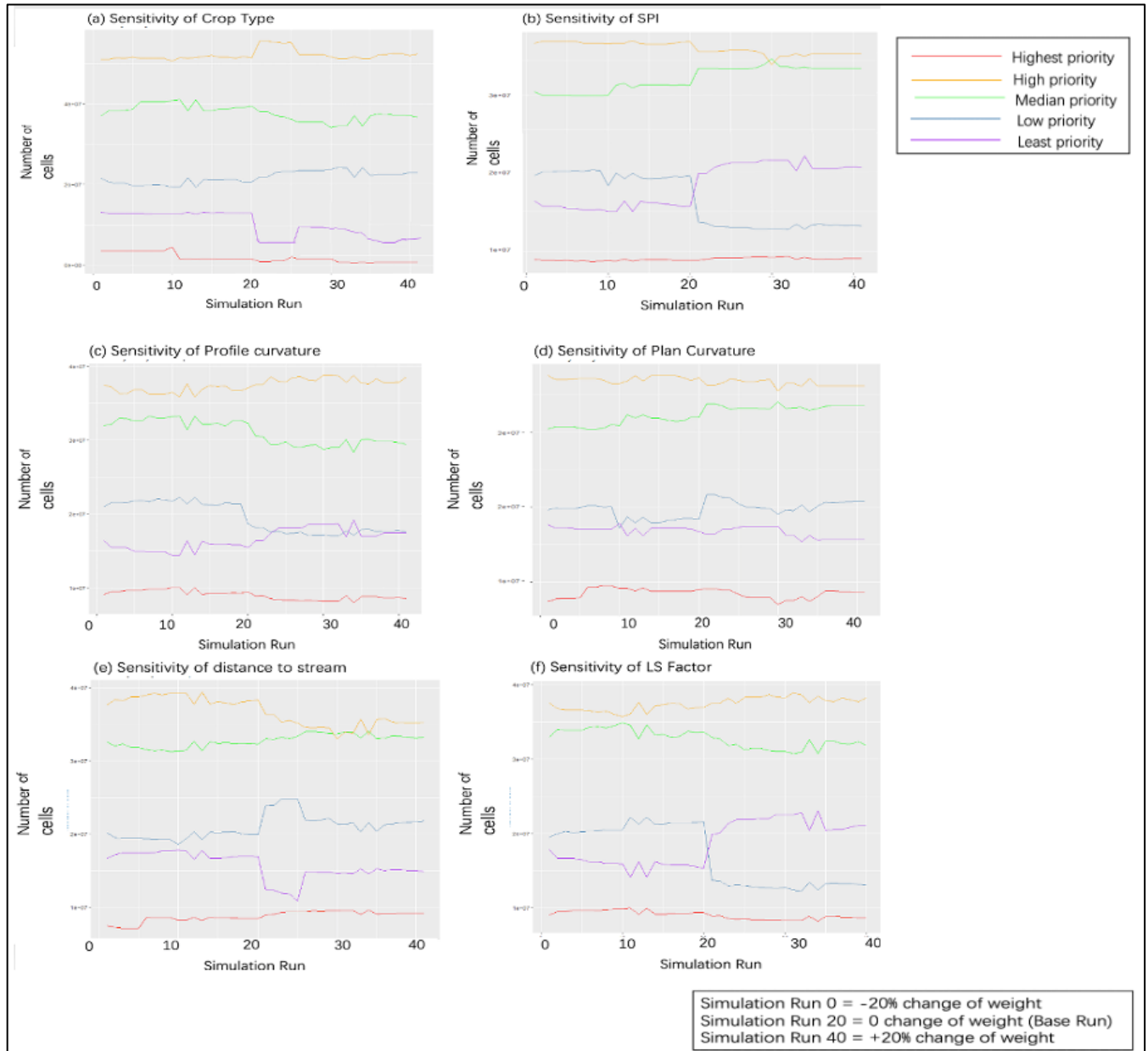


Figure 4.4.4 sensitivity analysis plots of selected criteria

In Figure 4.4.4, the count of cells in different priority levels is denoted by different colors, with x-axis representing the order of simulation runs and y-axis indicating the number of cells. It can be observed from plot c and plot (f) that SPI and LS factor belong to most sensitive criteria which can result in significant changes in priority category distribution when their weights are increased by more than 10%. These criteria also have the highest weight coefficients in WLC. Compared to other categories of priority level, the level of most priority denoted by red line is relatively stable, with slight variations in the number of cells, which remains the overall ranking. The stability of the most priority category indicates the relative independency of most of cells over most priority zone in weight adjustment of selected criteria. It is noticeable that the alteration of the weights of plan curvature and crop type have relatively weak impacts on the number of cells in median priority, low priority, and highest priority category, indicating their slight significance in WLC model. The most significant variations of priority level ranking happen in high priority category and least priority category, which are most sensitive to criteria weight alterations. There is a remarkable decrease of the number of cells in high priority category and significant increase in low priority category, with the increment in weights of LS and SPI. Overall, it can be observed from Figure 4.4.4 that the degree of sensitivity of each criterion is relatively consistent with their weights in WLC. The stability of the most priority category reveals the relative stability and reliability of the result from WLC.

4.5 Summary of Chapter

This chapter summarizes the results of digitization of GWWs, CTI model, SPI model and MCDA for GWWs implementation. 30 existing GWWs in the studied watershed have been identified and digitized, working as the ground truth data for threshold finding in topographic model and evaluation of outputs from CTI model, SPI model and MCDA. The CTI model with the threshold value of 600 has identified 29 existing GWWs, with good performance in predicting trajectory and length of GWWs. The close observation of the CTI output map can support the potential placement of GWWs in specific cropland. The predicted GWWs density distribution map by CTI model displays high density of potential GWWs situated in the northern and central part of the study area, which can provide general information and suggestion for decision makers of GWWs in watershed scale. The SPI threshold model has identified 23 existing GWWs with the threshold of 0.01 standard deviation, which has worse performance in occurrence prediction and length prediction of GWWs than that of CTI model. The output of SPI model displays several absences of predicted GWWs at the locations of existing GWWs and significant discontinuities along the trajectories of digitized GWWs. The

geographic distribution in GWWs density map by SPI threshold model is roughly similar to that of CTI model, revealing the high-density areas mainly located along the watercourses in the northern part of the Middle Thames River watershed. For the output from MCDA, 2 priority maps for GWWs implementation by WLC and FLA have been created respectively, both of which display the northern part of the watershed are occupied by higher priority zones. The priority levels in watershed are divided into 5 classes: least priority zone, low priority zone, median priority zone, high priority zone and most priority zone. The performance of two priority maps have been validated, which shows that the GWWs density in most priority zone is higher than those of lower priority zones. The sensitivity analysis has been conducted on WLC with 6 selected criteria. It shows that the degree of sensitivity of each criterion is relatively consistent with their weights in WLC. The stability of the most priority category reveals the relative stability and reliability of the result from WLC.

Chapter 5 Discussion

5.1 Threshold Finding

In this study, 5 critical CTI threshold (12, 30, 62, 75,100) reported as most appropriate thresholds in the literature (Daggupati et al., 2013; Parker et al., 2007; Thorne et al., 1986; Thorne and Zevenbergen, 1990) were tested in the CTI model, which all display poor performance in visual evaluation. The suitable CTI threshold value selected in this study is 600, which is much higher than those of previous studies. This difference in threshold values is likely owing to the impacts of soil type and lands use on forming ephemeral gully erosion, which are not considered in the CTI model. The main soil texture in the study area is silt loam combined with sandy loam, which is relatively different from those in existing studies including Clarion loam, Webster clay loam (Gali et al., 2015), Loring silt loam and Memphis silt loam (Parker et al., 2007). These soil types are relatively finer and better drained than those of studied watershed, which also have higher soil erodibility than those in the study area (Van et al., 2000). The land cover in the present study is mainly corn system and continuous row crops, while the primary land cover in study sites of previous studies is soybeans and mixed crop system. Apart from the soil type and land use, recent research highlighted that conservation practices, land management, meteorological conditions even piping system can influence the threshold values for different study sites (Piccarreta, & Capolongo, 2006; Parker et al., 2007). It is pointed out that these factors can influence the likelihood of ephemeral gully erosion and be unique to specific study sites. There are few theoretical bases for extracting suitable CTI threshold in different site conditions. Parker et al. (2007) provided a starting point for summarizing the threshold values selected in different site conditions. Further work on developing the databases of critical threshold values of CTI model with different site conditions are expected.

For the SPI model, four threshold values suggested by ACPF (from 2 to 5 standard deviations greater than the average SPI values of the study area) have been tested in this study. There is no existing GWWs identified by these thresholds. The value of 0.01 standard deviation was selected as suitable threshold in this study, which is much smaller than the thresholds suggested. This is possibly due to the localized nature of the threshold in SPI model. This model was originally developed by the USDA in ACPF to predict candidate locations for GWWs within the fields at the sub-watershed scale of 10000 to 40000 acres in the U.S. (Porter, 2018). There exist few studies to explore the applicability

and effectiveness of this model applied in other study sites outside the U.S. The SPI values throughout the Middle Thames River watershed have considerable variations which results in extremely large standard deviation value. This large value successively results in the relatively large value of critical value for identifying GWWs, thus some existing GWWs with moderate SPI value are omitted.

5.2 GWWs predicted by CTI and SPI model

The close observation of predicted GWWs in CTI and SPI model reveals that there exist significant discontinuities along the trajectory of digitized GWWs. Similar discontinuities are found among the raster cells with negative value in the plan curvature layer. The discontinuity in the output of CTI model is probably due to the involvement of plan curvature in the model, which can exclude raster cells with reduced flow convergence or flat areas in the GWWs (Parker et al., 2007; Daggupati et al., 2013). Several lower lawns and roadside ditches are predicted as GWWs, owing to the inclusion of plan curvature in the CTI model. There are 2 existing GWWs which were not predicted by CTI model. These GWWs are in the downstream area with relatively flat slope, which possibly causes they could not be predicted. The lower upslope drainage areas around these GWWs result in low CTI values of the pixels in these GWWs location. The flat slope leads to relatively small values in plan curvature of the cells in these GWWs location. Therefore, the CTI values of the cells in these areas are possibly lower than the critical threshold, and these GWWs can not be identified by CTI model. Further work of combining soil properties with CTI model to determine the areas for GWWs implementation is expected to improve the performance of identifying GWWs, which can overcome the strong dependency of topographic conditions. The GWWs density distribution map of CTI and SPI models have similar patterns in high density areas for GWWs, since both methods are significantly impacted by the slope gradient and drainage area. Both maps display several high-density areas in the northern part and central part of the study area, especially along the watercourses in the northern part of the Middle Thames River and Noussouri River. Closer observations of these high-density areas over the ariel image reveals that there is denser drainage network compared with other areas.

5.3 Relationship with RUSLE

The Revised Universal Soil Loss Equation (RUSLE) is considered as a comparatively robust empirical method to estimate the soil loss rates from the eroded area. Numerous studies have applied the RUSLE to identify areas prone to soil erosion (e.g., Efthimiou et al., 2016; Gayen et al., 2020). However, this model can not be employed to estimate soil loss rate from ephemeral gully erosion and assess areas' susceptibility to ephemeral erosion. The RUSLE was initially developed based on immense data from study sites (Bernard et al., 2010). There were no research plots which were big enough to experience ephemeral gully erosion, which can only predict rill and sheet erosion. Ephemeral gully erosion is mainly evolved by repeated incision process, which is less impacted by 'head-cut migration and erosion of gully walls' (Nachtergaele et al., 2002). Rill erosion is characterized as erosion in many small channels spreading along the slope, which has a different way of contributing to the drainage pattern from ephemeral gully erosion (Nachtergaele, 2002). Furthermore, the distribution of rill erosion is restrained by field boundaries, while ephemeral gully erosion usually crosses several fields. This difference indicates that rill erosion and ephemeral gully erosion have different impacts on soil transport: rill erosion usually moves soil within a single field, whereas ephemeral gully can redistribute soil particles across numerous farmlands in the watershed. Therefore, there exist no similar simple methods of estimating soil loss from ephemeral gully erosion (Bernard et al., 2010).

Although this simple empirical method can not be applied directly in predict ephemeral gully erosion, the factors comprised in RUSLE can play a significant role in studies of ephemeral gully erosion especially the presented study. There are five factors in RUSLE: R (rainfall erosivity factor), K (soil erodibility factor), LS (slope length and steepness factor), C (cover and management factor) and P (erosion control and practice factor) (Rowlands, 2019), which have different impacts on erosion process. It was concluded that the majority of existing modelling methods is dependent on "process-based representations" (Bernar et al., 2010). The processes of ephemeral gully erosion are founded to be affected by the same factors influencing the process of rill and sheet erosion, such as drainage network, drainage area and concentrated flow (Bernar et al. 2010). Therefore, the RUSLE provides the scientific basis for ephemeral gully erosion modelling.

5.4 MCDA

In this study, 12 factors were selected as criteria in MCDA, based on previous studies (Domazetović et al., 2019; Mohsen et al., 2017; Majumdar et al., 2021), data accessibility, and hydrological and geological knowledge. These criteria have different degrees of influence on the susceptibility of ephemeral gully erosion and suitability of GWWs construction. However, it is observed from Figure 4.4 that several thematic layers have similar geographic distribution throughout the study area, such as slope and stream density. There exist relative association among these topographic criteria; for example, the areas with steeper slope and more runoffs may have higher stream density, thus experiencing more erosion. Although there is no linear relationship established among these criteria, the association between these factors on topographic and hydrologic aspects is likely to generate the distribution of priority more similar to those of criteria. The influence of other criteria on the output map may be comparatively diminished. It remains unreasonable to conclude that the association among criteria in MCDA can have a negative influence on MCDA results, since there exist few studies to evaluate the influence of association among criteria on the performance of MCDA. Moreover, the performance of priority maps in this study have been validated. Additional research on the association among criteria in MCDA is suggested.

In the process of WLC, the SMARTER method was employed to assign weights to each criterion. The ‘proxy’ weights standing for an approximation of the ‘real’ weights not only reflect the relative importance of each criterion with separation, but also keep priority ranking of raster cells separate well in the output. Compared with the sets of coefficients for each criterion in previous ephemeral gully erosion susceptibility models, including frequency ratio, index of entropy and linear regression model (Zabihi et al., 2017; Conforti et al., 2010; Pournader et al., 2018), there is an approximate match of proportional relation between the SMARTER weights and coefficients in previous studies. The weights for highest ranked criteria in SMARTER method are relatively smaller than those in previous studies, which is likely due to the ‘smooth’ effect of ‘proxy’ weights on the ‘true’ weights with extreme values (Ambrasaitė et al., 2011). These effects may decrease the influence of highest ranked criteria on the priority scores. However, it is argued that the ‘smooth effect’ does not necessarily result in inaccuracy in the output, since the weight coefficients unique in previous studies may be unapplicable for this study site, which can not be referred as exact ‘true’ weights (Ambrasaitė et al., 2011). Overall, the SMARTER method is an easier way for decision makers to determine

weights; especially, it may generate more precise weights than that determined by decision makers who have more confidence in determining the ranking of the importance of each criterion than determining the raw weights (Barron and Barret, 1996).

In this study, the FLA was applied as the second method of MCDA. Compared with WLC, it does not demand the relative importance of criteria determined by decision makers directly. The FLA aggregates thematic layers using fuzzy operators, which requires least prior knowledge of relationships among criteria (Ki & Ray, 2014). This overlay method is particularly convenient when substantial thematic layers are aggregated, which also provides flexibility through changing GAMMA value when the priority scores of raster cells need to be adjusted. Comparing the priority maps from FLA and WLC, there exist some degree of biases in geographic distribution and priority division distribution. It can be observed that there exist more cells belonging to highest priority zones in the map of WLC, and the map of FLA have more pixels falling into least priority zones. These biases are likely due to different techniques of standardization and overlay in WLC and FLA: (1) the additive effect of the ranking system in WLC contributes to more high priority scores in the priority map, (2) the continuous rating scales in fuzzy membership function probably results in more low scores in the priority map of FLA. As for the bias in geographic distribution of two priority maps, some most priority areas of FLA map appear in the lower Oxford across the ‘Zorra & East Zorra Tavistock Line’, which cannot be observed in the map of WLC. Closer observation reveals that these areas are close to Strathallan swamp, which may influence the development of ephemeral gully erosion. In the priority map of WLC, these exist more areas of most priority along Nissouri Creek and Middle Thames River than those in FLA map, which is likely due to the additive effect of the ranking system on the drainage pattern. Overall, the priority maps of WLC and FLA display the similar priority distribution of GWWs implementation, with highest priority areas concentrated in the northern part of the studies watershed.

5.5 Limitations and Prospects

The accuracy, preciseness and integrity of this study are expected to be improved if more data are available and accessible, including GWWs inventory data and criteria data. For the lack of accurate inventory data of existing BMPs, the existing GWWs need to be identified and delineated. Field

reconnaissance surveys of GWWs were not possible owing to the restricted access to agricultural fields (private property) during the pandemic. Although the identification of GWW features was cross-checked with the technician from UTRCA and relevant experts throughout the digitizing process, the precision of GWWs' starting and ending points location together with their trajectories can be improved, if existing BMPs data record more accurate location of specific types of BMPs or field reconnaissance surveys can be conducted. Moreover, it is likely to identify more existing GWWs as ground truth data in the studied watershed, which can facilitate the validation process.

Apart from the GWWs inventory data, more thematic layers are expected to be applied in the MCDA, including lithology layer and meteorology layer. These thematic layers are commonly used as conditioning factors in existing studies of ephemeral gully erosion susceptibility, which are limited within the studies watershed. The number of meteorological stations within the study area is relatively inadequate to display the detailed spatial variation of meteorology through interpolation. Further works on retrieving more thematic layer data in good quality and combining into priority map are suggested, which can improve the robustness of the priority map.

There also exist limitations in the CTI model. The CTI model only considers the influence of terrain attributes in forming the ephemeral gully erosion, which overlooks the impacts of soil type and climate condition. In addition, the localized nature of threshold value may restrict the application of this method in other study areas where the ground truth data are not accessible. Additional research is suggested on strategies for finding thresholds in different site conditions. Besides, the discontinuities among the trajectories of predicted GWWs may influence the length prediction performance of GWWs. Further work on enhancement of length prediction and trajectory modification can support the application of this method in GWWs design.

Finally, the MCDA in this study faces challenge in weight determination. Firstly, it is restricted to consult a group of experts about their opinions on weight assignment in the Middle Thames River especially during the pandemic. Secondly, there are no similar studies of GWWs, or ephemeral gully erosion conducted in the Middle Thames River watershed. It increases the difficulty of criteria standardization and weight determination, which requires the combination of prior experience from

existing studies and the local characteristics of the study area. Thirdly, the existing GWWs data are not able to support statistical modelling (as training data) for retrieving the relative importance of each criterion. The suitability and effectiveness of existing GWWs remain unexplored. Moreover, it is unscientific to conclude that the areas without GWWs implementation at present belong to the areas with no need for GWWs. Therefore, more accurate GWWs data are expected to be applied to develop statistical modelling, which can derive the relative importance of each criterion for reference of weight assignments.

Further research on GWWs' effectiveness in different prioritized areas is suggested, including sediment reduction rate and runoff reduction rate, which is probably achieved by combining the CTI model with complex hydrological models such SWAT and AGNPS. Moreover, it is expected to design the potential GWWs (e.g., shape, grass type, and storm duration) at the field scales in prioritized areas based on specific meteorology and geographic condition. Besides, additional research on extending the application of methods developed in the present study to the provincial and national scales is expected. The parameters in the present study including CTI threshold, SPI threshold, criteria ranking, weight assignment and fuzzy membership need to be formalized. Alternatively, an inventory database of parameters specific to different study sites' conditions is expected to be created. Last but not least, a more integrated sensitivity analysis is needed to be conducted on total of 12 criteria. The variations in criteria weighting and priority distribution are expected to be visualized more explicitly.

Overall, the predicted GWWs and priority maps in this study can facilitate the targeted placement of GWWs within the Middle Thames River watershed. Considering the automatic, repeatable, and rapid characteristics of the methods in this study, it has a potential to be used as a preliminary or 'screening' tool incorporated into complex hydrology modeling process such as BMPDSS and AGNPS, which are currently unable to locate GWWs automatically.

5.6 Chapter Summary

In conclusion, the CTI and SPI model are rapid methods to predict potential GWWs in specific fields, which requires the threshold finding unique to study areas. The MCDA can generate priority maps for

GWWs implementation, which assists decision makers with watershed planning. This Section discussed the localized nature of threshold values and discontinuities along the trajectories of predicted GWWs in CTI and SPI model. The biases in overlay techniques and priority maps between WLC and FLA are explained. Finally, three main limitations of this study are presented, including (1) data availability of GWWs inventory data and criteria data; (2) limited application of CTI model; (3) challenges in weight assignments in MCDA. The methods in this study are expected to be automated and incorporated into complex hydrology models, which can enable conservation efficiency and assist landowners and local stakeholders with targeted placement of GWWs.

Chapter 6 Conclusions

Soil erosion remains considered to be a primary challenge in the 21st century threatening fresh water and crop land that supports more than 95% of global food production (Borrelli et al., 2020; FAO, 2020). It is of significance to plan for and prevent soil erosion in its initial stages rather than labor intensive repairing later (OMAFRA, 2018). The Middle Thames River watershed has suffered from severe erosion issues for more than ten years with 21% highly erodible lands throughout the basin, where extensive soil conservation measures are highly encouraged (UTRCA, 2017). Grassed waterways, as broad and shallow channels to move concentrated surface runoff, are considered as one of the most effective measures to prevent ephemeral soil erosion. Therefore, identifying the site-specific opportunities for GWWs implementation in the Middle Thames River watershed can support targeted soil conservation as well as the watershed planning.

This study aims to develop a fast and effective methodology to identify the potential areas for GWWs implementation from the field scale to the watershed scale. For the lack of inventory GWWs data, the identification and digitization of GWWs have been conducted using ariel images to delineate the existing GWWs as reference data for evaluation. The CTI model and SPI model has been developed to predict the existing and potential GWWs at the field level. The output maps of CTI and SPI model display the location and length of predicted GWWs in each field. The performance of CTI and SPI model have been assessed by visual evaluation, occurrence evaluation and length evaluation. To better visualize the results of CTI and SPI models, the density distribution maps of predicted GWWs throughout the studied watershed have been created based on the outputs from CTI and SPI. After developing CTI and SPI models, the MCDA has been conducted to map the priority areas for GWWs implementation at the watershed scale. Twelve factors were selected as criteria of MCDA based on literature review, data availability and geographic knowledge. Two methods including WLC and FLA were employed in MCDA, which produced two outputs maps of priority areas for GWWs implementation. The results of these two maps have been validated using existing GWWs.

The results of CTI model and SPI model display the existing and predicted GWWs in each field. The CTI model with the threshold of 600 has identified 30 existing GWWs, while the SPI model with the threshold of 0.01 standard deviation identified 23 GWWs. Several discontinuities exist in predicted

GWWs along the trajectories of digitized GWWs. The lengths of predicted GWWs by CTI model have a much better agreement with observation than that of SPI model. The density distribution map of CTI and SPI model presented high-density areas of predicted GWWs which are mainly situated in the northern and central part of the study area, especially the areas along the upstream of Middle Thames River and Nissouri creek. The low-density areas for GWWs implementation are mostly located in the southwestern part of the study area.

The results of WLC and FLA displayed the high-priority areas mainly located in the northwestern part of the watershed, especially along the upstream of Nissouri creek. It is found that these upstream areas have relatively steeper slope gradient than other areas in the studied watershed, with dominant soil type of sandy loam and silty loam. There are more areas belonging to lowest priority zone and lower areas falling into most priority level in FLA output map, compared with the map of WLC. The FLA required less prior knowledge of relationship among criteria, which provide more flexibility and convenience to decision makers. The validation of both WLC and FLA output maps display relatively good performance, based on the criteria that greater percentage of GWWs implementation must occur in the higher priority zones (Kanungo et al., 2009).

The main limitations and challenge of this study have been identified. For the lack of accurate inventory data of GWWs and constraints of field survey, the existing GWWs need to be delineated manually, which may produce more uncertainty. The second limitation is related to discontinuities and threshold finding in CTI and SPI model. The localized nature of threshold value in both CTI and SPI may restrict the application of this method in other study areas where the ground truth data are not accessible. The significant discontinuities among the trajectories of predicted GWWs can influence the length prediction performance of GWWs. The third challenge of this study is weight assignment in MCDA. There are no similar studies of GWWs, or ephemeral gully erosion conducted in the Middle Thames River watershed. Additionally, it is restricted to consult a group of experts about their opinions on weight assignment in the Middle Thames River especially during the pandemic.

To conclude, this study has identified existing and potential areas for GWWs implementation from the field scale to watershed scale. Future work on the automation of the methodology is expected. It has a potential to be used as a preliminary or ‘screening’ tool incorporated into complex hydrology modeling process such as BMPDSS and AGNPS. The results of this study can facilitate the targeted placement of GWWs within the Middle Thames River watershed.

References

- Ackerman, D., & Stein, E. D. (2008). Evaluating the Effectiveness of Best Management Practices Using Dynamic Modeling. *Journal of Environmental Engineering*, 134(8).
[https://doi.org/10.1061/\(ASCE\)0733-9372\(2008\)134:8\(628\)](https://doi.org/10.1061/(ASCE)0733-9372(2008)134:8(628))
- Ascough II, J. C., Baffaut, C., Nearing, M. A., & Liu, B. Y. (1997). The WEPPwatershed model: I. Hydrology and erosion. *Transactions of the ASAE*, 40(4), 921-933.
- Agence européenne pour l'environnement. (2005). The European environment: State and outlook 2005 (Vol. 1). European Communities.
- Ahiablame, L. M., Engel, B. A., & Chaubey, I. (2012). Effectiveness of low impact development practices: literature review and suggestions for future research. *Water, Air, & Soil Pollution*, 223(7), 4253-4273.
- Alvarez-Guerra, M., Viguri, J. R., & Voulvoulis, N. (2009). A multicriteria-based methodology for site prioritisation in sediment management. *Environment international*, 35(6), 920-930.
- Ambrasaitė, I., Barfod, M. B., & Salling, K. B. (2011). MCDA and risk analysis in transport infrastructure appraisals: The Rail Baltica case. *Procedia-Social and Behavioral Sciences*, 20, 944-953.
- Archer, G. E. B., Saltelli, A., & Sobol, I. M. (1997). Sensitivity measures, ANOVA-like techniques and the use of bootstrap. *Journal of Statistical Computation and Simulation*, 58(2), 99-120.
- Artita, K.S., P. Kaini, and J.W. Nicklow. 2013. Examining the possibilities: Generating al-ternative watershed-scale BMP designs with evolutionary algorithms. *Water Resources Management* 27(11):3849-3863
- Balmforth D., Digman C.J., Butler D., Shaffer P. (2006). Integrated Urban Drainage Pilots: Scoping Study. DEFRA.London
- Barron, F. H., & Barrett, B. E. (1996). The efficacy of SMARTER—Simple multi-attribute rating technique extended to ranking. *Acta Psychologica*, 93(1-3), 23-36.
- Bernard, J., Lemunyon, J., Merkel, B., Theurer, F., Widman, N., Bingner, R., ... & Wilson, G. (2010). Ephemeral gully erosion—A national resource concern. *National Sedimentation Laboratory Technical Research Rep*, 69.

- Bennett, S. J., Alonso, C. V., Prasad, S. N., & Romkens, M. J. M. (2000). Experiments on headcut growth and migration in concentrated flows typical of upland areas. *Water Resources Res.*, 36(7), 1911-1922.
- Begin, Z. B., & Schumm, S. A. (1979). Instability of alluvial valley floors: a method for its assessment. *Transactions of the ASAE*, 22(2), 347-0350.
- Bingner, R. L., Theurer, F. D., Gordon, L. M., Bennett, S. J., Parker, C., Thorne, C., & Alonso, C. V. (2007). AnnAGNPS ephemeral gully erosion simulation technology. In Javier Casalí, Rafael Giménez (eds.): *Progress in Gully Erosion Research. IV International Symposium on Gully Erosion*. September 17-19, 2007. Pamplona, Spain. Pamplona: Universidad Pública de Navarra/Nafarroako Unibertsitate Publikoa, 2007. Universidad Pública de Navarra/Nafarroako Unibertsitate Publikoa.
- Bennett, S. J., & Wells, R. R. (2019). Gully erosion processes, disciplinary fragmentation, and technological innovation. *Earth Surface Processes and Landforms*, 44(1), 46-53.
- Board, C. H. R., Authority, U. T. R. C., & Bocking, D. (2000). *The Thames Strategy: Managing the Thames as a Canadian Heritage River*. London, Ont.: Upper Thames River Conservation Authority.
- Boardman, J. (2001). Storms, floods and soil erosion on the South Downs, East Sussex, autumn and winter 2000-01. *Geography*, 346-355.
- Boardman, J. (2016). The value of Google Earth™ for erosion mapping. *Catena*, 143, 123-127.
- Borrelli, P., Robinson, D. A., Panagos, P., Lugato, E., Yang, J. E., Alewell, C., ... & Ballabio, C. (2020). Land use and climate change impacts on global soil erosion by water (2015-2070). *Proceedings of the National Academy of Sciences*, 117(36), 21994-22001.
- Bojorquez-Tapia LA, Cruz-BelloGM, Luna-Gonzalez L, Juarez L, Ortiz-PerezMA. V-DRASTIC: using visualization to engage policymakers in groundwater vulnerability assessment. *J Hydrol* 2009;373(1–2):242–55.
- Boufeldja, S., Hamed, K. B., Bouanani, A., & Belkendil, A. (2020). Identification of zones at risk of erosion by the combination of a digital model and the method of multi-criteria analysis in the arid regions: case of the Bechar Wadi watershed. *Applied Water Science*, 10(5), 1-18.

- Burrough, P. A., and McDonell, R. A., 1998. Principles of Geographical Information Systems (Oxford University Press, New York), 190 pp.
- Cevik, E., & Topal, T. (2003). GIS-based landslide susceptibility mapping for a problematic segment of the natural gas pipeline, Hendek (Turkey). *Environmental geology*, 44(8), 949-962.
- Chen, J., Hua, C., & Liu, C. (2019). Considerations for better construction and demolition waste management: Identifying the decision behaviors of contractors and government departments through a game theory decision-making model. *Journal of cleaner production*, 212, 190-199.
- Cheng, M. S., Zhen, J., & Shoemaker, L. (2009). BMP decision support system for evaluating stormwater management alternatives. *Frontiers of Environmental Science & Engineering in China*, 3(4), 453–463.
- Chow, T. L., Rees, H. W., & Daigle, J. L. (1999). Effectiveness of terraces/grassed waterway systems for soil and water conservation: A field evaluation. *J. Soil Water Cons.*, 54(3), 577-583.
- Curtiss, J. R. (1978). The Clean Water Act of 1977: Midcourse Corrections in the Section 404 Program. *Neb. L. Rev.*, 57, 1092.
- Clark, E. H., Haverkamp, J. A., & Chapman, W. (1985). Eroding soils. The off-farm impacts. Conservation Foundation.
- Clubb, F. J., Mudd, S. M., Attal, M., Milodowski, D. T., & Grieve, S. W. (2016). The relationship between drainage density, erosion rate, and hilltop curvature: Implications for sediment transport processes. *Journal of Geophysical Research: Earth Surface*, 121(10), 1724-1745.
- Conoscenti, C., Agnesi, V., Angileri, S., Cappadonia, C., Rotigliano, E., & Märker, M. (2013). A GIS-based approach for gully erosion susceptibility modelling: a test in Sicily, Italy. *Environmental Earth Sciences*, 70(3), 1179-1195.
- Conforti, M., Aucelli, P. P., Robustelli, G., & Scarciglia, F. (2011). Geomorphology and GIS analysis for mapping gully erosion susceptibility in the Turbolo stream catchment (Northern Calabria, Italy). *Natural hazards*, 56(3), 881-898.
- Dabney, S. M. (1998). Cover crop impacts on watershed hydrology. *Journal of Soil and Water Conservation*, 53(3), 207-213.

Daggupati, P., Douglas-Mankin, K. R., & Sheshukov, A. Y. (2013). Predicting ephemeral gully location and length using topographic index models. *Transactions of the ASABE*, 56(4), 1427-1440.

Daniel Obenour, Isabella Bertani, Nathan Manning, Drew Gronewold,, Craig Stow, and Donald Scavia. (2017). 2017 Western Lake Erie Harmful Algal Bloom (HAB) Forecast by NOAA Great Lakes Environmental Research Laboratory (GLERL), North Carolina State University and University of Michigan. Issued: 13 July 2017. Retrieved from https://www.glerl.noaa.gov/res/HABs_and_Hypoxia/docs/2017LakeErieBloomForecastRelease2.pdf

Dai, F. C., & Lee, C. F. (2001). Terrain-based mapping of landslide susceptibility using a geographical information system: a case study. *Canadian Geotechnical Journal*, 38(5), 911-923.

Den Biggelaar, C., Lal, R., Wiebe, K., & Breneman, V. (2004). The global impact of soil erosion on productivity. I. Absolute and relative erosion-induced yield losses. *Advances in agronomy*, 81(81), 1-48.

Denver, J. M., Tesoriero, A. J., & Barbaro, J. R. (2010). Trends and transformation of nutrients and pesticides in a Coastal Plain aquifer system, United States. *Journal of Environmental Quality*, 39(1), 154-167.

Desmet, P. J. J., Poesen, J., Govers, G., & Vandaele, K. (1999). Importance of slope gradient and contributing area for optimal prediction of the initiation and trajectory of ephemeral gullies. *Catena*, 37(3-4), 377-392.

Delphin, J. E., & Chapot, J. Y. (2001). Leaching of atrazine and deethylatrazine under a vegetative filter strip. *Agronomie*, 21(5), 461-470.

Delgado, M. G., & Sendra, J. B. (2004). Sensitivity analysis in multicriteria spatial decision-making: a review. *Human and ecological risk assessment*, 10(6), 1173-1187.

Domazetović, F., Šiljeg, A., Lončar, N., & Marić, I. (2019). Development of automated multicriteria GIS analysis of gully erosion susceptibility. *Applied geography*, 112, 102083.

Dosskey, M.G. (2002). Setting priorities for research on pollution reduction functions of agricultural buffers. *Environ. Manag.* 30, 641–650.

- Diebel, M. W., Maxted, J. T., Nowak, P. J., & Vander Zanden, M. J. (2008). Landscape planning for agricultural nonpoint source pollution reduction I: a geographical allocation framework. *Environmental management*, 42(5), 789-802.
- Efthimiou, N., Lykoudi, E., Panagoulia, D., & Karavitis, C. (2016). Assessment of soil susceptibility to erosion using the EPM and RUSLE Models: the case of Venetikos River Catchment. *Global NEST Journal*, 18(1), 164-179.
- Ellis, J. B., Deutsch, J. C., Mouchel, J. M., Scholes, L., & Revitt, M. D. (2004). Multicriteria decision approaches to support sustainable drainage options for the treatment of highway and urban runoff. *Science of the total Environment*, 334, 251- 260.
- Erener, A., Mutlu, A., & Düzgün, H. S. (2016). A comparative study for landslide susceptibility mapping using GIS-based multi-criteria decision analysis (MCDA), logistic regression (LR) and association rule mining (ARM). *Engineering geology*, 203, 45-55.
- EPA. (2017, April 07). Harmful Algal Blooms. Retrieved from
<https://www.epa.gov/nutrientpollution/harmful-algal-blooms>
- Esri. (2016). Kernel Density. ArcGIS for Desktop. Retrieved from
<https://desktop.arcgis.com/en/arcmap/10.3/tools/spatial-analyst-toolbox/kernel-density.htm>.
- Esri. (2016). How Slope works. ArcGIS for Desktop. Retrieved from
<https://desktop.arcgis.com/en/arcmap/10.3/tools/spatial-analyst-toolbox/how-slope-works.htm>
- Esri. (2016). How Fuzzy Membership Works. Retrieved from
<https://desktop.arcgis.com/en/arcmap/10.3/tools/spatial-analyst-toolbox/how-fuzzy-membership-works.htm>
- Esri. (2016). How Fuzzy Overlay works. Retrieved from
<https://desktop.arcgis.com/en/arcmap/10.3/tools/spatial-analyst-toolbox/how-fuzzy-overlay-works.htm>
- Esri. (2016). Curvature Function. Retrieved from <https://desktop.arcgis.com/en/arcmap/10.3/manage-data/raster-and-images/curvature-function.htm>.
- Foley, J. A., Ramankutty, N., Brauman, K. A., Cassidy, E. S., Gerber, J. S., Johnston, M., ... & Zaks, D. P. (2011). Solutions for a cultivated planet. *Nature*, 478(7369), 337-342.

- Foster, G. R. (1986). Understanding ephemeral gully erosion. In Soil Conservation: Assessing the National Resources Inventory (Vol. 2, pp. 90-125). Washington, D.C.: National Academies Press.
- Fiener, P., & Auerswald, K. (2003). Concept and effects of a multi - purpose grassed waterway. *Soil Use and Management*, 19(1), 65-72.
- Fiener, P., & Auerswald, K. (2006). Seasonal variation of grassed waterway effectiveness in reducing runoff and sediment delivery from agricultural watersheds in temperate Europe. *Soil and Tillage Research*, 87(1), 48-58.
- Floress, K., Reimer, A., Thompson, A., Burbach, M., Knutson, C., Prokopy, L., ... & Ulrich-Schad, J. (2018). Measuring farmer conservation behaviors: Challenges and best practices. *Land use policy*, 70, 414-418.
- Gaddis, E., Voinov, A., Seppelt, R., & Rizzo, D. (2014). Spatial optimization of best management practices to attain water quality targets. *Water Resources Management*, 28(6), 1485-1499.doi:10.1007/s11269-013-0503-0
- Gayen, A., Saha, S., & Pourghasemi, H. R. (2020). Soil erosion assessment using RUSLE model and its validation by FR probability model. *Geocarto International*, 35(15), 1750-1768.
- Gigović, L., Drobnjak, S., & Pamučar, D. (2019). The application of the hybrid GIS spatial multi-criteria decision analysis best-worst methodology for landslide susceptibility mapping. *ISPRS International Journal of Geo-Information*, 8(2), 79.
- Garnett, T., Appleby, M. C., Balmford, A., Bateman, I. J., Benton, T. G., Bloomer, P., ... & Godfray, H. C. J. (2013). Sustainable intensification in agriculture: premises and policies. *Science*, 341(6141), 33-34.
- Gali, R. K., Soupir, M. L., Kaleita, A. L., & Daggupati, P. (2015). Identifying potential locations for grassed waterways using terrain attributes and precision conservation technologies. *Transactions of the ASABE*, 58(5), 1231-1239.
- Greene, R., Devillers, R., Luther, J. E., & Eddy, B. G. (2011). GIS - based multiple - criteria decision analysis. *Geography compass*, 5(6), 412-432.

- Gómez-Gutiérrez, Á., Conoscenti, C., Angileri, S. E., Rotigliano, E., & Schnabel, S. (2015). Using topographical attributes to evaluate gully erosion proneness (susceptibility) in two mediterranean basins: Advantages and limitations. *Natural Hazards*, 79(1), 291-314.
- Gordon, L. M., Bennett, S. J., Alonso, C. V., & Bingner, R. L. (2008). Modeling long-term soil losses on agricultural fields due to ephemeral gully erosion. *J. Soil Water Cons.*, 63(4), 173-181.
- Government of Ontario. (2006). Clean Water Plan. Retrieved from
<https://www.ontariocanada.com/registry/view.do?postingId=3782&language=en>
- Gutiérrez, Á. G., Schnabel, S., & Contador, F. L. (2009). Gully erosion, land use and topographical thresholds during the last 60 years in a small rangeland catchment in SW Spain. *Land Degradation & Development*, 20(5), 535-550.
- Holland, J. M. (2004). The environmental consequences of adopting conservation tillage in Europe: reviewing the evidence. *Agriculture, ecosystems & environment*, 103(1), 1-25.
- Holmes, K. W., Chadwick, O. A. and Kyriakidis, P. C. (2000). Error in a USGS 30-meter digital elevation model and its impact on terrain modeling. *Journal of Hydrology*, 233. 154 – 173.
- Hu, G., Wu, Y., Liu, B., Yu, Z., You, Z., & Zhang, Y. (2007). Short-term gully retreat rates over rolling hill areas in black soil of Northeast China. *Catena*, 71(2), 321-329.
- Jia, H., Yao, H., Tang, Y., Shaw, L. Y., Zhen, J. X., & Lu, Y. (2013). Development of a multi-criteria index ranking system for urban runoff best management practices (BMPs) selection. *Environmental monitoring and assessment*, 185(9), 7915-7933.
- John Greig. (2017). Canada's soils still degrading, albeit more slowly. AGCanada. Retrieved from
<https://www.agcanada.com/daily/canadas-soils-still-degrading-albeit-more-slowly>.
- Kanungo, D. P., Arora, M. K., Sarkar, S., & Gupta, R. P. (2009). A fuzzy set based approach for integration of thematic maps for landslide susceptibility zonation. *Georisk*, 3(1), 30-43.
- Khawlie M, Awad M, Shaban A, BouKheir R, Abdallah C (2002) Remote sensing for environmental protection of the eastern Mediterranean rugged mountainous areas, Lebanon. *ISPRS J Photogramm Remote Sens* 57:13–23

- Khosravi, F., Fischer, T. B., & Jha-Thakur, U. (2019). Multi-criteria analysis for rapid strategic environmental assessment in tourism planning. *Journal of Environmental Assessment Policy and Management*, 21(04), 1950013.
- Ki, S. J., & Ray, C. (2014). Using fuzzy logic analysis for siting decisions of infiltration trenches for highway runoff control. *Science of the total environment*, 493, 44-53.
- Kincheloe, S. (1994). Tools to aid management: The use of site specific management. *Journal of soil and water conservation*, 49(2), S43-S43.
- Kirkby, M. J., & Beven, K. J. (1979). A physically based, variable contributing area model of basin hydrology. *Hydrological Sciences Journal*, 24(1), 43-69.
- Koch, B. J., Febria, C. M., Gevrey, M., Wainger, L. A., & Palmer, M. A. (2014). Nitrogen removal by stormwater management structures: A data synthesis. *JAWRA Journal of the American Water Resources Association*, 50(6), 1594-1607.
- Knapen, A., & Poesen, J. (2010). Soil erosion resistance effects on rill and gully initiation points and dimensions. *Earth Surface Processes and Landforms: The Journal of the British Geomorphological Research Group*, 35(2), 217-228.
- Knisel, W. G. (1980). CREAMS: A field scale model for chemicals, runoff, and erosion from agricultural management systems (No. 26). Department of Agriculture, Science and Education Administration.
- Knisel, W., Di Nicuolo, A., Pfohl, M., Müller, H., Risler, T., Eggstein, M., & Seifried, E. (1993). Different effects of two methods of low - density lipoprotein apheresis on the coagulation and fibrinolytic systems 3. *Journal of internal medicine*, 234(5), 479-487.
- Kumar, S., Soukup, M., & Elbaum, R. (2017). Silicification in grasses: variation between different cell types. *Frontiers in Plant Science*, 8, 438.
- Liu, Y., Yang, W., Leon, L., Wong, I., McCrimmon, C., Dove, A., & Fong, P. (2016). Hydrologic modeling and evaluation of Best Management Practice scenarios for the Grand River watershed in Southern Ontario. *Journal of Great Lakes Research*, 42(6), 1289-1301.
- Liu, Y., Engel, B. A., Flanagan, D. C., Gitau, M. W., Mcmillan, S. K., & Chaubey, I. (2017). A review on effectiveness of best management practices in improving hydrology and water quality:

Needs and opportunities. *Science of The Total Environment*, 601-602, 580-593. doi: 10.1016/j.scitotenv.2017.05.212

Locatelli, G., & Mancini, M. (2012). A framework for the selection of the right nuclear power plant. *International Journal of Production Research*, 50(17), 4753-4766.

Logan, T. J. (1990). Agricultural best management practices and groundwater protection. *Journal of Soil and Water Conservation*, 45(2), 201-206.

Logan, T. J. (1993). Agricultural best management practices for water pollution control: current issues. *Agriculture, Ecosystems & Environment*, 46(1-4), 223-231.

Lucà, F., Conforti, M., & Robustelli, G. (2011). Comparison of GIS-based gullying susceptibility mapping using bivariate and multivariate statistics: Northern Calabria, South Italy. *Geomorphology*, 134(3-4), 297-308.

Marttunen, M., Mustajoki, J., Dufva, M., & Karjalainen, T. P. (2015). How to design and realize participation of stakeholders in MCDA processes? A framework for selecting an appropriate approach. *EURO Journal on Decision Processes*, 3(1-2), 187-214.

Martin, C., Ruperd, Y., & Legret, M. (2007). Urban stormwater drainage management: The development of a multicriteria decision aid approach for best management practices. *European journal of operational research*, 181(1), 338-349.

Majumdar, S., Kose, M., & Chatterjee, U. (2021). Gully Erosion Mapping by Multi-criteria Decision Analysis Techniques and Geoinformatics in Adana Province, Turkey. *Earth Systems and Environment*, 1-12.

Malczewski, J., & Rinner, C. (2015). Multicriteria decision analysis in geographic information science (pp. 220-228). New York: Springer.

Martin YE, Franklin SE (2005) Classification of soil- and bedrock dominated landslides in British Columbia using segmentation of satellite imagery and DEM data. *Int J Remote Sens* 26:1505–1509.

Michalak, A. M., Anderson, E. J., Beletsky, D., Boland, S., Bosch, N. S., Bridgeman, T. B., . . . Zagorski, M. A. (2013). Record-setting algal bloom in Lake Erie caused by agricultural and meteorological trends consistent with expected future conditions. *Proceedings of the National Academy of Sciences*, 110(16), 6448-6452. doi:10.1073/pnas.1216006110

- Momm, H. G., Bingner, R. L., Wells, R. R., & Wilcox, D. (2012). AGNPS GIS-based tool for watershed-scale identification and mapping of cropland potential ephemeral gullies. *Appl. Eng. Agric.*, 28(1), 1-13.
- Momm, H. G., Bingner, R. L., Wells, R. R., Rigby, J. R., & Dabney, S. M. (2013). Effect of topographic characteristics on compound topographic index for identification of gully channel initiation locations. *Trans. ASABE*, 56(2), 523-537.
- Moore, I. D., & Burch, G. J. (1986). Physical basis of the length - slope factor in the universal soil loss equation. *Soil Science Society of America Journal*, 50(5), 1294-1298.
- Moore, I. D., Burch, G. J., & Mackenzie, D. H. (1988). Topographic effects on the distribution of surface soil-water and the location of ephemeral gullies. *Trans. ASAE*, 31(4), 1098-1107.
- Moriasi, D. N., Arnold, J. G., Van Liew, M. W., Bingner, R. L., Harmel, R. D., & Veith, T. L. (2007). Model evaluation guidelines for systematic quantification of accuracy in watershed simulations. *Transactions of the ASABE*, 50(3), 885-900.
- Nachtergaele, J., Poesen, J., Steegen, A., Takken, I., Beuselinck, L., Vandekerckhove, L., & Govers, G. (2001). The value of a physically based model versus an empirical approach in the prediction of ephemeral gully erosion for loess-derived soils. *Geomorphology*, 40(3-4), 237-252.
- Nachtergaele, J., Poesen, J., & Govers, G. (2002). Ephemeral gullies. A spatial and temporal analysis of their characteristics, importance, and prediction. *Belgeo. Revue belge de géographie*, (2), 159-182.
- Natural Resources Conservation Services (n.d.). Conservation Choices: Grassed Waterway. Natural Resources Conservation Services. United States Department of Agriculture. Retrieved from <https://www.nrcs.usda.gov/wps/portal/nrcs/detail/null/?cid=nrcseprd415210>.
- Nebel, S., Brick, J., Lantz, V. A., & Trenholm, R. (2017). Which Factors Contribute to Environmental Behaviour of Landowners in Southwestern Ontario, Canada? *Environmental Management*, 60(3), 454-463. doi:10.1007/s00267-017-0849-9
- Novotny, V. (2002). Water quality: diffuse pollution and watershed management. John Wiley & Sons.

- Nyssen, J., Poesen, J., Moeyersons, J., Haile, M., Deckers, J., 2008. Dynamics of soil erosion rates and controlling factors in the Northern Ethiopian Highlands towards a sediment budget. *Earth Surface Processes and Landforms* 33, pp. 695-711.
- Odu, G. O. (2019). Weighting methods for multi-criteria decision-making technique. *Journal of Applied Sciences and Environmental Management*, 23(8), 1449-1457.
- Ontario Ministry of Agriculture Food and Rural Affairs (2016). Sustaining Ontario's Agricultural Soils: Towards a Shared Vision. Retrieved from
<http://www.omafra.gov.on.ca/english/landuse/soil-paper.pdf>
- Ontario Ministry of Agriculture Food and Rural Affairs (2018). Soil Erosion- Causes and Effect. Factsheet, order No.12-053. Retrieved from
<http://www.omafra.gov.on.ca/english/engineer/facts/12-053.htm>
- Ontario Soil and Crop Improvement Association. (2016). Farmland Health Incentive Program Website. Retrieved from
<http://www.ontariosoilcrop.org/wp-content/uploads/2015/12/FHIP-2016-Brochure-WEBcompressed.pdf>
- Oostwoud Wijdenes, D. J., & Bryan, R. (2001). Gully - head erosion processes on a semi - arid valley floor in Kenya: a case study into temporal variation and sediment budgeting. *Earth Surface Processes and Landforms*, 26(9), 911-933.
- Parker, C., Thorne, C. L., Bingner, R., Wells, R., & Wilcox, D. (2007). Automated mapping of potential for ephemeral gully formation in agricultural watersheds. Research Report No. 56. Oxford, Miss.: USDA-ARS National Sedimentation Laboratory.
- Paustian, K., Lehmann, J., Ogle, S., Reay, D., Robertson, G. P., & Smith, P. (2016). Climate-smart soils. *Nature*, 532(7597), 49-57.
- Patton, P. C., & Schumm, S. A. (1975). Gully erosion, Northwestern Colorado: a threshold phenomenon. *Geology*, 3(2), 88-90.
- Piccarreta, M., Faulkner, H., Bentivenga, M., & Capolongo, D. (2006). The influence of physico-chemical material properties on erosion processes in the badlands of Basilicata, Southern Italy. *Geomorphology*, 81(3-4), 235-251.

- Poesen, J. (1993). Gully typology and gully control measures in the European loess belt. *Farmland Erosion in Temperate Plains Environments and Hills*. Proceedings, 221-239.
- Poesen, J., Nachtergaele, J., Verstraeten, G., & Valentin, C. (2003). Gully erosion and environmental change: importance and research needs. *Catena*, 50(2-4), 91-133.
- Poesen J. & Valentin C., 2003. Gully Erosion and Global Change. Proc. First International Symposium on Gully Erosion, Leuven, Belgium, April 2000. *Catena* 50 (2–4): 87–562.
- Pournader, M., Ahmadi, H., Feiznia, S., Karimi, H., & Peirovan, H. R. (2018). Spatial prediction of soil erosion susceptibility: an evaluation of the maximum entropy model. *Earth Science Informatics*, 11(3), 389-401.
- Poesen J., Torri D. & Vanwalleghem T., 2011. Gully Erosion: Procedures to Adopt When modelling Soil Erosion in Landscapes Affected by Gullying. In: Morgan R.P.C. & Nearing M.A. (eds.) *Handbook of Erosion Modelling*. Blackwell Publishing Ltd, Chichester, UK. Chapter 19: 360–386 + Plates 16–19.
- Pulice, I., Cappadonia, C., Scarciglia, F., Robustelli, G., Conoscenti, C., De Rose, R., ... & Agnesi, V. (2012). Geomorphological, chemical and physical study of “calanchi” landforms in NW Sicily (southern Italy). *Geomorphology*, 153, 219-231.
- Rahmati, O., Pourghasemi, H. R., & Zeinivand, H. (2016). Flood susceptibility mapping using frequency ratio and weights-of-evidence models in the Golastan Province, Iran. *Geocarto International*, 31(1), 42-70.
- Rahmati, O., Tahmasebipour, N., Haghizadeh, A., Pourghasemi, H. R., & Feizizadeh, B. (2017). Evaluation of different machine learning models for predicting and mapping the susceptibility of gully erosion. *Geomorphology*, 298, 118-137.
- Ravalico, J. K., Dandy, G. C., & Maier, H. R. (2010). Management Option Rank Equivalence (MORE)—A new method of sensitivity analysis for decision-making. *Environmental Modelling & Software*, 25(2), 171-181.
- Rao, N. S., Easton, Z. M., Schneiderman, E. M., Zion, M. S., Lee, D. R., & Steenhuis, T. S. (2009). Modeling watershed-scale effectiveness of agricultural best management practices to reduce phosphorus loading. *Journal of Environmental Management*, 90(3), 1385-1395. doi: 10.1016/j.jenvman.2008.08.011

Rowlands, L. (2019). Erosion and Sediment Control—WSUD During the Construction Phase of Land Development. In Approaches to Water Sensitive Urban Design (pp. 163-176). Woodhead Publishing.

Roberts, R., & Goodwin, P. (2002). Weight approximations in multi - attribute decision models. Journal of Multi - Criteria Decision Analysis, 11(6), 291-303.

Saarikoski, H., Mustajoki, J., & Marttunen, M. (2013). Participatory multi-criteria assessment as ‘opening up’vs.‘closing down’of policy discourses: a case of old-growth forest conflict in Finnish Upper Lapland. Land use policy, 32, 329-336.

Saha, A. K., Gupta, R. P., Sarkar, I., Arora, M. K., & Csaplovics, E. (2005). An approach for GIS-based statistical landslide susceptibility zonation—with a case study in the Himalayas. Landslides, 2(1), 61-69.

Servenay A, Prat C (2003) Erosion extension of indurated volcanic soils of Mexico by aerial photographs and remote sensing analysis. Geoderma 117:367–375

Schaller, F. W., & Bailey, G. W. (Eds.). (1983). Agricultural management and water quality. Iowa State Press.

Schroter, J. B., & Kansas, H. (n.d.). Grassed Waterways versus Underground Outlet Tile. Retrieved from

<https://www.nrcs.usda.gov/wps/portal/nrcs/detail/ks/newsroom/features/?cid=stelprdb1242792>

Schindler, D. W., & Fee, E. J. (1974). Experimental Lakes Area: Whole-Lake Experiments in Eutrophication. Journal of the Fisheries Research Board of Canada, 31(5), 937-953. doi:10.1139/f74-110

Schmitt, T., Dosskey, M. G., & Hoagland, K. D. (1999). Filter strip performance and processes for different vegetation, widths, and contaminants.

Sharpley, A., Richards, P., Herron, S., & Baker, D. (2012). Case study comparison between litigated and voluntary nutrient management strategies. Journal of Soil and Water Conservation, 67(5), 442-450.

- Shoemaker, L., Riverson, J., Khalid, A., Zhen, J., Sabu, P., & Rafi, T. (2009). SUSTAIN, a framework for placement of best management practices in urban watersheds to protect water quality. Report EPA/600/R-09/095, USEPA, Washington, DC, USA.
- Stone, R., & McKague, K. (2009). Grassed waterways: Ontario Ministry of Agriculture, Food and Rural Affairs Factsheet, 09-021.
- Strauss, P., Leone, A., Ripa, M. N., Turpin, N., Lescot, J. M., & Laplana, R. (2007). Using critical source areas for targeting cost - effective best management practices to mitigate phosphorus and sediment transfer at the watershed scale. *Soil Use and Management*, 23, 144-153.
- Srivastava, P., Hamlett, J. M., & Robillard, P. D. (2003). Watershed Optimization Of Agricultural Best Management Practices: Continuous Simulation Versus Design Storms. *Journal of the American Water Resources Association*, 39(5), 1043-1054. doi:10.1111/j.1752-1688.2003.tb03691.x
- Thorne, C. R., & Zevenbergen, L. W. (1984). On-site prediction of ephemeral gully erosion (Doctoral dissertation, Colorado State University. Libraries).
- Thorne, C. L., Zevenbergen, L. W., Grissinger, E. H., & Murphrey, J. B. (1986). Ephemeral gullies as sources of sediment. In Proc. 4th Federal Interagency Sedimentation Conf. (vol. 3, pp. 152-153). Reston, Va.: U.S. Geologica Survey.
- Theresa Peluso. (2020). Ten years of environmental destruction in Ontario: Soil pollution. The Milestones. Science and Nature. Retrieved from <https://millstonenews.com/ten-years-of-environmental-destruction-in-ontario-soil-pollution/>.
- Tomer, M. D., & Locke, M. A. (2011). The challenge of documenting water quality benefits of conservation practices: A review of USDA-ARS's conservation effects assessment project watershed studies. *Water Science and Technology*, 64(1), 300-310.
- Tomer, M.D., K.M.B. Boomer, S.A. Porter, B.K. Gelder, D.E. James, and E. McLellan. 2015. Agricultural Conservation Planning Framework: 2. Classification of riparian buffer design-types with application to assess and map stream corridors. *J. Environ. Qual.* 44(3):768-779.
- Triantaphyllou, E. (2000). Multi-Criteria Decision Making: A Comparative Study. Dordrecht, The Netherlands: Kluwer Academic Publishers (now Springer). p. 320. ISBNÂ 0-7923-6607-7.

Trujillo-Barrera, A., Pennings, J. M., & Hofenk, D. (2016). Understanding producers' motives for adopting sustainable practices: the role of expected rewards, risk perception and risk tolerance. European Review of Agricultural Economics, 43(3), 359-382.

Tyndall, J., and T. Bowman (2016) Iowa Nutrient Reduction Strategy Best Management Practice cost overview series: Riparian buffers, vegetated filter strips, saturated buffers. Department of Ecology & Natural Resource management, Iowa State University.

Upper Thames River Conservation Authority(n.d.). Farmland Best Management Practices (BMPs). Retrieved from <http://thamesriver.on.ca/landowner-grants-stewardship/farmland-bmps/>.

Upper Thames River Conservation Authority (2017). Mud Creek Watershed Report Card 2017. Retrieved from http://thamesriver.on.ca/wp-content/uploads//WatershedReportCards/RC_Mud.pdf

Upper Thames River Conservation Authority (2017). Middle Thames Corridor Watershed Report Card 2017. Retrieved from http://thamesriver.on.ca/wp-content/uploads//WatershedReportCards/RC_MiddleThames.pdf

USDC, & NOAA. (2017, August 07). Lake Erie Harmful Algal Bloom. Retrieved from <https://www.weather.gov/cle/lakeeriehab>

U.S. Geological Survey and U.S. Department of Agriculture, Natural Resources Conservation Service, 2013, Federal Standards and Procedures for the National Watershed Boundary Dataset (WBD) (4 ed.): Techniques and Methods 11–A3, 63 p., <http://pubs.usgs.gov/tm/11/a3/>.ISSN: 2328-7055 (online)

Van der Knijff, J. M., Jones, R. J. A., & Montanarella, L. (2000). Soil erosion risk: assessment in Europe.

Vatn, A. (2009). An institutional analysis of methods for environmental appraisal. Ecological Economics, 68(8-9), 2207-2215.

Verstraeten, G., Van Oost, K., Van Rompaey, A., Poesen, J., Govers, G., 2002. Evaluating an integrated approach to catchment management to reduce soil loss and sediment pollution through modelling. Soil Use Manag. 19, 386–394.

Verstraeten, G., & Poesen, J. (1999). The nature of small-scale flooding, muddy floods and retention pond sedimentation in central Belgium. Geomorphology, 29(3-4), 275-292.

- Watters, A. (2019). Freshwater Scarcity: The Current Situation in Southern Ontario.
- Wang, Y., Montas, H. J., Brubaker, K. L., Leisnham, P. T., Shirmohammadi, A., Chanse, V., & Rockler, A. K. (2017). A diagnostic decision support system for BMP selection in small urban watershed. *Water Resources Management*, 31(5), 1649-1664.
- Wijdenes, D. J. O., Poesen, J., Vandekerckhove, L., & Ghesquiere, M. (2000). Spatial distribution of gully head activity and sediment supply along an ephemeral channel in a Mediterranean environment. *Catena*, 39(3), 147-167.
- Wu, Q., (2020). geemap: A Python package for interactive mapping with Google Earth Engine. *The Journal of Open Source Software*, 5(51), 2305. <https://doi.org/10.21105/joss.02305>
- Wu, Q., Lane, C. R., Li, X., Zhao, K., Zhou, Y., Clinton, N., DeVries, B., Golden, H. E., & Lang, M. W. (2019). Integrating LiDAR data and multi-temporal aerial imagery to map wetland inundation dynamics using Google Earth Engine. *Remote Sensing of Environment*, 228, 1-13. <https://doi.org/10.1016/j.rse.2019.04.015> (pdf | source code)
- Wu, W., & Wang, S. S. Y. (2005). Empirical-numerical analysis of headcut migration. *International Journal of Sediment Research*, 20(3), 233-243.
- Yates, A. G., Bailey, R. C., & Schwindt, J. A. (2007). Effectiveness of best management practices in improving stream ecosystem quality. *Hydrobiologia*, 583(1), 331-344. doi:10.1007/s10750-007-0619-4
- Zabihi, M., Mircholi, F., Motevalli, A., Darvishan, A. K., Pourghasemi, H. R., Zakeri, M. A., & Sadighi, F. (2018). Spatial modelling of gully erosion in Mazandaran Province, northern Iran. *Catena*, 161, 1-13.
- Zevenbergen, L. W., & Thorne, C. R. (1987). Quantitative analysis of land surface topography. *Earth surface processes and landforms*, 12(1), 47-56.

Appendix

The digitization of GWWs and visual evaluation of CTI model and SPI model were conducted through geemap in Google Earth Engine (GEE) using Python script and drawing tools, which can support interactive mapping in GEE. The scripts in geemap are presented below.

```
// creating a feature collection from digitized GWW polygons
var GWPolygon_1 = ee.FeatureCollection(GWPolygon)

// export the feature collection to the drive as shapefile format, specifying the folder name and task
name
Export.table.toDrive({
  collection: GWPolygon_1,
  description:'GWW_POLY',
  folder:'Digitization',
  fileFormat: 'SHP'
})

// Load shapefiles of SPI (with 1st to 5th standard deviation threshold) , CTI (threshold from 100 to
1000), watershed boundary and BMP point and visualize them.

Map.addLayer(table0,{color:'FF396E'},'SPI_1ST');

Map.addLayer(table1,{color:'FF3D00'},'SPI_2ST')

Map.addLayer(table2,{color:'FF4500'},'SPI_3ST');

Map.addLayer(table3,{color:'grey'},'SPI_4ST')

Map.addLayer(table4,{color:'green'},'SPI_5ST');

Map.addLayer(table5,{color:'red'},'CTI_Line100')

Map.addLayer(table6,{color:'red'},'CTI_Line200');

Map.addLayer(table7,{color:'red'},'CTI_Line300);
```

```

Map.addLayer(table8,{color:'red'},' CTI_Line400);

Map.addLayer(table9,{color:'red'},' CTI_Line500);

Map.addLayer(table10,{color:'red'},' CTI_Line600);

Map.addLayer(table11,{color:'red'},' CTI_Line700);

Map.addLayer(table12,{color:'red'},' CTI_Line800);

Map.addLayer(table13,{color:'red'},' CTI_Line900);

Map.addLayer(table14,{color:'red'},' CTI_Line1000);

Map.addLayer(table15,{color:'red',pointRadius: 5},'BMPPoint');

// visualize the watershed boundary without filling color

var ecoregions = ee.FeatureCollection(table16)

var empty = ee.Image().byte();

var outlines = empty.paint({ 

  featureCollection: ecoregions,
 
  color: 'BIOME_NUM',
 
  width: 2.5
});

var palette = ['FF0000', '00FF00', '0000FF'];

Map.addLayer(outlines, {palette: palette, max: 14}, 'buffered watershed boundary');

```